1999

Dual fuel conversion of a direct-injection diesel engine

Talus Park
West Virginia University

DUAL FUEL CONVERSION OF A DIRECT INJECTION DIESEL ENGINE

by

Talus Park

THESIS

Submitted to the College of Engineering and Mineral Resources
at
West Virginia University

in partial fulfillment of the requirements for the degree of

Master of Science
in
Mechanical Engineering

Nigel N. Clark, Ph. D., Chair
Christopher M. Atkinson, Sc. D.
Thomas R. Long, Ph. D.

Department of Mechanical and Aerospace Engineering

Morgantown, West Virginia
1999

Keywords: Dual Fuel, Pilot Injection, Diesel, Natural Gas, CNG

Acknowledgements

First and foremost, I thank Richard Atkinson, the resident electronics guru, for his invaluable guidance and assistance throughout this project. I also extend thanks (excuse the wart) to Dr. Nigel Clark for this research opportunity and for quality advising over the course of this project, and to Dr. Chris Atkinson and Dr. Tom Long for serving on my committee. Many thanks go to Mike Traver who provided much data acquisition assistance, to Tom McDaniel who keeps the Engine Research Center running like a well oiled machine, and to Wayne Hildebrand for performing the gas chromatograph analysis. I also thank IMPCO Technologies, Inc. for donating the natural gas control valve and the pressure regulator used in this project. Finally, immeasurable gratitude to my wife, Natalie, for supporting me both financially and emotionally, even while pursuing a Master's degree of her own, and to my son, whose imminent arrival provided the kick in the pants I needed to complete this thesis.

Abstract

Dual fuel pilot-injected diesel natural gas engines offer significant potential to reduce oxides of nitrogen (NO_x) and particulate matter (PM) emissions while maintaining diesel-like efficiency. A 1994 Navistar T444E turbocharger V-8 diesel engine was converted to dual fuel diesel and compressed natural gas (CNG). In an attempt to reduce the overall cost and complexity of conversion, the engine was left completely original, including the diesel fuel injection system. Also, for the sake of simplicity, the method of intake manifold fumigation through an IMPCO, Inc. electronic natural gas control valve was chosen to deliver the CNG. A microprocessor-based electronic control unit was developed to manage the hydraulically-actuated, electronically-controlled unit injectors (HEUI). Pilot injection parameters (start of injection, injection duration, and injection pressure) were varied along with the CNG flowrate to minimize NO_x production while still considering hydrocarbon (HC), carbon dioxide (CO_2), carbon monoxide (CO), and PM limits. Thermal efficiency and diesel fuel replacement ratio were noted as well. In-cylinder pressure data was collected and used to calculate run-time combustion parameters such as indicated mean effective pressure (IMEP), heat release rate (HRR) and to observe the ignition delay period. Comparative diesel and dual fuel tests were completed at intermediate load (1500 rpm, 335 N-m) and high load (1500 rpm, 580 N-m) operating conditions to determine the emissions benefits of the dual fuel conversion. Compared to diesel operation, optimized dual fuel operation at intermediate load produced a 32% decrease in NO_x and a 57% decrease in PM. Dual fuel operation at high load produced a 19% decrease in NO_x and a 72% decrease in PM. However, these reductions came with an increase in HC and CO emissions over standard diesel operation.

Table of Contents

Table of Figures

Table of Tables

Nomenclature

Abbreviations and Symbols

ADC	Analog to Digital Converter
ADV	Injection Advance
APS	Accelerator Pedal Sensor
ATDC	After Top Dead Center
ATS	Air Temperature Sensor
BSFC	Brake Specific Fuel Consumption
BTDC	Before Top Dead Center
BTU	British Thermal Unit
CA	Crank Angle
CMP	Camshaft Position
CNG	Compressed Natural Gas
CO	Carbon Monoxide
CO_2	Carbon Dioxide
COV	Coefficient of Variation
D2	Number 2 Diesel (light diesel)
DAS	Data Acquisition System
DF	Dual Fuel
DI	Direct Injected
ECT	Engine Coolant Temperature
ECU	Electronic Control Unit
EEC-IV	Ford Motor Company electronic control unit
EGR	Exhaust Gas Recirculation
EOI	End Of Injection
EOP	Engine Oil Pressure
EOT	Engine Oil Temperature
FID	Flame Ionization Detector
FIPW	Fuel Injection Pulse Width
GC	Gas Chromatograph
HC	Hydrocarbon
HEUI	Hydraulically-Actuated Electronically-Controlled Unit Injection
HRR	Heat Release Rate
Hz	Hertz
ICP	Injection Control Pressure
ICPR	Injection Control Pressure Regulator
IDM	Injector Drive Module
IMEP	Indicated Mean Effective Pressure
IMEPg	Gross Indicated Mean Effective Pressure
Log	Logarithm
LPG	Liquefied Petroleum Gas
MAP	Manifold Absolute Pressure
NMHC	Non Methane Hydrocarbons

NO_x	Oxides of Nitrogen
P	Pressure
PID	Proportional Integral Differential
PING	Pilot-Injected Natural Gas
PM	Particulate Matter
PWM	Pulse Width Modulation
R	Universal Gas Constant
RPM	Revolutions Per Minute
SCFM	Standard Cubic Feet Per Minute
SI	Spark-Ignited
SOI	Start Of Injection
TDC	Top Dead Center
THC	Total Hydrocarbons
V	Volume
VPM	Vehicle Personality Module
WVU	West Virginia University

1 Introduction & Objectives

1.1 Introduction

With increasing government restriction of tailpipe emissions from vehicles powered by internal combustion engines and a growing concern over the use of imported oil, alternative fuels have gained popularity. Natural gas has become a widely used alternative fuel for a variety of reasons including ready availability and its low emissions potential. Spark-ignited natural gas engines are common but suffer lowered efficiency due to pumping losses from intake throttling and therefore, cannot match the thermal efficiency of a diesel engine. Existing diesel engines may be converted readily to operate primarily on natural gas, using pilot injection of diesel to achieve ignition. However, many initial attempts to implement this technology were crude, leading to excessive diesel usage, over fueling to achieve acceptable power levels, and unacceptably high emissions. Pilot-injected natural gas (PING) engines show significant potential to rival diesel engines in their part and full load efficiency. While diesel engines have significant advantages over spark-ignited (SI) natural gas engines in terms of fuel efficiency, they cannot presently match the low emissions benefits of dedicated SI engines, particularly in their emissions of particulate matter (PM) and oxides of nitrogen (NO_x). This research is aimed at reducing the emissions from diesel engines through dual fuel conversion and the adoption of advanced engine control strategies, while maintaining diesel-like thermal efficiency and minimizing diesel fuel consumption.

1.2 Objectives

The overall objective of this project was to produce an engine control strategy to facilitate engine operation that was efficient, reduced exhaust emissions, and minimized diesel fuel usage. In order to fulfill this goal three steps were taken: First, complete control of all engine parameters had to be obtained to allow maximum flexibility in developing an engine control strategy. This required replacing the stock engine control unit with one that offered the advanced control needed. Since no such engine controller was commercially available, one was built. Secondly, a natural gas delivery system was designed and fitted to the engine. An attempt was made to keep the conversion as simple and inexpensive as possible in order to make this technology more appealing to industry. Low cost, off-the-shelf products were used wherever possible with minimal modification to the engine's stock configuration. Finally, the engine was comparison tested while operating in both diesel-only and dual fuel mode to verify completion of the overall objective.

2 Literature Review

Pilot-injected dual fuel engines are internal combustion engines designed or converted to run primarily on a gaseous air-fuel mixture. This homogeneous mixture is drawn into the cylinder on the intake stroke and deliberately ignited slightly before top dead center on the compression stroke by a small amount of diesel fuel injected into the cylinder. Because there is premixing of the primary fuel with air before it enters the cylinder, the combustion process in dual fuel engines is similar to SI engines. However, since dual fuel engines rely on the autoignition of the pilot diesel fuel, then they also have some of the properties of compression ignition engines [1][*].

Dual fuel engines can use nearly any type of gaseous fuel such as propane, compressed natural gas (CNG), low BTU wood gas, and hydrogen gas as well as liquefied petroleum gas (LPG). The use of these fuels is desirable because they provide a means to increase domestic energy use, have the potential to reduce emissions, and in some cases offer significant fuel cost savings [2, 3, 4, 5, 6]. A study found that dual fuel engine conversions cost less than $1000 per ton of NO_x eliminated, which is much less than the cost of some existing measures such as exotic alternative compression ignition fuels and catalyst exhaust after-treatment [1]. Of all the options available, CNG is the most widely used in dual fuel applications. This is mainly because, of the fuels listed above, only CNG offers a fuel cost savings that can justify the increased cost of operation and the initial cost of conversion [7]. Compressed natural gas is highly knock resistant with a research octane number of 120 to 130 which makes it ideal for use as the homogeneous charge fuel in high compression diesel engines [1]. In addition, many

[*] Numbers in brackets denote references listed at the end of the document.

years of proven use in reciprocating engines makes CNG the preferred choice for a dual fuel engine [8].

There are many advantages that dual fuel engines have over their dedicated diesel and spark-ignited counterparts. Most dual fuel engines can operate on gaseous fuel with diesel pilot or on diesel fuel alone. This makes dual fuel engines particularly attractive in vehicular applications where range is a concern because of a lack of CNG refueling facilities. Another advantage is that an existing diesel engine can be converted to dual fuel with relative ease as opposed to converting a diesel engine to spark-ignited CNG operation. The original cylinder head can be used and the compression ratio can be retained because of CNG's good antiknock characteristics.

Under certain operating conditions, dual fuel engines are capable of achieving thermal efficiencies equal to that of dedicated diesel engines and greater than that of spark-ignited engines. Two factors make dual fuel engine efficiency superior to spark-ignited. First, since dual fuel engines are almost never throttled, pumping losses are reduced to a minimum [1]. Second, when the pilot fuel is sprayed into the combustion chamber and autoignition occurs, many individual ignition sources are created, allowing for more complete and rapid combustion of the CNG-air mixture than with a single spark plug [9]. One efficiency problem with dual fuel engine conversions is the valve overlap in many diesel engines. In most diesel engines, the intake valves are opened before the exhaust valves have closed, allowing some of the intake air to escape out through the exhaust which promotes good exhaust scavenging [1]. This is perfectly acceptable in a diesel engine because the fuel does not enter the cylinder with the intake air, but in a dual fuel engine the intake stroke draws in a fuel-air mix and therefore, some fuel escapes out

the exhaust before it ever has a chance to be burned which compromises thermal efficiency. However, reducing the valve overlap requires a new camshaft profile which would greatly increase the cost of a dual fuel conversion.

The main advantage of dual fuel engines is reduced exhaust emissions, namely oxides of nitrogen (NO_x) and particulate matter (PM). However, these emissions reductions are only realized during moderate to high load operating conditions, leaving emissions reduction at light load an area for increased research [1].

Poor combustion at light load brings about losses in thermal efficiency as well as increased emissions. Dual fuel engines are seldom throttled which causes very lean fuel-air mixtures at light load. At these light load operating conditions the bulk of the energy released comes from the pilot fuel combustion and any gaseous fuel-air mixture that is entrained in the pilot zone at the time of ignition. The remaining gaseous fuel-air mixture is very lean which slows propagation of the flame front and makes combustion difficult, if not impossible. In order to ensure complete combustion of the gaseous fuel-air mixture, it then becomes necessary to increase the pilot quantity to a greater amount than would be required at high load conditions [10]. Methods have been investigated to improve dual fuel engine performance and emissions at light load. Gebert et al. [11] have tried several methods, including injection timing optimization, skip firing, and turbocharger air bypass. They found that advancing injection timing increased NO_x production, while retarding the injection timing resulted in reduced NO_x but increased hydrocarbon (HC), carbon monoxide (CO), and smoke emissions as well as reduced thermal efficiency. Skip firing requires the engine to run on a reduced number of cylinders at light load to bring the fuel-air ratio closer to stoichiometric in the cylinders

that are used. This was determined to be a very effective method to improve light load operation and even allowed idle operation with a 95% diesel substitution which would otherwise be impossible. An observed problem with skip firing was rough operation that caused visible shaking of the engine on the dynamometer. At some engine speed and load points it is desirable to redirect the turbocharger boost to decrease the mass of air filling the combustion chamber and therefore increase the equivalence ratio of the mixture. Turbocharger boost bypassing was tried and shown to reduce HC and CO emissions. Daisho et al. [3] used hot and cooled exhaust gas recirculation (EGR) to increase the fuel-air ratio and thus improve combustion at light loads. They found that hot EGR at light loads improved the thermal efficiency due to the charge temperature increase. Hot EGR also reduced NO_x and smoke formation. Cooled EGR gave slightly lower thermal efficiency but provided an even greater NO_x reduction than hot EGR. Along similar lines, Poonia et al. [6] found that intake air heating improved thermal efficiency at light load. Karim's [12] research of light load dual fuel operation produces some more suggestions for improving performance and emissions. He suggests fuel charge stratification to produce a slightly richer gaseous mixture in the areas surrounding the pilot zone. This would allow a greater percentage of the gaseous mixture to be burned before the lean limit is reached. The use of auxiliary fuels such as hydrogen or gasoline vapor to improve the combustion characteristics of the natural gas is recommended. This, however, adds great complexity to a dual fuel engine. Finally, reducing the engine operational speed is suggested to increase the time that the piston remains near top dead center and therefore increase the time for ignition and flame propagation through the lean fuel-air charge. It has been shown that ignition delay

increases as the fuel-air mixture becomes leaner and reduced engine speed would minimize the detrimental effects of this delay increase [13].

Dual fuel engine emissions and efficiency can also be improved by modifying the pilot fuel properties. Li et al. [14] found that in a diesel engine, nitrate and peroxide type cetane enhancing additives produced a reduction in CO at all load ranges and a NO_x reduction at low load. This information is pertinent to dual fuel operation because, during dual fuel operation at low load, the primary energy source is the pilot fuel. Another investigation of pilot fuel cetane number in dual fuel engines by Gunea et al. [15] also found that the use of pilot fuels with a higher cetane rating led to improved dual fuel engine performance and allowed lower pilot fuel quantities to be used.

Pilot fuel delivery systems for dual fuel engines have been another focus. With research being done to reduce pilot quantities, the limitation of emissions reduction becomes the ability to reduce the flow of the diesel injectors to the miniscule amounts that the new fueling parameters require. Most diesel fuel injection systems have a turn-down ratio of about 10, which means that the injector's minimum flow per injection can only be about 10% of the maximum flow per injection. For this reason BKM, Inc. has developed the Servojet electro-hydraulic, accumulator type unit fuel injection system that is capable of delivering down to 2 mm^3 per injection which represents 2% of the total energy required to run a 7.6 liter Navistar DT-466 at full load [16]. FEV Motortechnik GmbH & Company has developed a piezoelectric fuel injection system that allows precise time controlled fuel injection of very small amounts of diesel with minimal cycle-to-cycle variations [9].

Other research being done in the area of dual fuel engines is computer modeling of the dual fuel combustion process. Liu and Karim [17] developed a multi-zone thermodynamic dual fuel model that can be used to predict autoignition characteristics, the onset of knock, and exhaust emissions as well as the overall performance of a dual fuel engine at both high and low load. Catalyst development is also an area of research that can assist in the progress of dual fuel engines. Since an unthrottled dual fuel engine runs very lean at light load, there are large quantities of excess oxygen in the exhaust. This excess oxygen reduces the ability of a conventional catalyst to reduce the NO_x emissions. A new type of catalyst has been developed that stores NO_x during lean burn operation for reduction when the engine is running near stoichiometric. This type of technology may be applicable to a vehicular dual fuel engine that operates alternately at light load and full load [18]. A plasma-assisted catalyst is another method with which NO_x from a dual fuel engine operating at light load can be reduced. This catalyst uses plasma to oxidize NO into NO_2, which is then reacted with the hydrocarbons with another catalyst. By using the plasma to first oxidize the NO into NO_2, new more durable and more active catalysts can be used to reduce the remaining NO_2. Since this technology involves complex exhaust plumbing, it would be feasible only for stationary dual fuel engines [19].

3 Experimental Setup

3.1 Engine, Conversion & Instrumentation

3.1.1 Engine

A 1994 Navistar T444E diesel engine was selected for this project. It is a direct injected medium duty diesel engine that utilizes the Hydraulically-Actuated Electronically-Controlled Unit Injection (HEUI) fuel delivery system. This system is ideal for use in a dual fuel conversion because of its flexibility. Since this system is electronically actuated rather than mechanically, the rate of injection can be controlled independently of engine speed. The start of injection (SOI) and end of injection (EOI) can be controlled regardless of engine speed as well. Another advantage of this system is the ability to readily change the injection pressure by changing the hydraulic oil injection control pressure (ICP) which allows injection pressures between 3,000 and 21,000 psi at any engine speed, including idle.

Stock Engine Specifications:	
Type	Diesel, 4 stroke
Cooling System	Water cooled
Intake System	Turbocharged, intercooled
Fuel System	HEUI
Engine Control System	Ford EEC-IV electronic control unit
Cylinder Configuration	V8
Displacement	7.3 liter (444 c.i.)
Bore and Stroke	104.39 mm x 106.20 mm (4.11 in x 4.18 in)
Compression Ratio	17.5:1
Valve Train	2 valves/cylinder, pushrod
Firing Order	1-2-7-3-4-5-6-8
Rated Power	142 kW @ 2600 rpm (190 hp)
Peak Torque	650 N-m @ 1500 rpm (485 ft-lb)

Table 1: Engine Specifications for 1994 Navistar T444E model A190F

3.1.2 Natural Gas Delivery

One of the goals of this project was to develop a dual fuel conversion that was simple but effective. Intake manifold fumigation was the chosen method to deliver CNG to the engine because of simplicity. The CNG flow was controlled by a simple valve and entered the intake stream at a single point between the intercooler and the intake manifold. No costly gaseous fuel injectors or extensive intake manifold porting were required for this setup. IMPCO Technologies, Inc. is an established manufacturer of CNG delivery systems including regulators and CNG control valves. An IMPCO natural gas control valve (model number GMSZ30) and a low pressure regulator (PEV-1-7) were procured for this project. Both of these parts are used on the Chevrolet C/K Bi-Fuel pickup truck.

The IMPCO natural gas control valve is of the servo-actuated throttle plate type that operates at 1.5 kPa over the intake manifold pressure. It is equipped with a hot-wire flow meter with built in temperature correction. This valve makes it possible to set the desired CNG flow by simply supplying a 1000 Hz to 1600 Hz signal and read back the actual CNG flow by recording a 508 Hz to 2724 Hz signal. Calibration curves provided by IMPCO allowed conversion of the signal from frequency to CNG flow in grams per second.

The IMPCO low pressure regulator is a diaphragm-type, capable of reducing CNG pressures of as high as 1170 kPa down to 1.5 kPa, a range which is more than adequate for the 345 kPa house gas supply that was used. The regulator was referenced to the intake manifold pressure to maintain a constant 1.5 kPa pressure differential over the entire range of both vacuum and turbocharger boost.

These two components along with a solenoid-actuated shut-off valve and some rubber hose comprise the complete natural gas delivery system.

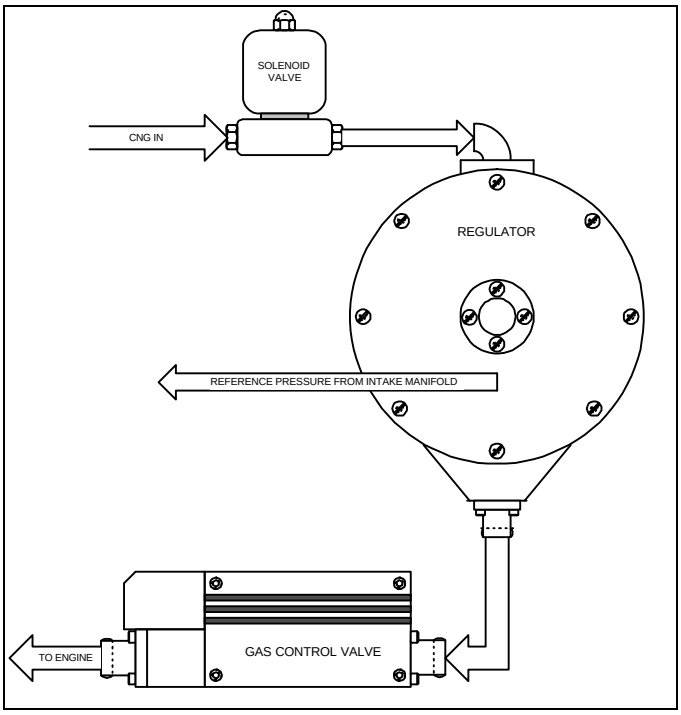

Figure 1: Schematic of the natural gas delivery system

3.1.3 Instrumentation

Upon review of the control requirements of this project, it was determined that in-cylinder pressure data would be necessary for understanding the dual fuel combustion process and for the development of a control scheme for the engine when running in dual fuel mode. A new cylinder head for the Navistar T444E was procured. The glow plug ports of two adjacent, centrally located cylinders were adapted to accept PCB Piezotronics, Inc. quartz piezoelectric in-cylinder pressure transducers. The modified cylinder head was then fitted to the engine.

Pressure Sensor Specifications	
Model	145A01
Type	Quartz piezoelectric
Dynamic Range	27,580 kPa (4,000 psi)
Maximum Static Pressure	34,475 kPa (5,000 psi)
Resolution	0.69 kPa (0.01 psi)
Sensitivity	0.131 pC/kPa (0.9 pC/psi)
Operating Temperature Range	-54°C to 350°C (-65°F to 660°F)
Maximum Flash Temperature	1650°C (3000°F)
Supporting Hardware	
In-line charge amplifier	PCB Model number 422E03
Charge to voltage converter	PCB Model number 483A

Table 2: Pressure measurement hardware specifications

The angular position of the crankshaft must be known precisely when taking pressure measurements so that the pressure in the cylinder can be related to the position of the piston or the instantaneous cylinder volume during the cycle. A Sumtak optical shaft encoder (model number LEI-037-1024) was purchased to perform this task. It provided 1024 pulses per revolution which allowed for very precise (360°/1024 or 0.3516° resolution) measurement of the crankshaft position.

Other engine run-time parameters were recorded to monitor the engine operating conditions. Wherever possible, the stock engine sensors were used for both engine control and for monitoring through the data acquisition system. The sensors were calibrated for conversion of the signals into engineering units. These parameters and the sensors that were used are listed in the following table.

Engine Sensors	
Engine Oil Pressure (EOP)	Navistar part # 1813658C2
Engine Oil Temperature (EOT)	Navistar part # 1814320C1
Engine Coolant Temperature (ECT)	Navistar part # 1814320C1
Manifold Absolute Pressure (MAP)	Navistar part # 1807330C1
Cam Position (CMP)	Navistar part # 1821720C97
Injection Control Pressure (ICP)	Navistar part # 1812818C2
Air Temperature Sensor (ATS)	Navistar part # 1814320C1
Exhaust Temperature (pre turbo)	Omega grounded K-type, part # KQSS-18G-12
Intake Temperature	Omega grounded K-type, part # KQSS-18G-12

Table 3: List of engine sensors with part numbers

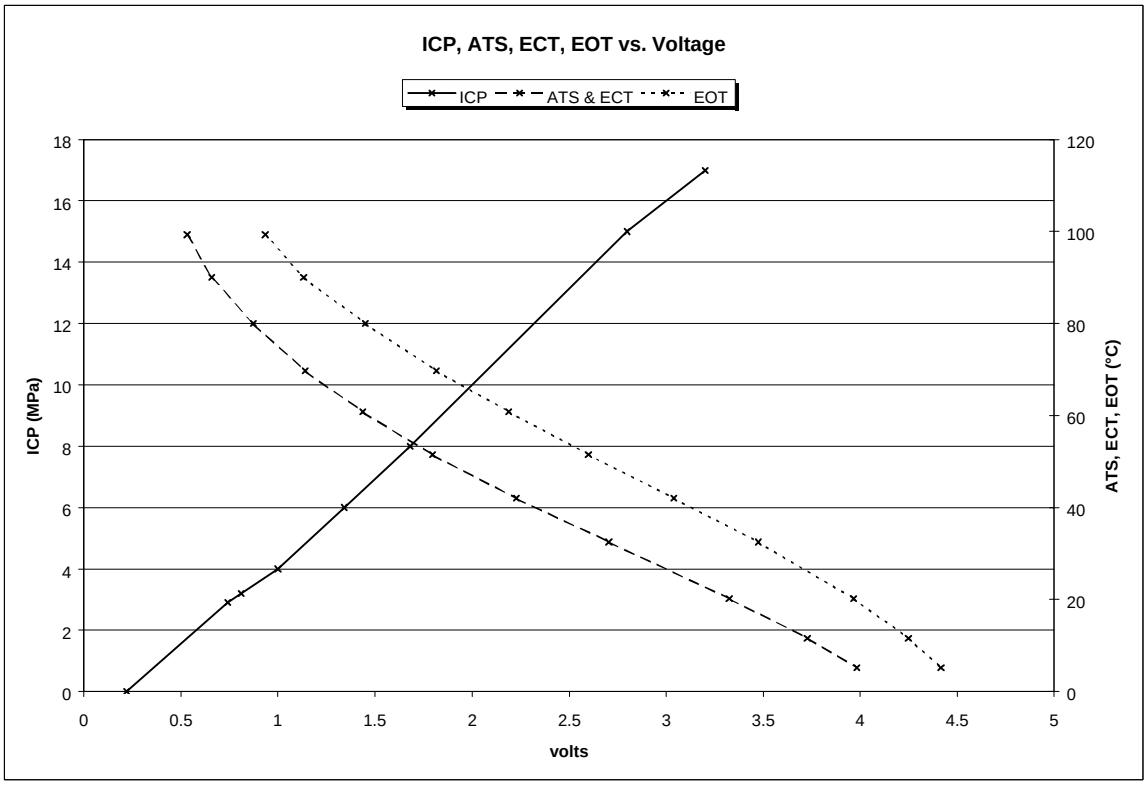

Figure 2: Calibration of Navistar temperature and pressure sensors

All of the signals from the engine including the in-cylinder pressure, crank position and various temperatures and pressure were monitored and stored using a computerized data acquisition system. A Gateway, Inc. 486 personal computer was equipped with a Cyber Research DAS-16 analog to digital data acquisition board for slow speed data acquisition of analog signals. The engine run-time parameters came from a

Ford-Rotunda EEC-IV breakout box (model number 007-00033) that allowed monitoring of the signals traveling between the engine and ECU without interrupting or affecting engine operation. Emissions, dynamometer, and dilution tunnel data were also collected with the DAS-16. Also installed in the data acquisition computer was a Keithley DAS-58 analog to digital acquisition board capable of storing up to 1 megasample ($1.048x10^6$ samples) of data for high speed data acquisition of the in-cylinder pressure and crank position, and a Cyber Research CTM-10 counter-timer board for time based signals.

Cyber Research DAS-16	Engine Coolant Temperature (ECT)
	Engine Oil Temperature (EOT)
	Accelerator Pedal Sensor (APS)
	Exhaust Temperature
	Intake Temperature
	Dynamometer Torque
	HC Analyzer
	NO_x Analyzer
	CO_2 Analyzer
	CO Analyzer
	Venturi Temperature
	Venturi Pressure
Cyber Research CTM-10	Manifold Absolute Pressure (MAP)
	Injection Control Pressure (ICP)
	Engine Speed
	CNG Flow
Keithley DAS-58	In-cylinder Pressure
	Crank Position (TDC Location)

Table 4: Data acquisition card assignments

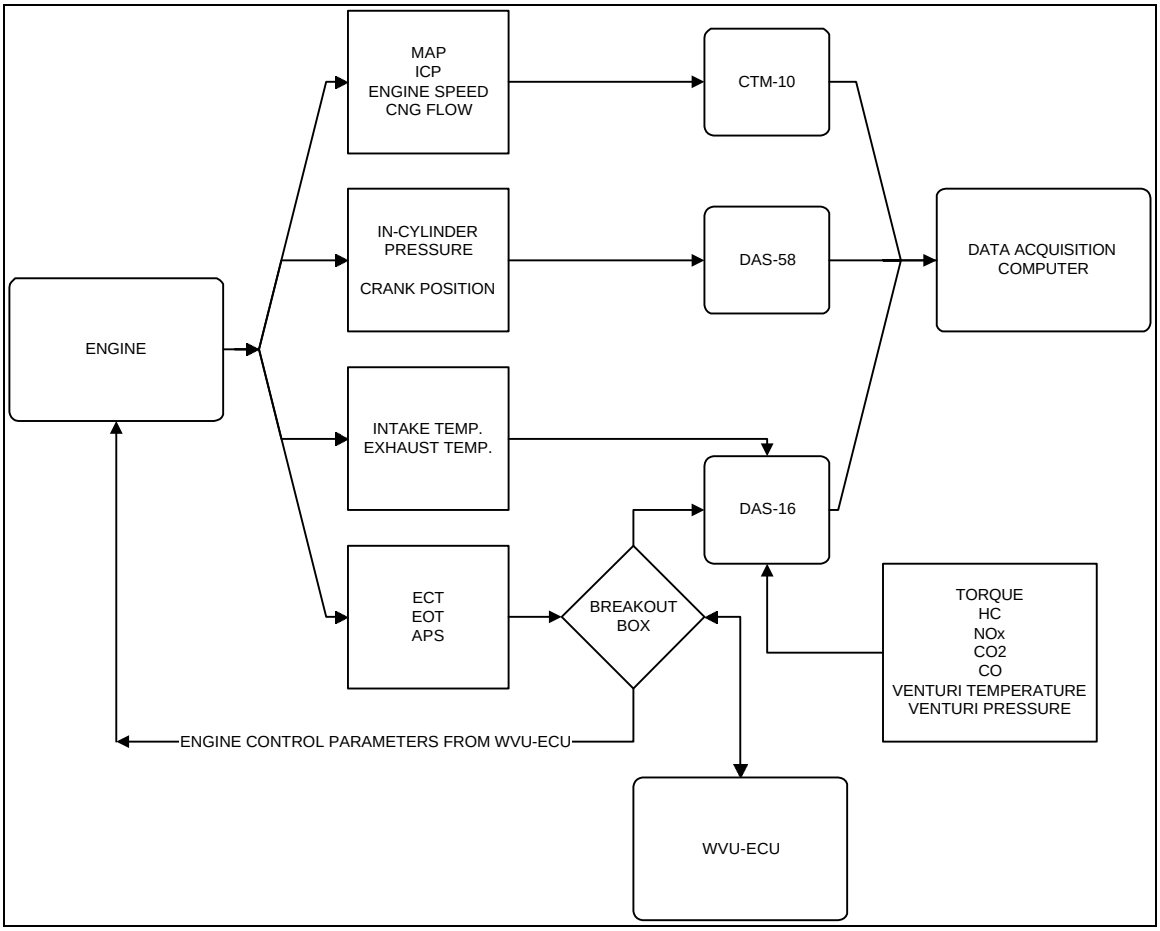

Figure 3: Block diagram of data acquisition setup

A data acquisition program (written by M. Traver, West Virginia University) displayed the signals on the screen in engineering units, compiled the individual signals into a data file, and saved this on the hard drive. Another program (also written by M. Traver and modified by the author) took the data files from each test and performed pressure smoothing and peak finding to extract pertinent information from the pressure traces. The slow speed data from the DAS-16 was also reduced into engineering units, and specific engine performance parameters such as thermal efficiency, indicated mean effective pressure (IMEP), and brake specific emissions were calculated.

3.1.4 Electronic Control Unit

A fully functional electronic control unit (ECU) was designed and built cooperatively by Richard J. Atkinson from West Virginia University, and the author. The ECU was designed to control diesel fuel injection pulse width (FIPW), injection advance (ADV) or start of injection, ICP, and CNG flow. The ECU uses two Microchip PIC-based microcontrollers; one to perform initialization of a Silicon Systems 67F687 engine interface peripheral and the other to perform the run-time algorithms. This ECU was developed by reverse engineering the stock Ford EEC-IV controller to determine the required signal protocol and then designing a system to mimic it.

The stock Ford EEC-IV engine control system consisted of three separate units: (1) the EEC-IV engine controller that contains the fueling, timing, injection pressure, and temperature compensation maps; (2) the injector drive module (IDM) that receives the desired fueling in the form of a digital pulsewidth modulated (PWM) signal and the desired injection advance in the form of a cylinder identification signal and fuel injection synchronization pulse; and (3) the vehicle personality module (VPM) which supplies the EEC-IV with information about the vehicle in which it is installed. The signal from the IDM to the fuel injectors was viewed on an oscilloscope and it was determined that this signal would be extremely difficult to reproduce because of its complexity. The fueling signals from the EEC-IV to the IDM, however, were simple square waves and could be easily mimicked and so the IDM was retained for use with the WVU-ECU. The VPM was ignored for this stage of the project.

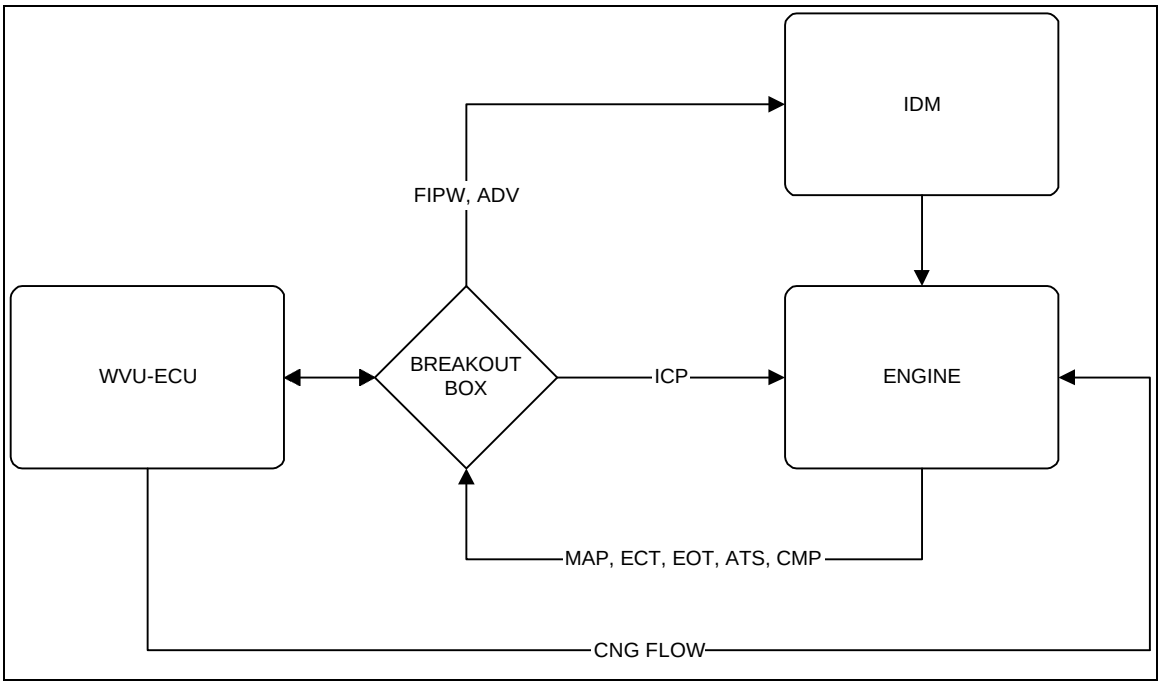

Figure 4: Experimental electronic control system setup

The WVU-ECU was designed to allow manual adjustment of engine control parameters with the engine running. This makes development of the control strategy simpler, since the ECU does not have to be taken off-line to upload new maps or change control algorithms. The ECU has four potentiometers that are used to set FIPW, ADV, ICP, and CNG flow manually. However, at the discretion of the user, any one of these parameters may be controlled automatically through the accelerator pedal sensor (APS) input. The dynamometer control computer uses a proportional-integral-differential (PID) feedback control algorithm that generates a throttle position (rack position on a diesel) signal to maintain a set engine torque. This signal is read by the WVU-ECU as the APS which is then used to vary the selected control parameter to maintain the desired torque. The DC dynamometer described in Section 3.2.2 is used to control the desired speed of the engine. The ECU operation has two stages: the first stage is initialization where the

Microchip PIC16C84 uploads initialization routines such as cam wheel configuration and PWM signal frequency settings to the Silicon Systems (SSi) 67F687 engine interface peripheral. The second stage is when the Parallax BASIC Stamp II microcontroller takes over control of the SSi67F687 and runs the engine based on the potentiometer settings. The primary function of the SSi67F687 is to act as a communications link between the engine and the microcontroller. It uses a tooth counting scheme - the Navistar T444E has an indexed wheel attached to the camshaft which the SSi67F687 uses to keep track of the exact position of the crank at all times and, in turn, updates the microcontroller. It also takes the diesel FIPW, ADV, ICP, and CNG flow values from the microcontroller and sends them to the appropriate devices as square waves or PWM signals. A Maxim MAX147 12-bit, 8 channel analog to digital converter (ADC) is used to read the analog voltage signals from sensors on the engine such as engine oil temperature (EOT), engine coolant temperature (ECT), intake air temperature (IAT), and accelerator pedal position (APS) and the potentiometer settings and transfer the values to the microcontroller in digital form.

This setup allows the operator to have precise, "on the fly", control of the engine operating parameters by adjusting the potentiometers on the ECU while viewing the exact settings as they appear on the data acquisition computer screen. The goal of this project is to use the ECU as a development tool to optimize engine operation. In the future, when optimized engine control algorithms or lookup tables are generated, this ECU is capable of bypassing the potentiometer inputs and running autonomously from the stored algorithms or tables.

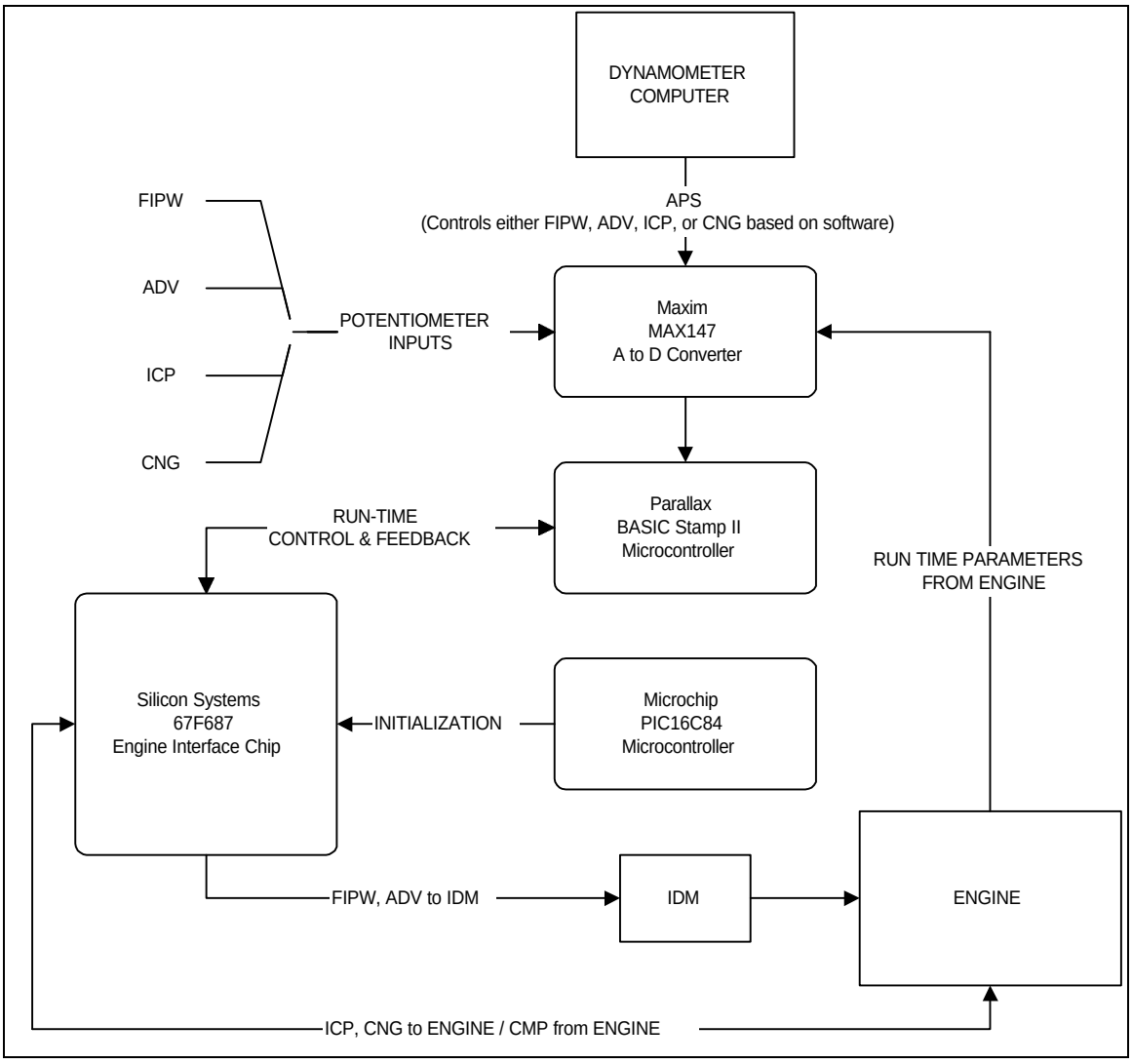

Figure 5: Simplified block diagram of WVU-ECU

3.2 Testing Facility & Equipment

The experiments for this project were completed at the West Virginia University Mechanical & Aerospace Engineering Department Engine & Emissions Research Center.

3.2.1 Analyzers & Dilution Tunnel

Analyzers to measure the concentration of HC, NO_x, CO, and CO_2 (carbon dioxide) in the diluted exhaust were used. The HC analyzer was a flame ionization detector (FID) (model number 402) manufactured by Rosemount Analytical, Inc.. Prior

to testing, the FID was "peaked" to determine the optimum flame air-fuel ratio for detector sensitivity. The NO_x analyzer (Rosemount model number 955) uses a chemiluminescent method of detection and was efficiency tested using a Rosemount NO_x efficiency tester. The CO (Rosemount model number 880A) and the CO_2 analyzer (Beckman Industrial model number 868) are both non-dispersive infrared analyzers. The exhaust samples were drawn from the dilution tunnel and transferred to the analyzers through heated probes and heated lines to prevent condensation of the water vapor and heavy hydrocarbons present in the exhaust gases.

The dilution tunnel was used to mix the exhaust gases with ambient air before sampling to simulate the mixing and reactions that take place when the exhaust leaves the tailpipe of a vehicle. The flow of air and exhaust into the tunnel was prescribed with a set of critical flow venturis. The pressure and temperature at the venturis were measured to calculate the mass flow rate through the tunnel. Prior to testing, the dilution tunnel was tested for leaks by propane injection with a Horiba propane injection kit. During a propane injection, a measured quantity of propane was injected into the tunnel and compared with the amount of propane detected by the hydrocarbon analyzer. The sample plane, where the gases are extracted from the dilution tunnel, is located 4.57 m from the tunnel opening.

To measure PM, 70 mm microfiber filters were conditioned at 21°C and 50% relative humidity for at least four hours and then weighed. The filters were then loaded with a continuous 4 scfm flow from the dilution tunnel during a test. After the test, the filters were again conditioned for four hours and weighed. The difference between the loaded and unloaded filter weights was used to calculate the engine's PM production.

Sample bags were filled with dilute exhaust from the dilution tunnel for further speciation analysis in a Varian model 3600 gas chromatograph (GC). Gas chromatography is useful for determining the concentration of methane (MHC) and non-methane hydrocarbons (NMHC) in a particular sample as well as complete component identification. The GC draws a 250 microliter sample into a holding area called the loop where it is conditioned to 35°C. From there it is injected into a J&W Scientific Co. column that is conditioned at 35°C for 2.5 minutes and then raised to 200°C at a rate of 20°C per minute to slowly drive the gasses out of the column. The gas exiting the column is analyzed using a flame ionization detector (FID). The sample analysis is then compared to a 300 part per million (ppm) methane standard calibration gas to determine the methane concentration in the sample.

3.2.2 Dynamometer

The engine was loaded with a transient-capable General Electric DC dynamometer. The dynamometer was controlled with a rack-mounted computer to maintain user specified speeds at all times. Software on the computer was designed to allow the user to input operational set points of engine speed and load. The dynamometer maintained the set speed throughout the test and the software attempted to maintain the specified torque by varying the throttle or rack position (APS value) with a proportional-integral-differential (PID) control algorithm.

3.3 Experimental Approach

In order to determine the benefits of a dual fuel conversion of a production diesel engine, it was necessary to conduct emissions tests. The engine was tested while

operating on diesel fuel in original condition to compare with the dual fuel emissions collected later. The information gathered from the diesel tests would also be used to find general engine parameter starting points for the dual fuel experimentation to be carried out later. The Navistar T444E was tested at two steady state set points with a speed and load of 1500 rpm, 335 N-m and 1500 rpm, 580 N-m. These points were selected because they represented the intermediate speed of the engine at half and near-full load and would most likely represent the operating conditions of the engine while cruising. Exhaust concentrations of HC, NO_x, CO_2, CO and PM filter weights were recorded. Engine operation parameters such as FIPW, ADV, and ICP were also recorded. In-cylinder pressure data was taken to calculate heat release rate (HRR), gross indicated mean effective pressure (IMEPg), and ignition delay. Each four minute set-point was repeated three times.

Once the engine was tested in original condition, the WVU-ECU was fitted to the wiring harness and the engine was tested once again on diesel fuel only. Sweeps of FIPW and ADV at a speed of 1500 rpm were done to characterize the fuel injectors and to determine the emissions effects. PM data was not collected for these tests because the number of filters required to measure PM at each sweep point would have been prohibitively large. The torque curves generated from the FIPW sweeps were used to determine the minimum FIPW for the injectors.

Dual fuel sweeps of diesel FIPW and ADV were carried out with CNG flow controlled with the APS signal to maintain the set torque. The ICP sweeps were executed with FIPW controlled by the APS. For each set of sweeps, the minimum emissions points (with emphasis on NO_x) were found and those values were used for the next set of

sweeps. Through this method, optimum values for diesel FIPW, ADV, ICP, and CNG flow were determined for 1500 rpm, 335 N-m and 1500 rpm, 580 N-m.

Finally, the dual fuel steady state tests were run at 1500 rpm, 335 N-m and 1500 rpm, 580 N-m to compare the emissions (including PM), efficiency, diesel fuel usage, and in-cylinder pressure data with the stock, diesel-only tests conducted earlier. These tests were conducted in exactly the same manner as the tests with the engine in stock configuration to maximize the validity of the comparison.

Diesel Tests	
EEC-IV Baseline	1500 rpm; 335 N-m & 580 N-m
FIPW Sweep	ADV: 6.5° BTDC; ICP: 10.5 MPa
ADV Sweep	FIPW: 900 μs & 2380 μs; ICP 10.5 MPa
Dual Fuel Tests	
FIPW Sweep	ADV & ICP constant; APS controlled CNG
ADV Sweep	Optimum FIPW; ICP constant; APS controlled CNG
ICP Sweep	Optimum ADV; CNG constant; APS controlled FIPW
Dual Fuel Steady State Tests	1500 rpm; 335 N-m & 580 N-m

Table 5: Diesel and dual fuel test table

3.3.1 Analysis of In-Cylinder Pressure Data

Before testing began, proper phasing (location relative to TDC) of the index pulse from the Sumtak had to be verified. The index pulse must be located at exactly TDC or erroneous values derived from pressure data will be generated. Verification is done by evaluating a logarithmic P-V diagram for certain telltale signs of improper phasing. According to Lancaster et al. [20], to ensure proper phasing the compression line on the logarithmic P-V diagram must be without curvature. There also must be no crossover of the compression and expansion lines on the diagram. It can be seen in Figure 7 that neither of these indicators is present. The compression line is straight and there is no crossover of the compression and expansion lines.

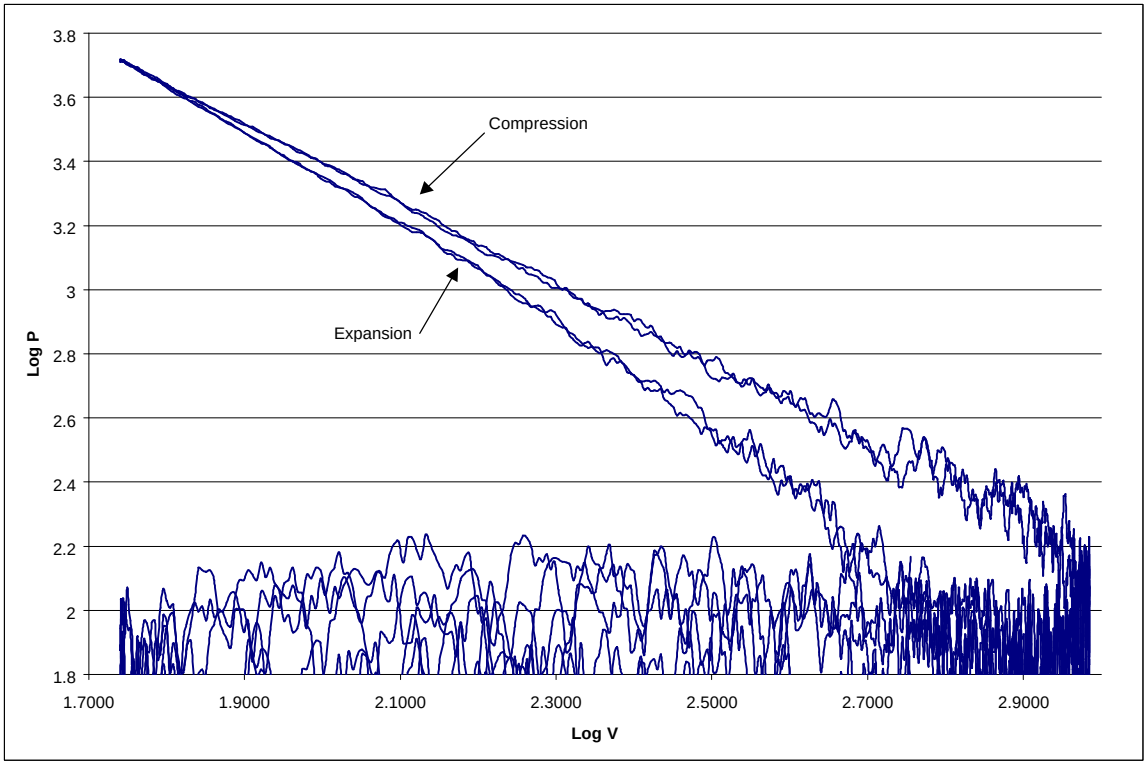

Figure 6: Log P vs Log V diagram for 2 consecutive motoring cycles to verify proper phasing

In-cylinder pressure data versus crank angle can offer valuable insight into the combustion process taking place in the cylinder. Heat release rate (HRR) is an important calculated parameter because from it, many other values such as ignition delay, premixed combustion phase and diffusion combustion phase are derived. It can be seen from Figure 7 that there is significant data scatter during the diffusion combustion phase. This is likely due to the physical characteristics of the pressure transducers. Pressure transducers that operate on the piezoelectric phenomenon can only measure dynamic pressures. Near-static pressures over an extended period of time will produce excessive drift and erratic readings.

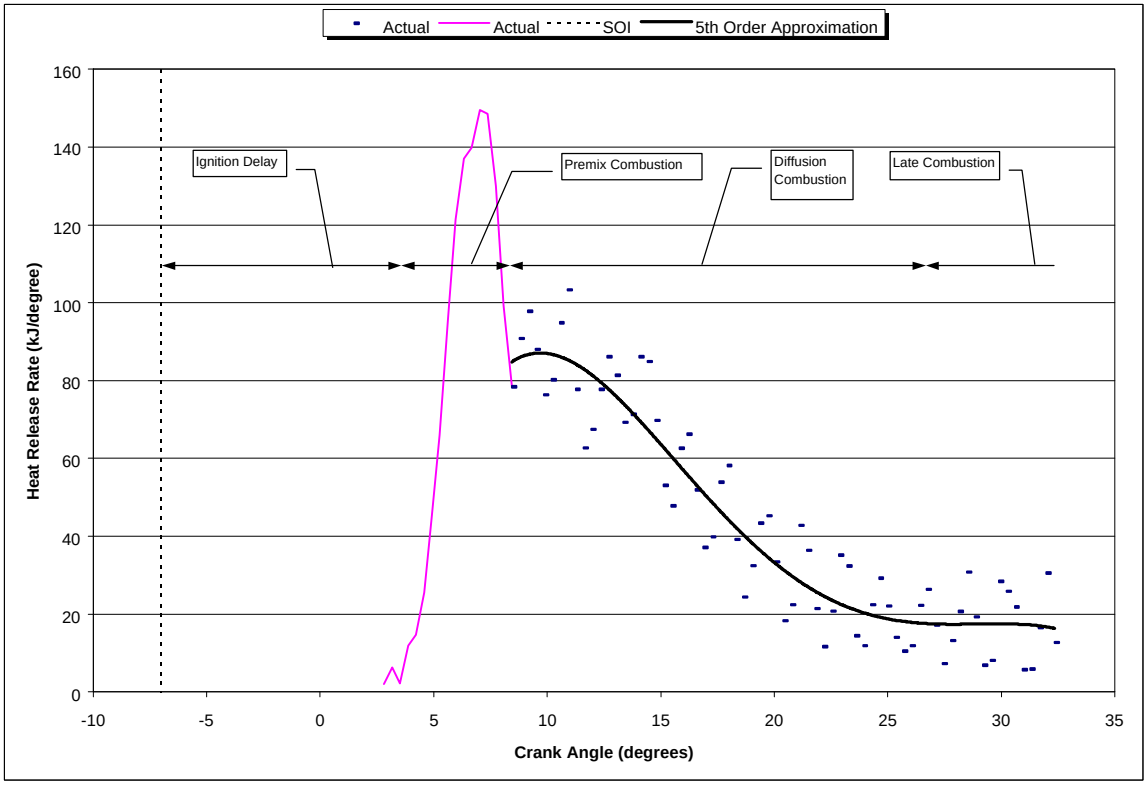

Figure 7: Example diesel-only heat release rate diagram with combustion stages labeled (1500 rpm; 335 N-m)

The following derivation of the HRR equation is adapted from Heywood [21]: In a direct injected diesel engine, the combustion chamber is a single open system in which the only flow across the boundary when the valves are closed is the fuel (neglecting crevice flow or blow-by). The first law equation for this system is:

$$\frac{dQ}{dt} - p\frac{dV}{dt} + \dot{m}_f h_f = \frac{dU}{dt} \tag{1}$$

Now, if the net heat release rate is assumed to be the difference between the heat released due to combustion (positive) and the heat transfer out of the system (negative) the equation becomes:

$$\frac{dQ_n}{dt} = \frac{dQ_{ch}}{dt} - \frac{dQ_{ht}}{dt} = p\frac{dV}{dt} + \frac{dU_s}{dt} \tag{2}$$

If the cylinder contents are assumed to be an ideal gas the equation becomes:

$$\frac{dQ_n}{dt} = p\frac{dV}{dt} + mc_v\frac{dT}{dt} \tag{3}$$

Then, from the ideal gas law with constant R:

$$\frac{dp}{p} + \frac{dV}{V} = \frac{dT}{T} \tag{4}$$

Using the above equation to remove T, net heat release rate is:

$$\frac{dQ_n}{dt} = \frac{g}{g-1}p\frac{dV}{dt} + \frac{1}{g-1}V\frac{dp}{dt} \tag{5}$$

Where $\gamma = c_p/c_v$ (ratio of specific heats, 1.35 was used for both the diesel and dual fuel analysis)

The indicated mean effective pressure (IMEP) is a useful measure of an engine's ability to do work with respect to engine size. The gross mean effective pressure (IMEPg) is the IMEP with the pumping and frictional losses omitted. The pressure data are related to an incremental change in the cylinder volume and numerical integration is applied from the beginning of the compression stroke (180° BTDC) to the end of the power stroke (180° ATDC). The IMEPg is computed by dividing the numerically integrated sum by the displacement of one cylinder. Finding the cycle-to-cycle coefficient of variation (COV) of the IMEPg is useful for providing an indication of the relative combustion stability or "smoothness" of the engine. The COV(IMEPg) is the standard deviation in IMEPg divided by the mean IMEPg and is usually expressed as a percentage [21]:

$$COV(IMEPg) = \frac{s_{IMEPg}}{IMEPg} \times 100 \tag{6}$$

The COV(IMEPg) is used to as a standard indication of the cycle-to-cycle variations of the combustion in the engine and is generally considered to have an upper limit of 10% before the engine becomes undriveable [22].

Although not derived from the in-cylinder pressure data, thermal efficiency which is also known as fuel conversion efficiency, is an important indicator of engine performance. This is defined as the ratio of the work produced by the engine and the amount of fuel energy supplied to the engine [21].

$$h = \frac{W}{m_f Q_{LHV}} \tag{7}$$

Where W = work, m_f = mass of fuel, and Q_{LHV} = lower heating value of the fuel. If the brake specific fuel consumption (BSFC) is used then equation 7 becomes:

$$h = \frac{1}{BSFC \cdot Q_{LHV}} \tag{8}$$

For diesel-only operation the Q_{LHV} was 43.2 MJ/kg, for dual fuel operation the Q_{LHV} was a composite value based on the diesel/natural gas mass ratio and the respective Q_{LHV} of each fuel (43.2 MJ/kg for diesel, 50 MJ/kg for CNG) [21].

4 Data, Results & Discussion

4.1 Diesel Operation

4.1.1 Diesel Steady State Test Data Using EEC-IV

The emissions results of the two steady state set points (1500 rpm, 335 N-m and 1500 rpm, 580 N-m) were collected and converted to brake specific values. Exhaust concentrations of THC, NO_x, CO_2, CO, and PM were recorded. Table 6 shows the averaged results of these tests.

	PM (g/kWh)	THC (g/kWh)	NMHC (g/kWh)	CO (g/kWh)	CO_2 (g/kWh)	NO_x (g/kWh)
335 N-m	0.076	0.087	0.087	0.533	764.7	8.92
580 N-m	0.213	0.026	0.026	4.610	746.6	7.78

Table 6: Averaged diesel emissions with EEC-IV (335 N-m & 580 N-m at 1500 rpm)

Dilution bags for each test were taken and analyzed using gas chromatography to determine the concentration of non-methane hydrocarbons and methane in the exhaust. Only trace amounts of methane were detected in the samples so it was determined that the exhaust contained predominantly non-methane hydrocarbons. It should also be noted that the brake specific HC production is very low. This is characteristic of direct injection (DI) diesel engines which typically have very complete fuel combustion.

In-cylinder pressure data were recorded for each mode and analyzed to characterize the engine. The IMEPg, ignition delay, and HRR were calculated from the in-cylinder pressure. A P-V diagram for each mode was also generated. From table 7 it can be seen that the diesel combustion process is very stable with the highest COV(IMEPg) of less than 3%. The ignition delay is defined as the difference between the start of injection and the location of the first positive value of IMEPg on the

compression stroke. The switch of HRR from negative to positive during the compression stroke indicates that combustion of the fuel has initiated and is sufficient to overcome the heat loss due to compression alone. Table 7 shows the average COV(IMEPg) and ignition delay for each mode.

	COV(IMEPg) %	Ign. Delay °After SOI
335 N-m	2.19	10.37
580 N-m	1.44	9.33

Table 7: COV(IMEPg) & ignition delay for diesel with EEC-IV

The in-cylinder pressure data were averaged over 128 engine cycles to smooth out any noise and cycle-to-cycle variations which provided a good representation of the cylinder pressure over time. The heat release rates were calculated from these averaged in-cylinder pressure traces. PdV/dq was also calculated and plotted versus crank angle to show the net energy release during the compression and expansion strokes.

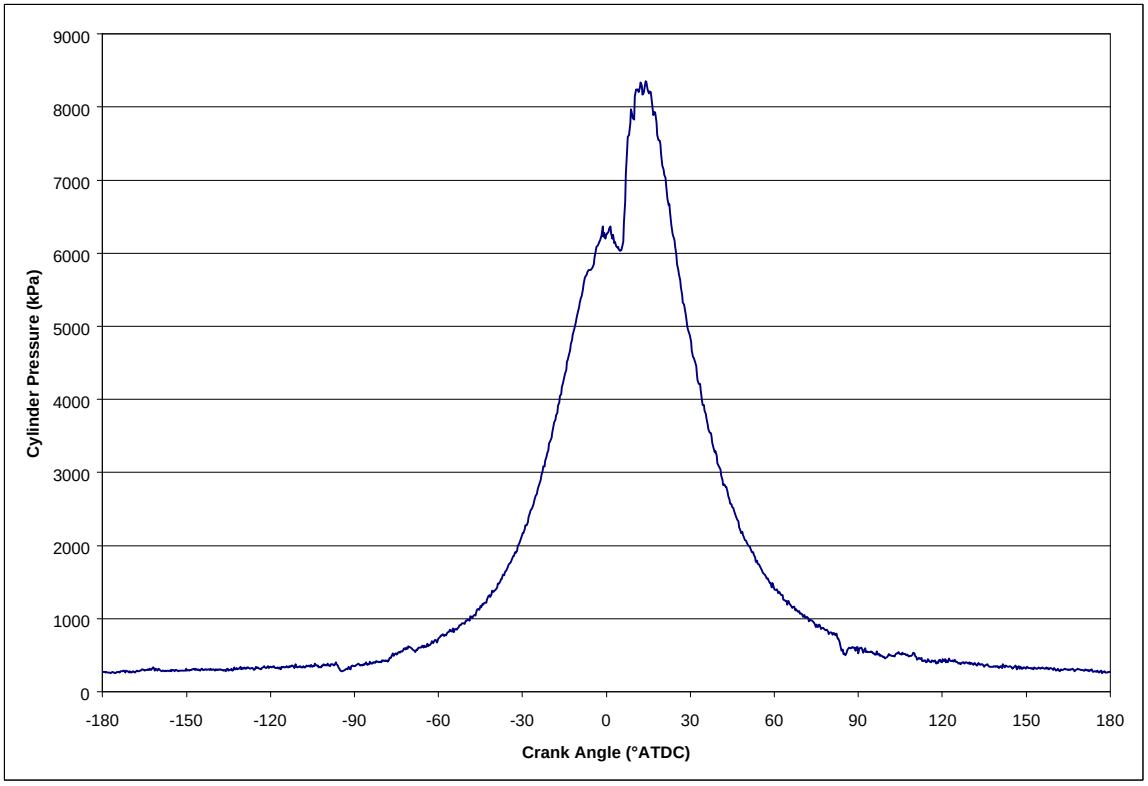

Figure 8: In-cylinder pressure vs. CA for diesel EEC-IV (1500 rpm; 335 N-m)

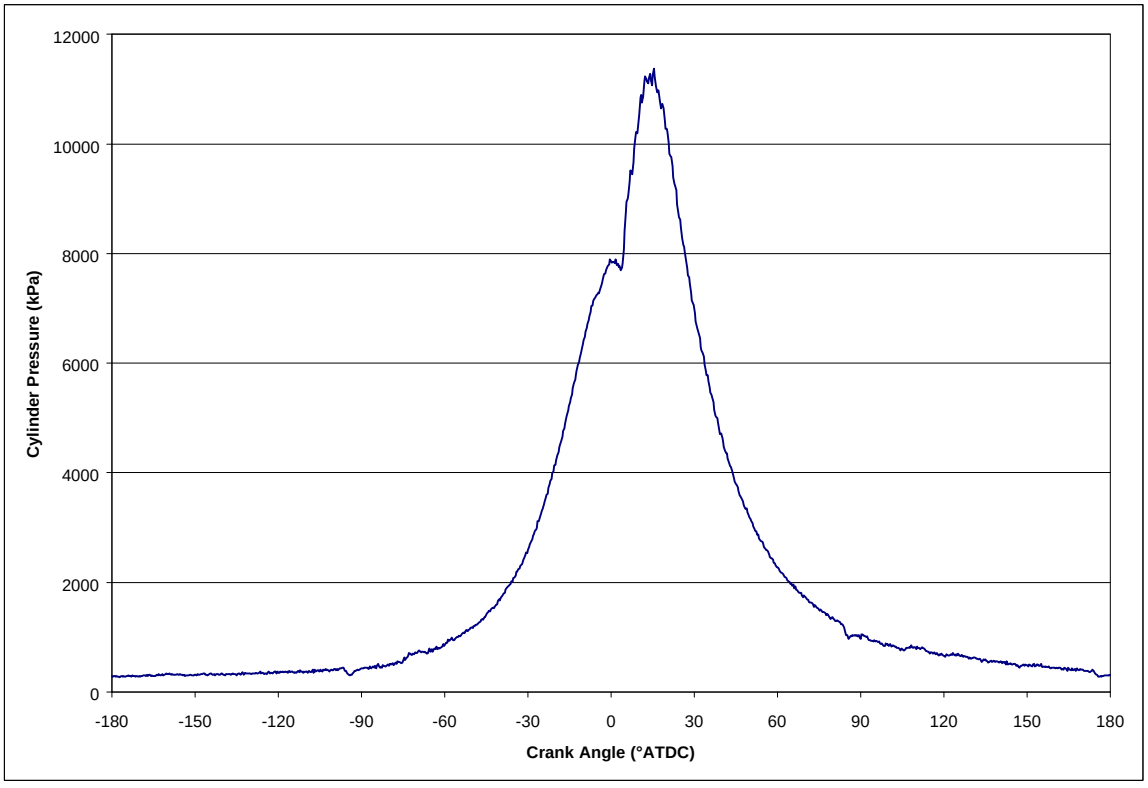

Figure 9: In-cylinder pressure vs. CA for diesel EEC-IV (1500 rpm; 580 N-m)

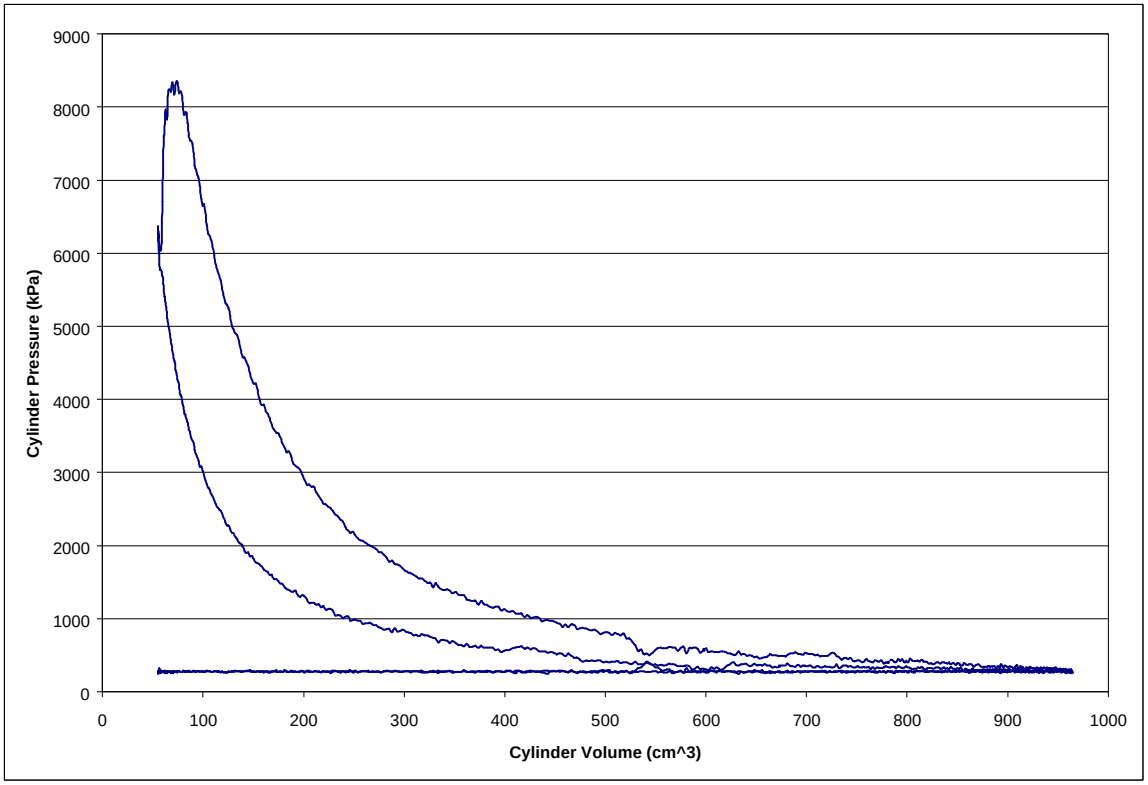

Figure 10: P-V diagram for diesel EEC-IV (1500 rpm; 335 N-m)

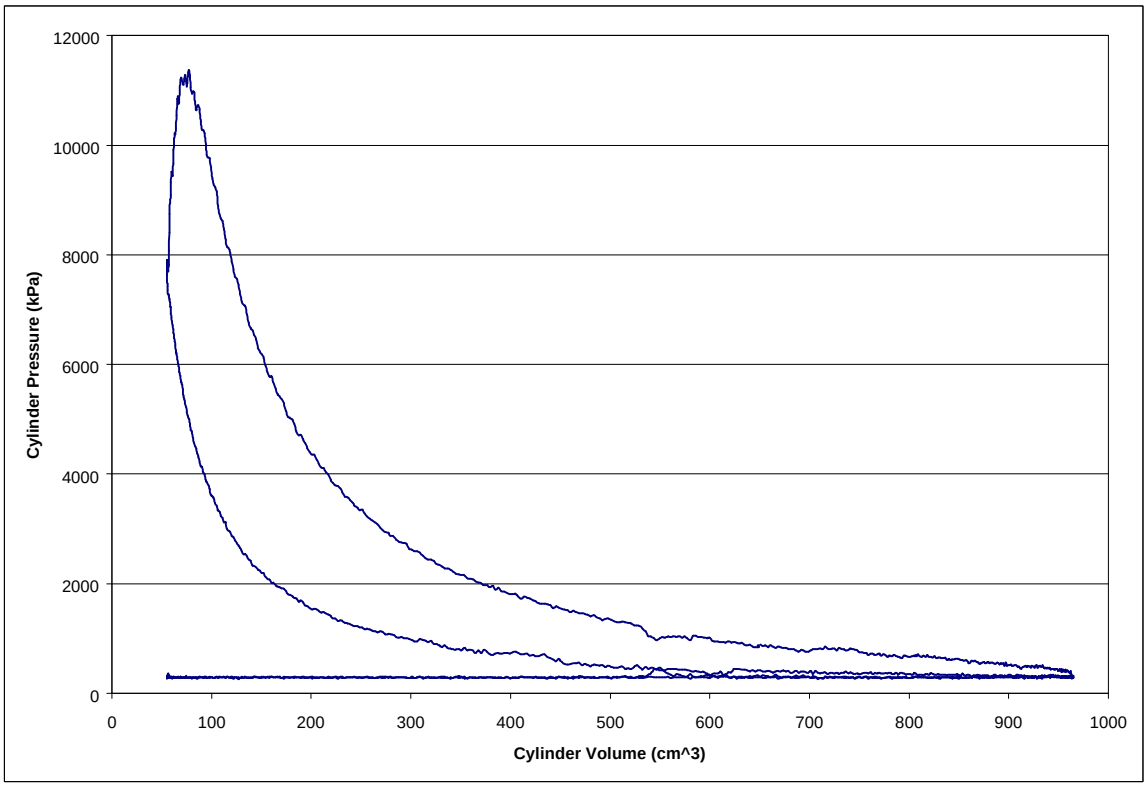

Figure 11: P-V diagram for diesel EEC-IV (1500 rpm; 580 N-m)

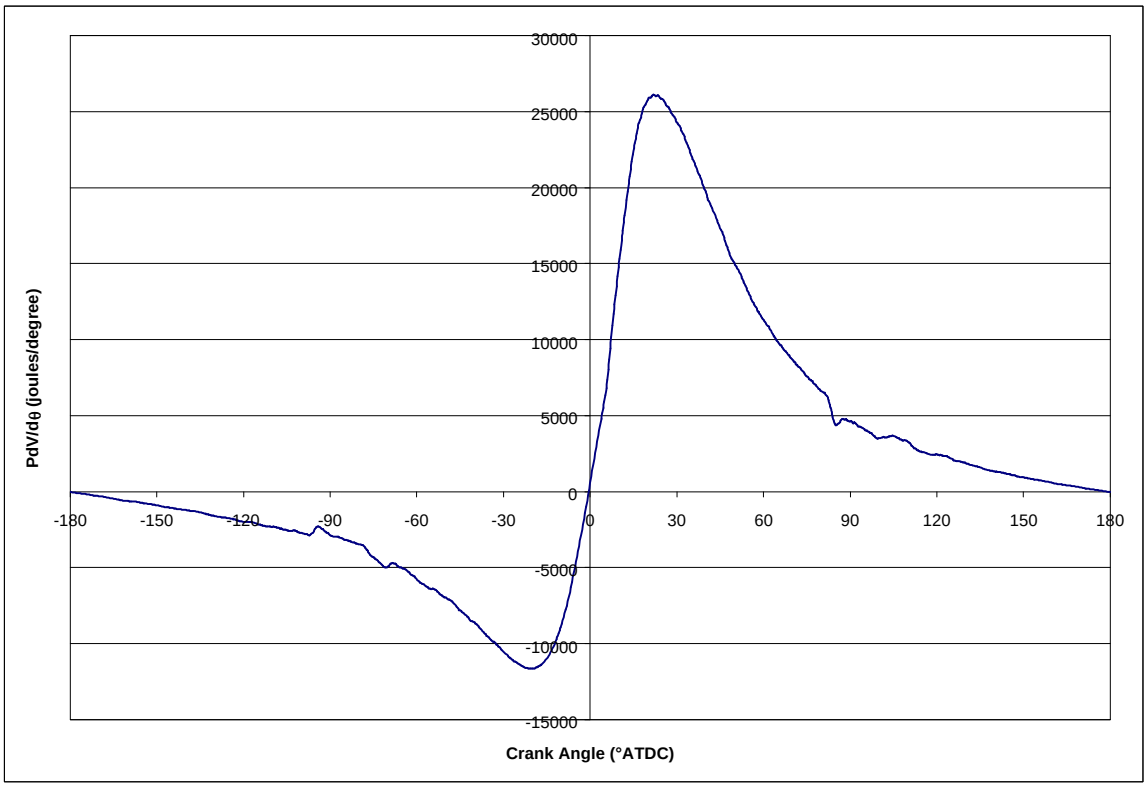

Figure 12: PdV/dθ vs. CA for diesel EEC-IV (1500 rpm; 335 N-m)

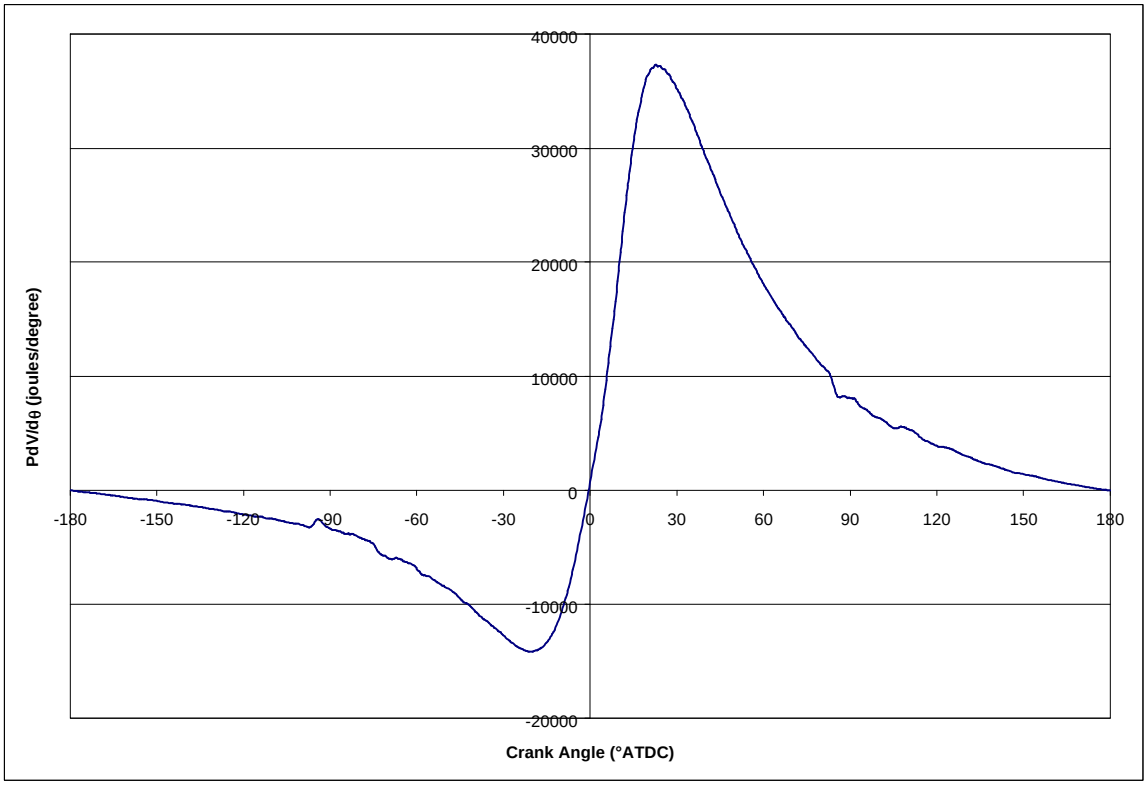

Figure 13: PdV/dθ vs. CA for diesel EEC-IV (1500 rpm; 580 N-m)

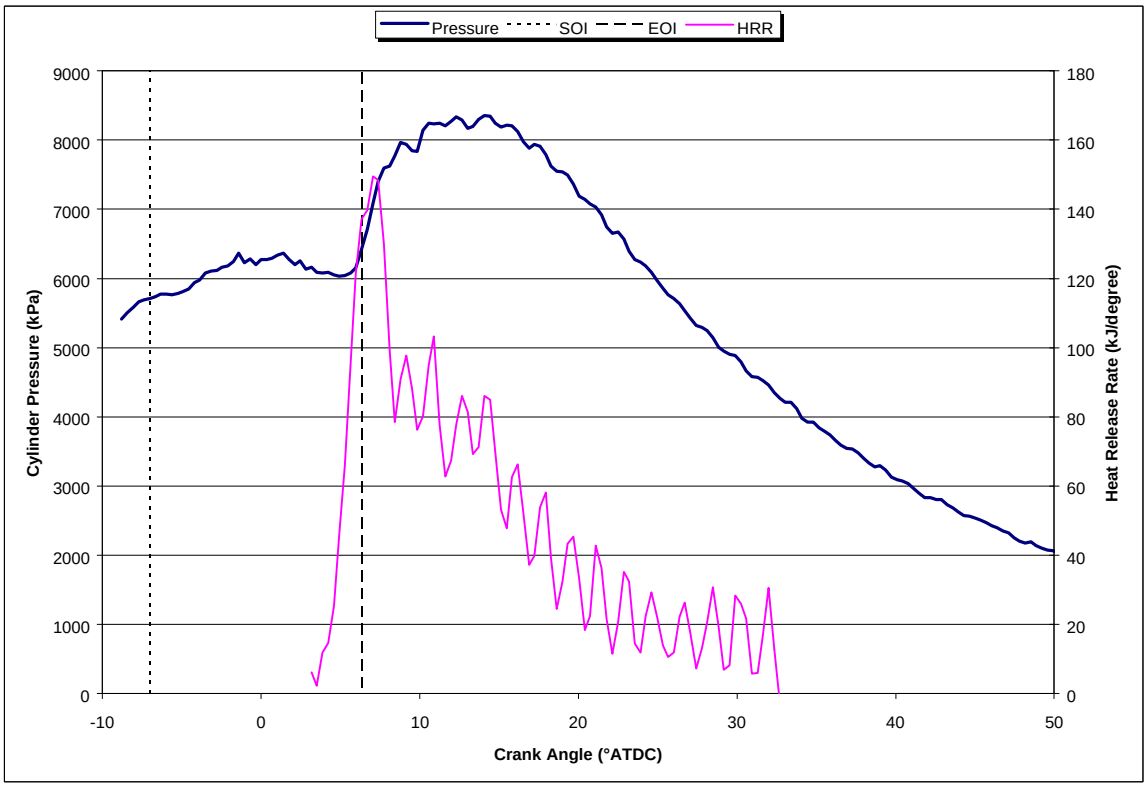

Figure 14: HRR & in-cylinder pressure for diesel EEC-IV (1500 rpm; 335 N-m)

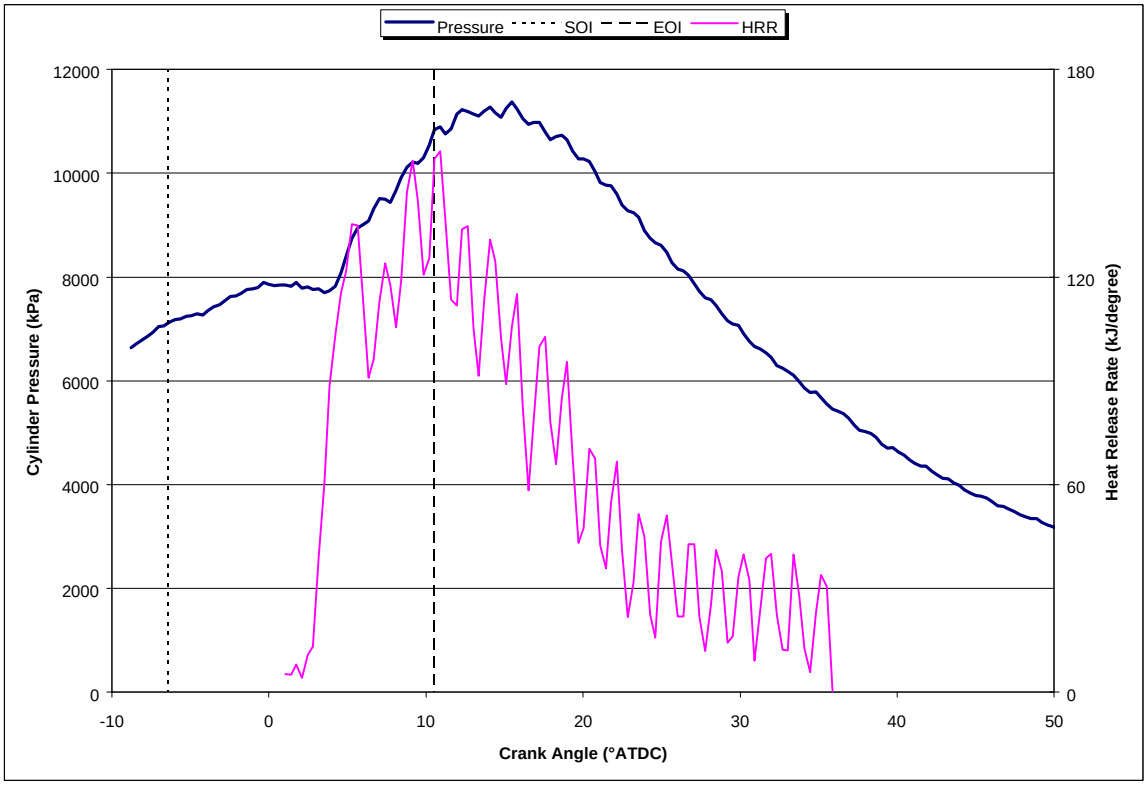

Figure 15: HRR & in-cylinder pressure for diesel EEC-IV (1500 rpm; 580 N-m)

4.1.2 Diesel Sweep Data Using WVU-ECU

It was necessary to characterize the engine running on diesel fuel using the WVU-ECU. Sweeps of FIPW over the entire range of operation were performed to determine what engine torque and emissions were produced. It was found from the FIPW sweep that there were some peculiar injector characteristics with which to contend. It can be seen from Figure 16 that FIPW between 650 μs and 900 μs causes the engine torque to drop off significantly and the engine produces no torque at about 800 μs. From the visible drop in exhaust emissions in Figure 17 it is evident that the injectors were not delivering the expected fuel between 650 μs and 900 μs. From this information, it was decided that the injectors were operating outside of their designed range below 900 μs and that all future tests would be carried out above this FIPW to take advantage of the near linear characteristics of the injectors in this range. No tests were carried out with FIPW below 900 μs.

The effects of ADV and FIPW were also explored. ADV was increased from 0° BTDC to 17° BTDC in one degree increments and the thermal efficiency was calculated at each point. Figure 21 shows that ADV had little effect on the thermal efficiency, which increased from 34% to 35% at high load (2373 μs FIPW) and remained relatively constant at about 16% at low load (900 μs FIPW).

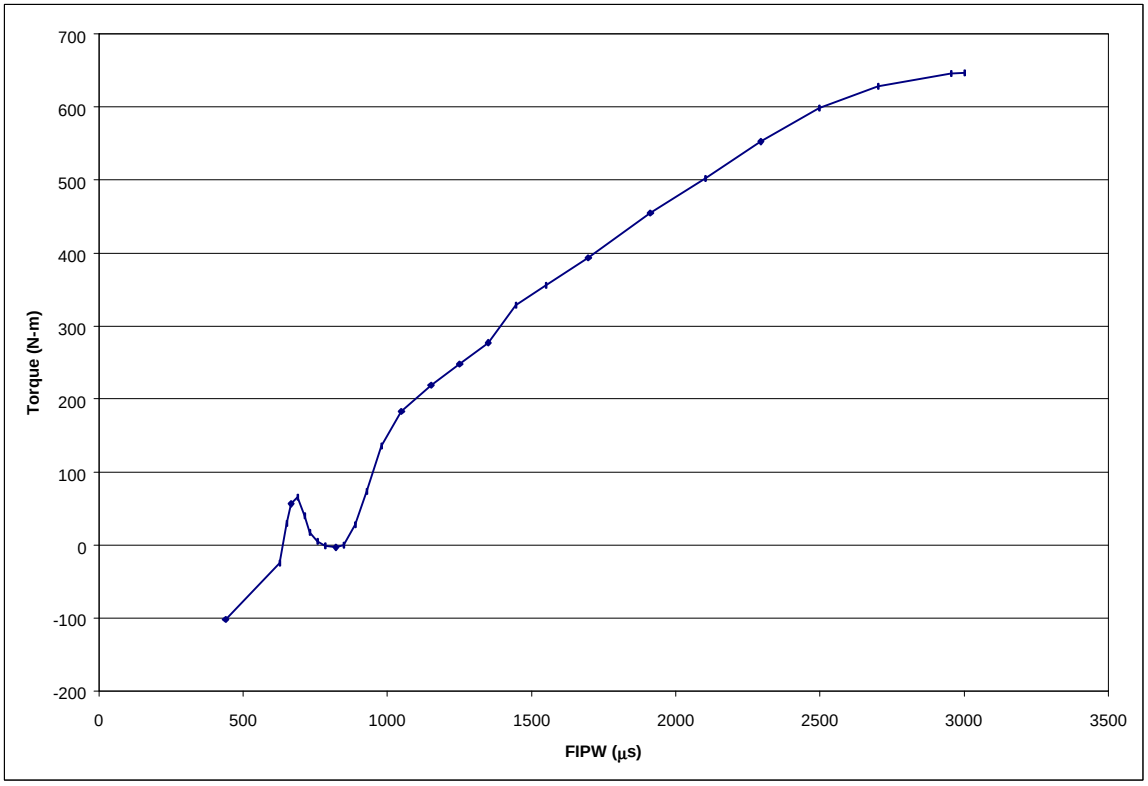

Figure 16: Torque vs. FIPW for diesel WVU-ECU (1500 rpm; 6.5° ADV; 10-10.5 MPa ICP)

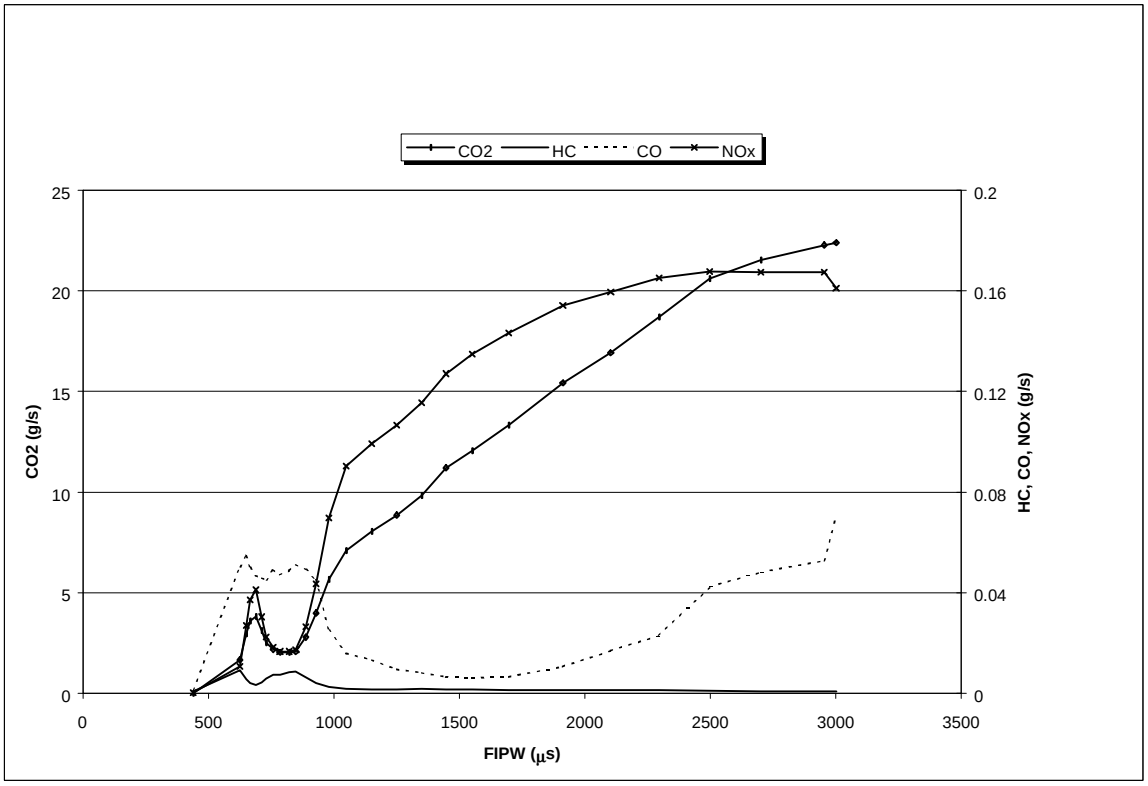

Figure 17: Emissions vs. FIPW for diesel WVU-ECU (1500 rpm; 6.5° ADV; 10-10.5 MPa ICP)

It can be seen from Figure 18 that the thermal efficiency is affected by the amount of fuel injected (which is a direct function of the FIPW). As the FIPW is increased from 900 μs to 3000 μs the efficiency rapidly increases from 15% to a maximum of 34% at 1500 μs. The low efficiency at small FIPW is likely caused by the engine running at near no-load conditions. At low loads, the frictional losses account for a higher percentage of the total fuel energy available which lowers thermal efficiency. This means that the engine was using most of the fuel energy it consumed to overcome the internal losses and produced very little net power, therefore causing lower thermal efficiency.

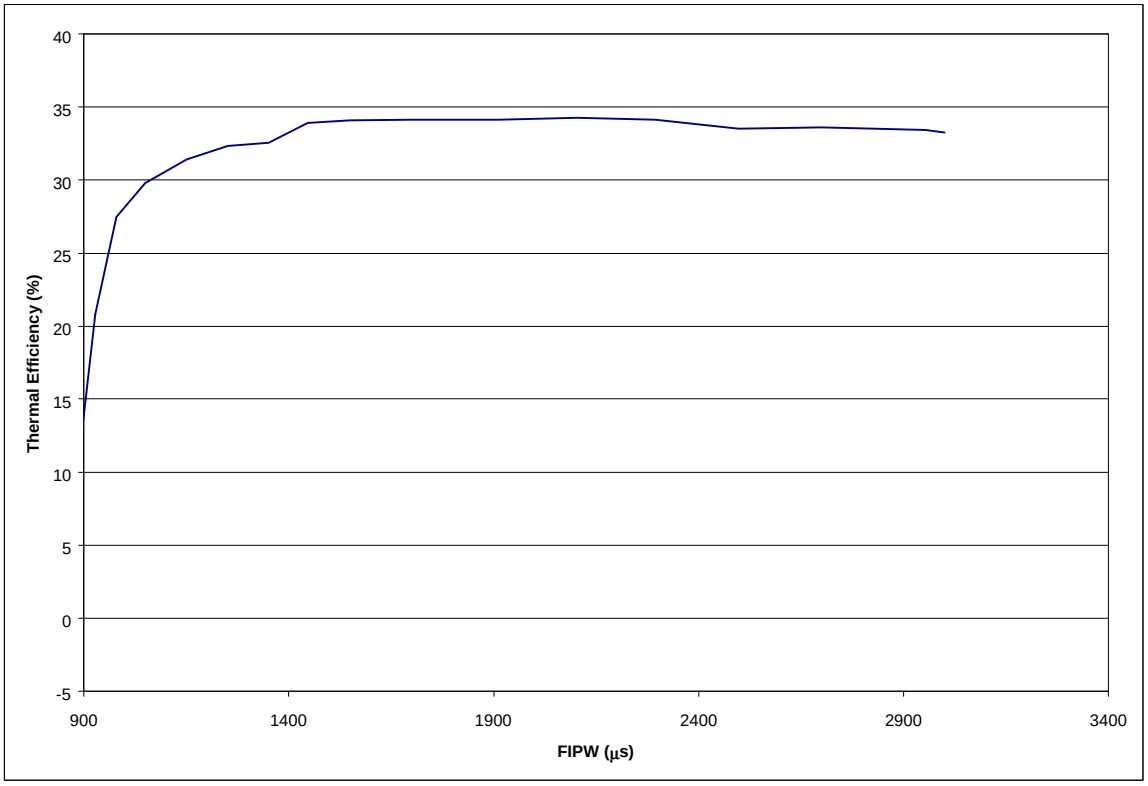

Figure 18: Thermal efficiency vs. FIPW for diesel WVU-ECU (1500 rpm; 6.5° ADV; 10-10.5 MPa ICP)

Exhaust emissions are also affected by injection advance. Once again ADV was swept from 0° BTDC to 17° BTDC and emissions data were recorded. For light load (FIPW: 900 μs) all exhaust emissions except for NO_x underwent a sudden decrease as

advance went from 0° BTDC to 6° BTDC and then leveled off. NO_x, however, steadily increased across the entire range. At high load (FIPW: 2373 μs) ADV was swept from 3° BTDC to 17° BTDC. HC emissions remained very low throughout, CO_2 decreased, and CO and NO_x both increased. The increase in NO_x production as ADV increased is caused by a shift in the location of peak pressure. The closer to TDC the peak pressure occurs, the higher the overall in-cylinder pressure, and therefore also temperature. The high temperatures cause the increased NO_x production.

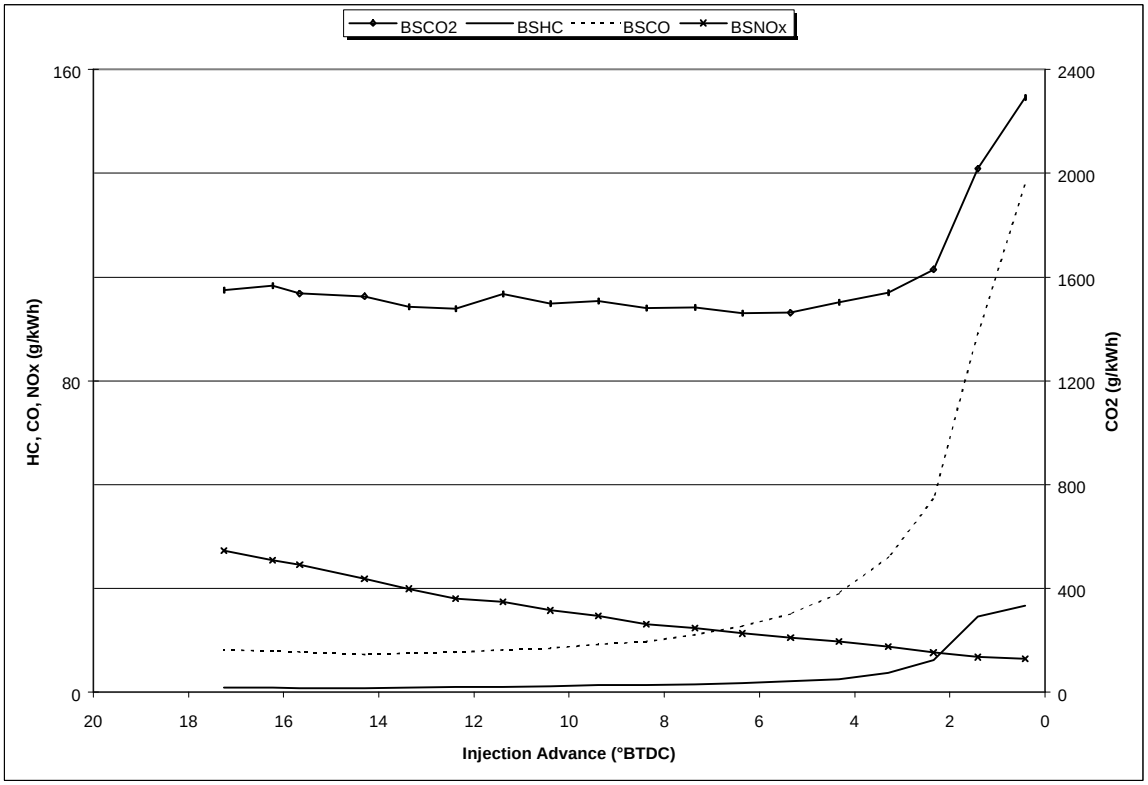

Figure 19: Emissions vs. ADV for diesel WVU-ECU (1500 rpm; 900 μs FIPW; 10-10.5 MPa ICP)

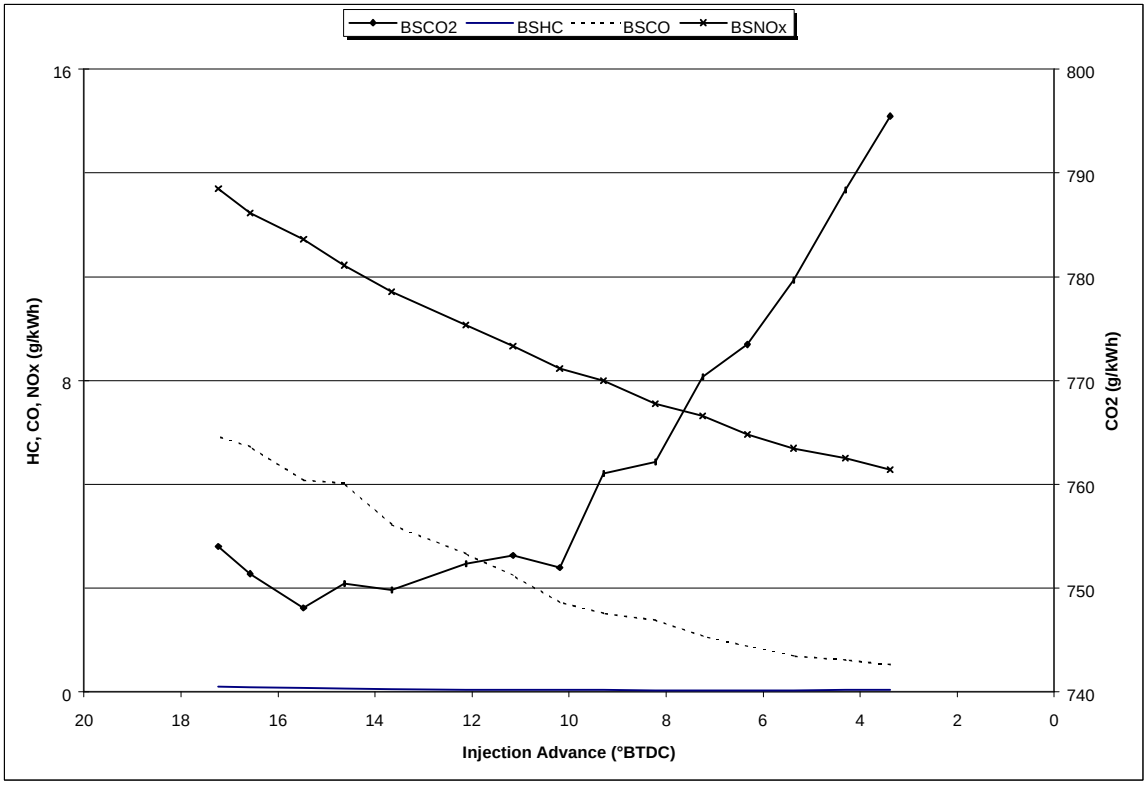

Figure 20: Emissions vs. ADV for diesel WVU-ECU (1500 rpm; 2373 μs FIPW; 10-10.5 MPa ICP)

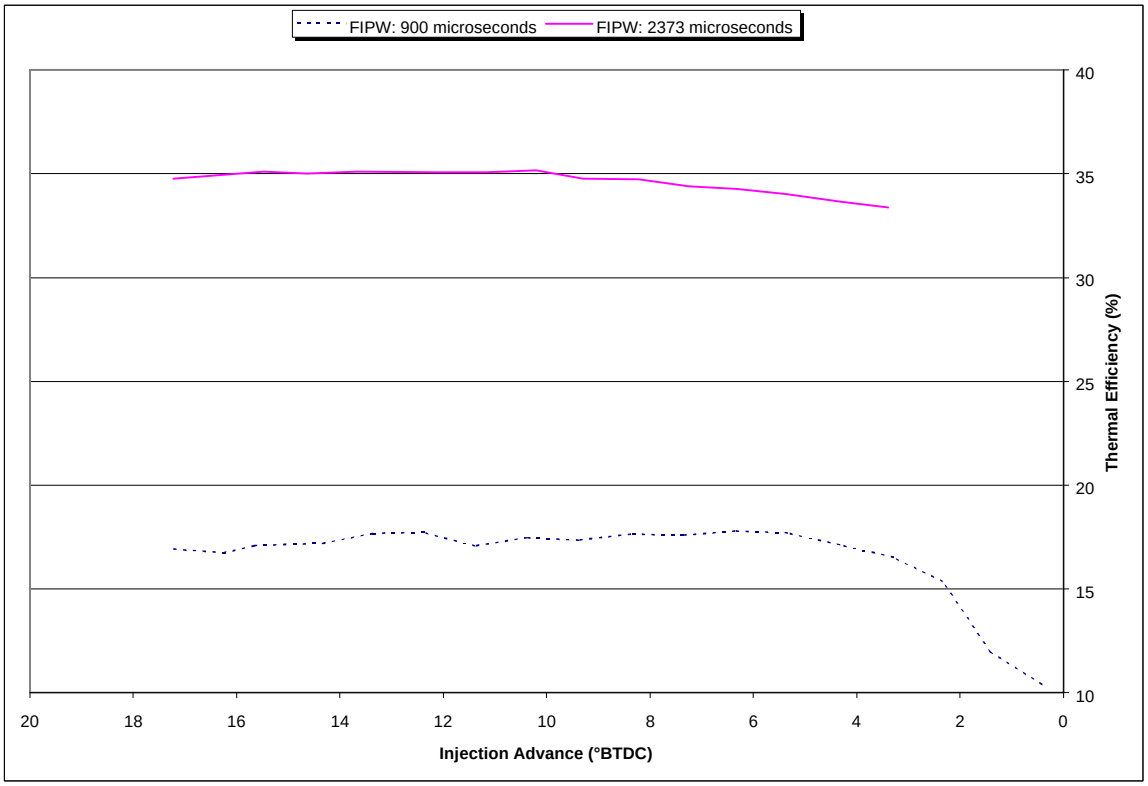

Figure 21: Thermal Efficiency vs. ADV for diesel WVU-ECU (1500 rpm; 10-10.5 MPa ICP)

4.2 Dual Fuel Operation

Operation of the engine in dual fuel mode was carried out in two stages. The first stage consisted of a series of sweeps designed to optimize FIPW, ADV, ICP, and CNG flow, to minimize exhaust emissions, and maximize diesel replacement while maintaining diesel-like thermal efficiencies. The second stage was a set of steady state tests identical to those performed during diesel operation with the Ford EEC-IV to provide a comparison between the two modes of operation.

4.2.1 Dual Fuel Sweep Data Using WVU-ECU

The first set of sweeps was of FIPW. The FIPW was stepped up in discrete increments while ADV and ICP were held constant. The CNG flow was then adjusted to hold the torque output steady.

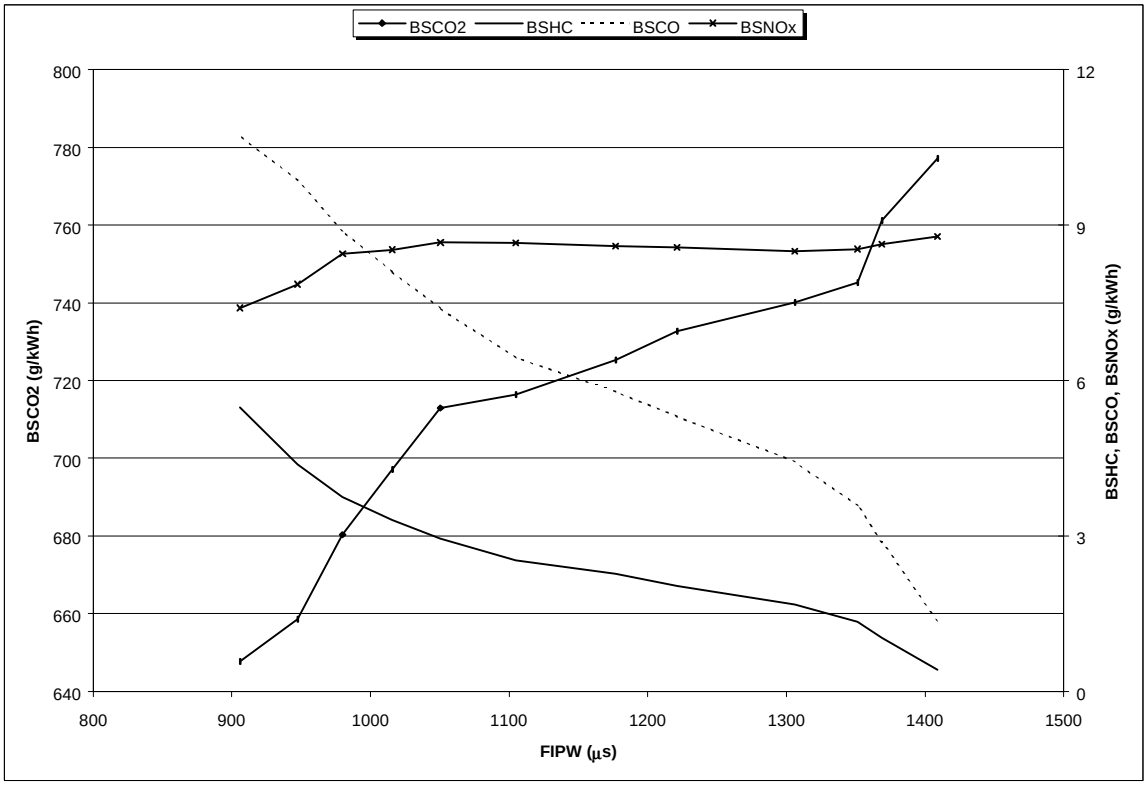

Figure 22: Dual fuel emissions vs. FIPW (1500 rpm; 335 N-m; 6.5° BTDC; 11 MPa ICP)

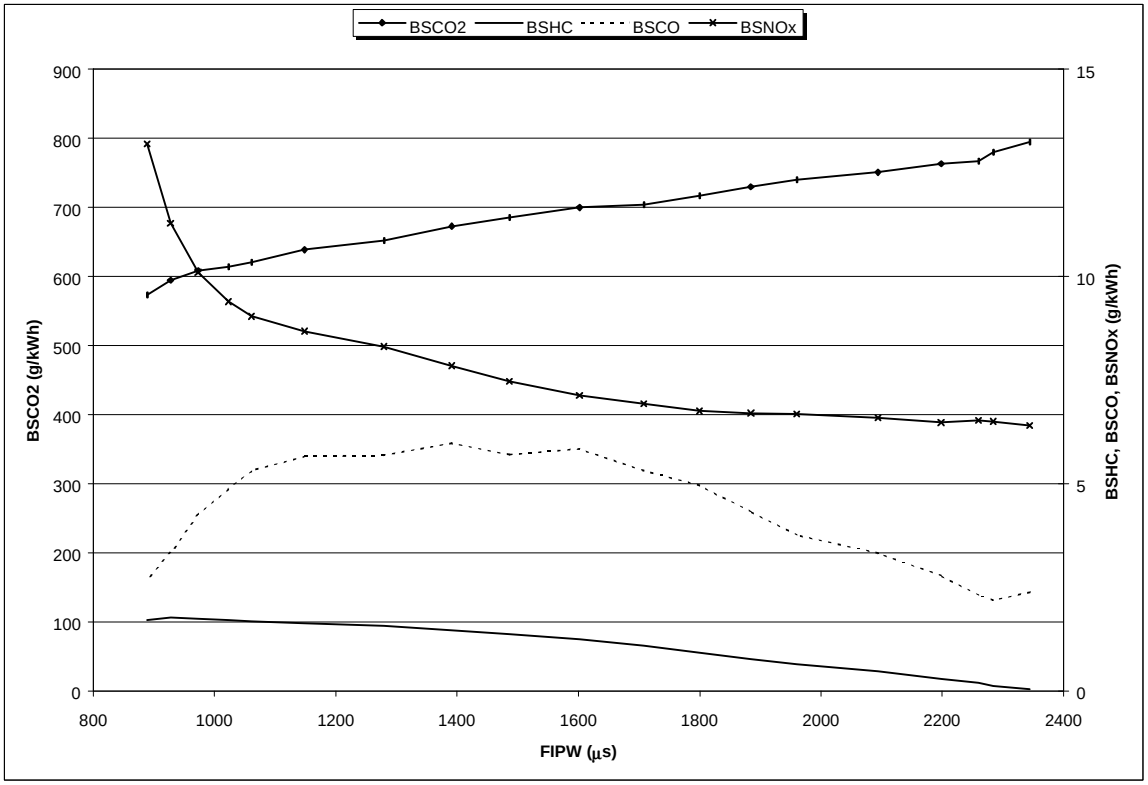

Figure 23: Dual fuel emissions vs. FIPW (1500 rpm; 580 N-m; 6.5° BTDC; 11 MPa ICP)

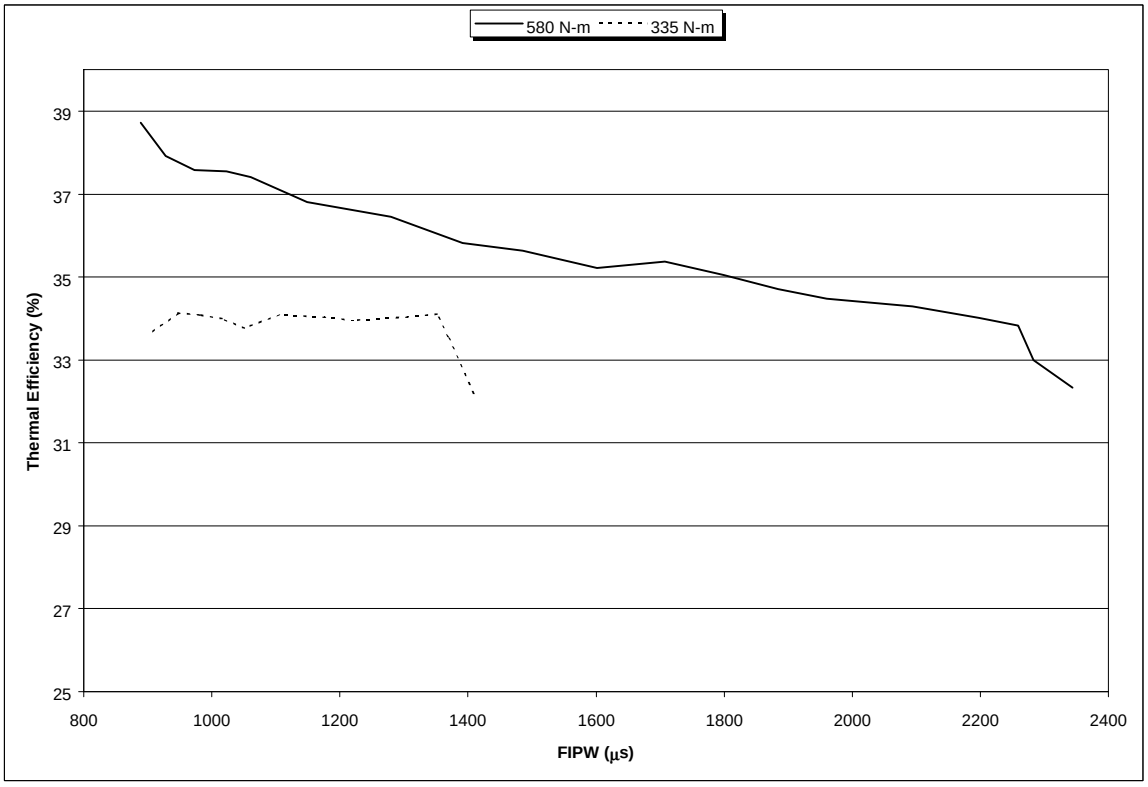

Figure 24: Dual fuel efficiency vs. FIPW (1500 rpm; 335 N-m & 580 N-m)

Since maximizing the diesel replacement was a goal of this project, a FIPW of 900 μs was chosen for subsequent sweeps of ADV. Figure 22 shows that the lowest NO_x and CO_2 emissions were produced at 900 μs, which coincides with previously chosen pilot injection FIPW. Figure 23, however, shows that the NO_x emissions were highest at 900 μs for 580 N-m. Thermal efficiency, at nearly 34%, was high at 900 μs FIPW for 335 N-m, but was even higher for 580 N-m at nearly 39% (Figure 24).

Sweeps of ADV were done at 335 N-m and 580 N-m with FIPW of 900 μs and ICP of 11-11.5 MPa. Again, CNG flow rate was varied to keep torque constant at either 335 N-m or 580 N-m and emissions and thermal efficiency were recorded for each point. The HC-NO_x tradeoff was of particular interest for this set of tests and it was determined from this information that the optimum ADV at 335 N-m was 4.5° BTDC (Figure 27) and 2.5° BTDC at 580 N-m (Figure 28). The HC-NO_x tradeoff also can be equated to a NO_x-efficiency tradeoff because the efficiency is directly related to the amount of unburned hydrocarbons in the exhaust. CO2 emissions decreased with increasing ADV for both modes while CO decreased at 335 N-m and remained relatively unchanged at 580 N-m with increasing ADV (Figures 25 & 26). It can be seen from Figure 29 that the thermal efficiency benefits greatly from advancing the start of injection, exceeding 39% at 9° BTDC for the 580 N-m set point and 37% at 13° BTDC for the 335 N-m set point. However, this efficiency increase does come with a significant NO_x penalty (NO_x-efficiency tradeoff) which is unacceptable.

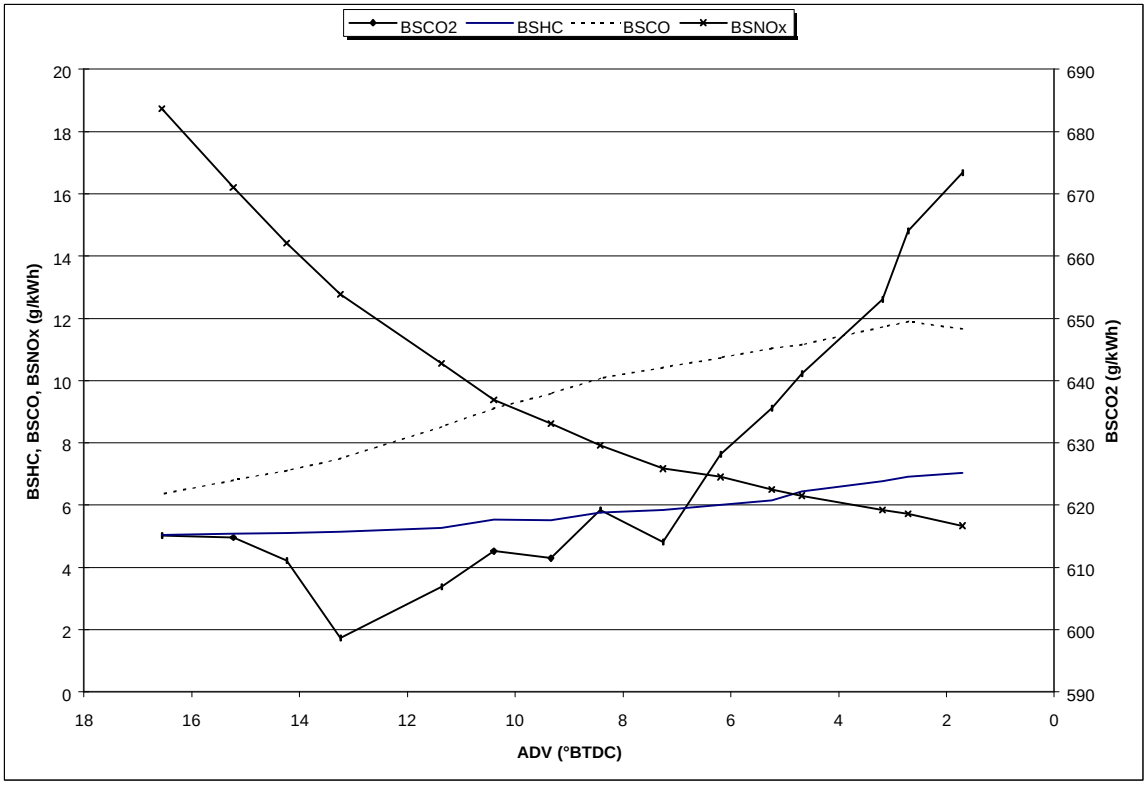

Figure 25: Dual fuel emissions vs. ADV (1500 rpm; 335 N-m; 900µs FIPW; 11 MPa ICP)

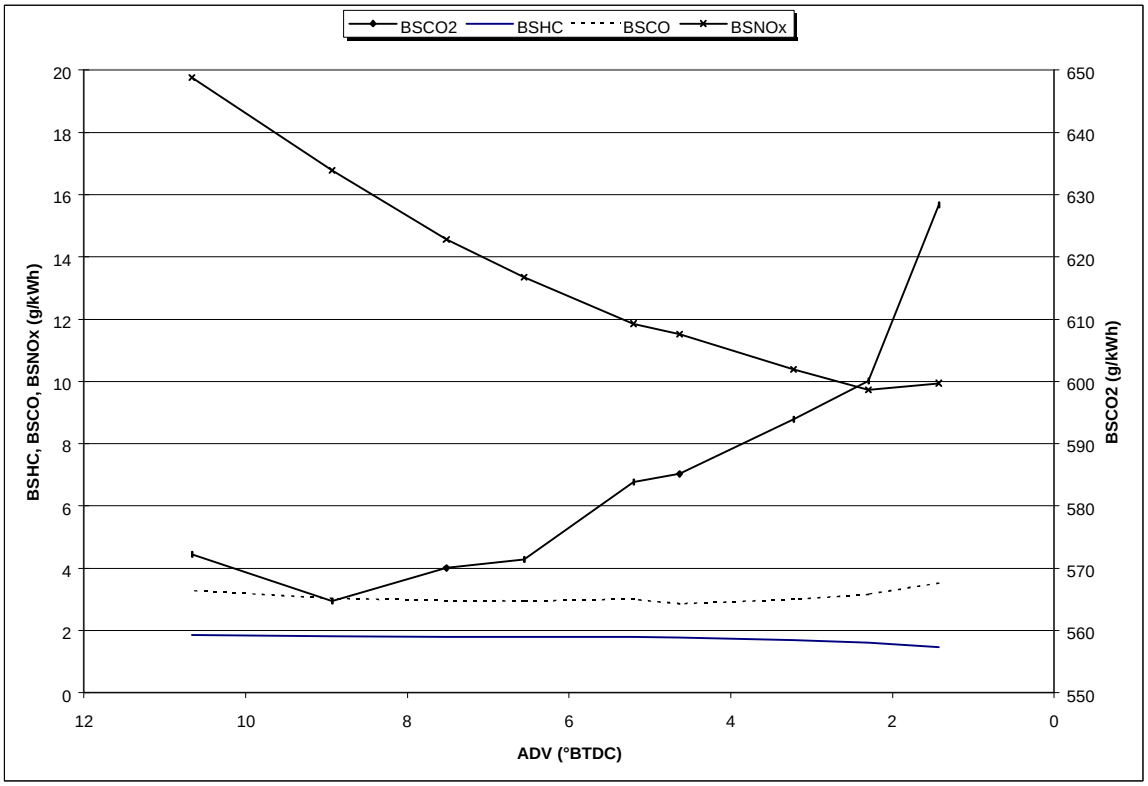

Figure 26: Dual fuel emissions vs. ADV (1500 rpm; 580 N-m; 900µs FIPW; 11 MPa ICP)

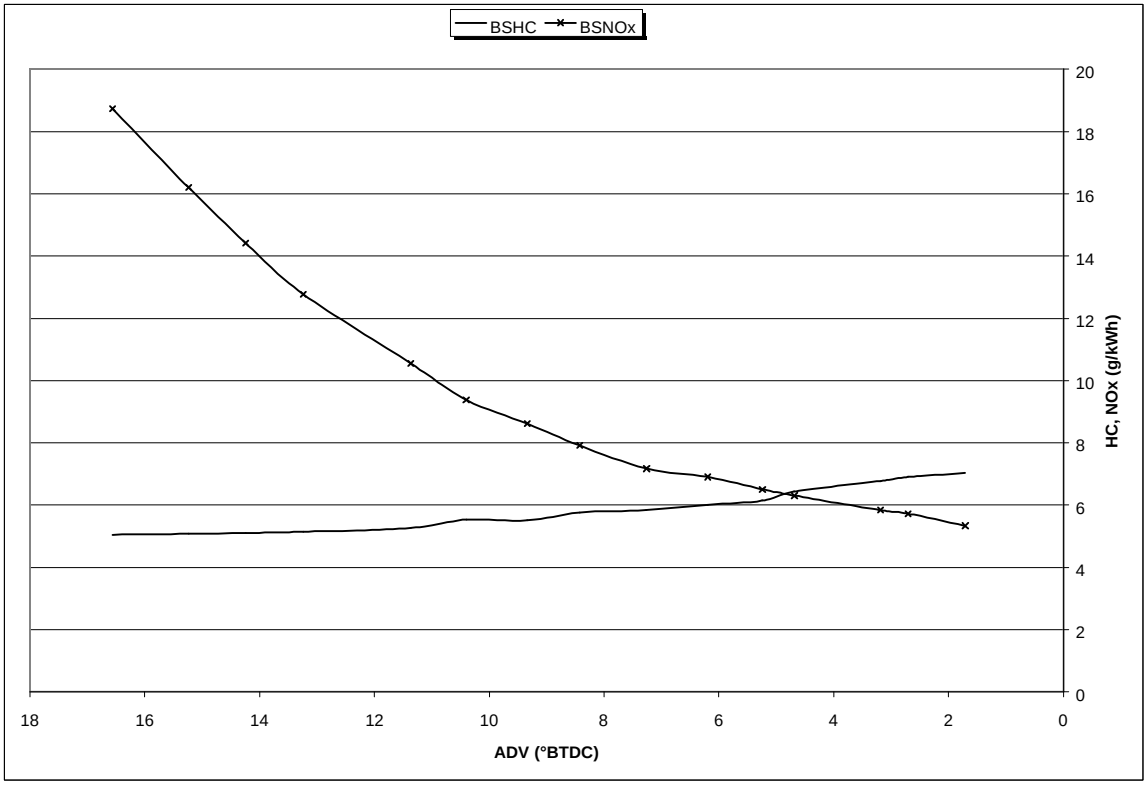

Figure 27: HC - NO_x Tradeoff (1500 rpm; 335 N-m; 900µs FIPW; 11 MPa ICP)

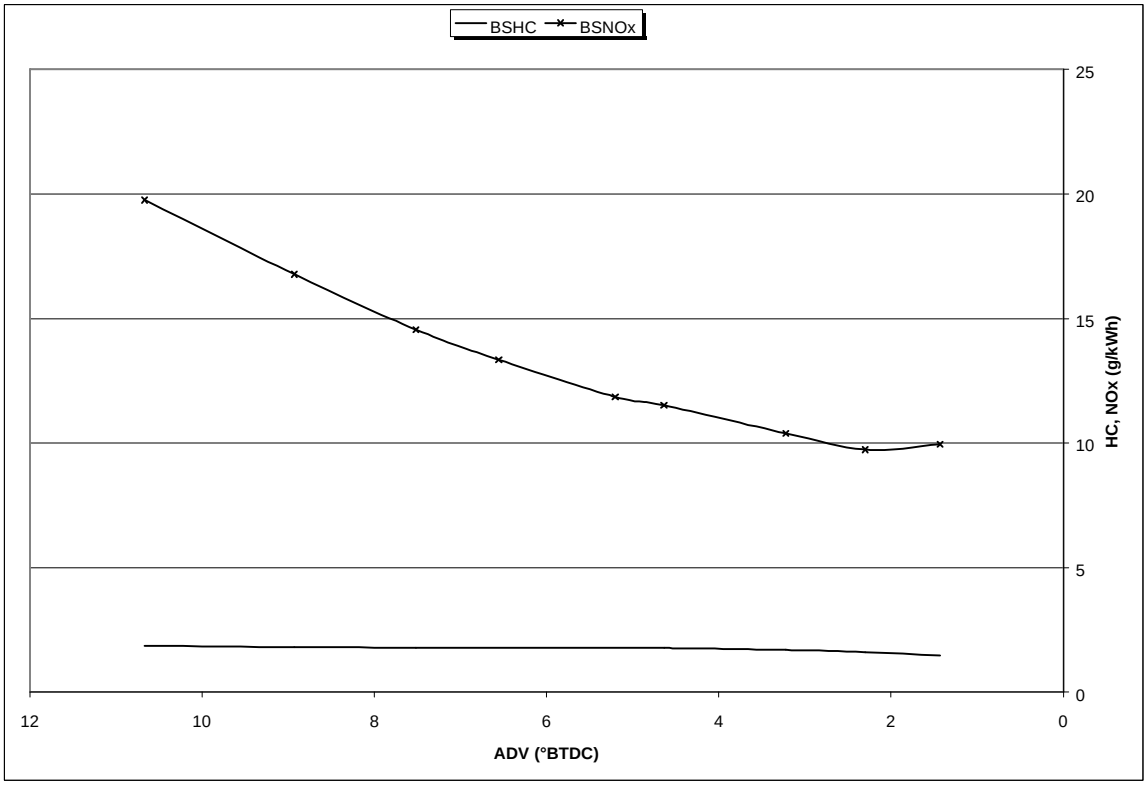

Figure 28: HC - NO_x Tradeoff (1500 rpm; 580 N-m; 900µs FIPW; 11 MPa ICP)

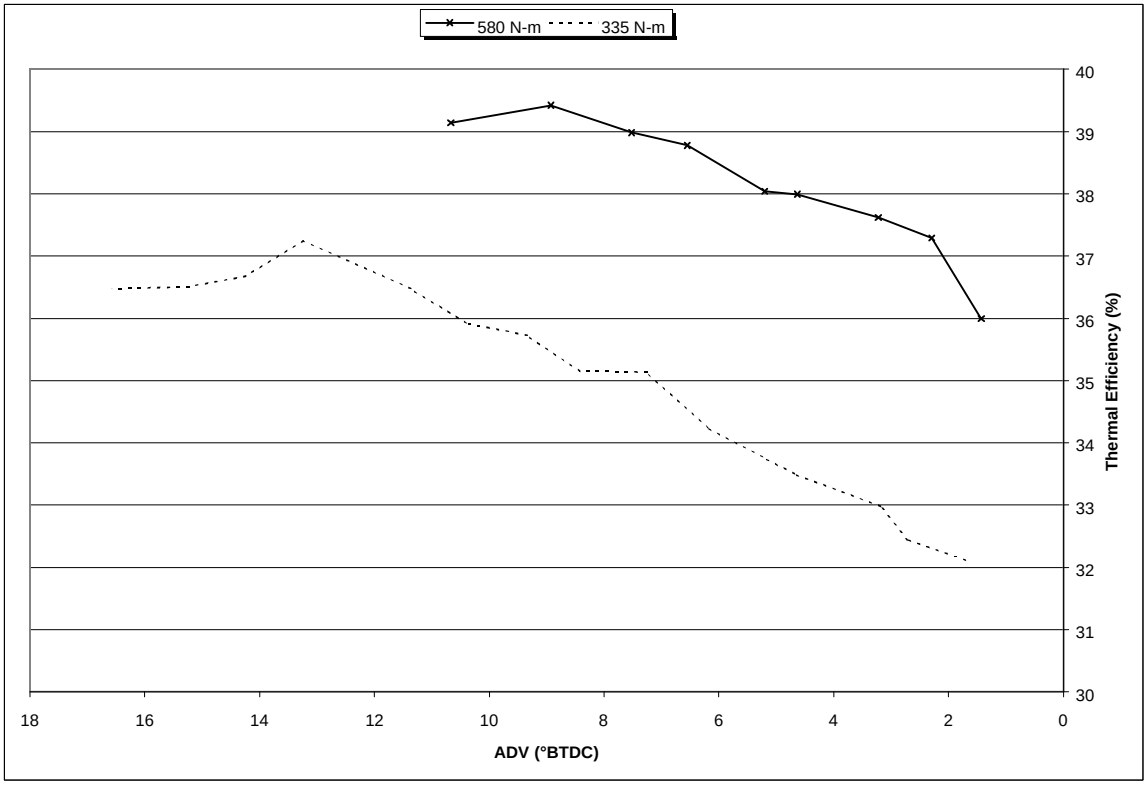

Figure 29: Dual fuel efficiency vs. ADV (1500 rpm; 335 N-m & 580 N-m)

Finally, the effects of ICP were investigated. ICP and FIPW control the amount of diesel fuel injected. ICP was stepped from 4 to 14 MPa in 1 MPa increments and the FIPW was adjusted to maintain a constant torque. CNG flow and ADV were held constant and emissions and thermal efficiency were recorded. From Figures 30 & 31 it can be seen that the NO_x levels were lowest at the lowest ICP, but from Figure 32 thermal efficiencies were also at a minimum (33% at 335 N-m and 35% at 580 N-m) at this point. At 335 N-m, HC and CO were at a maximum at the lowest ICP, while at 580 N-m, CO_2 and CO were at maximum levels at the lowest ICP. This data shows how emissions change when the pilot is delivered in a short, high pressure burst or in a long, low pressure stream. Table 8 shows that the peak pressure increases as ICP increases which accounts for the NO_x increase at high ICP. From this information, an ICP of 6 MPa for the 335 N-m set point and 4.5 MPa for the 580 N-m set point were chosen.

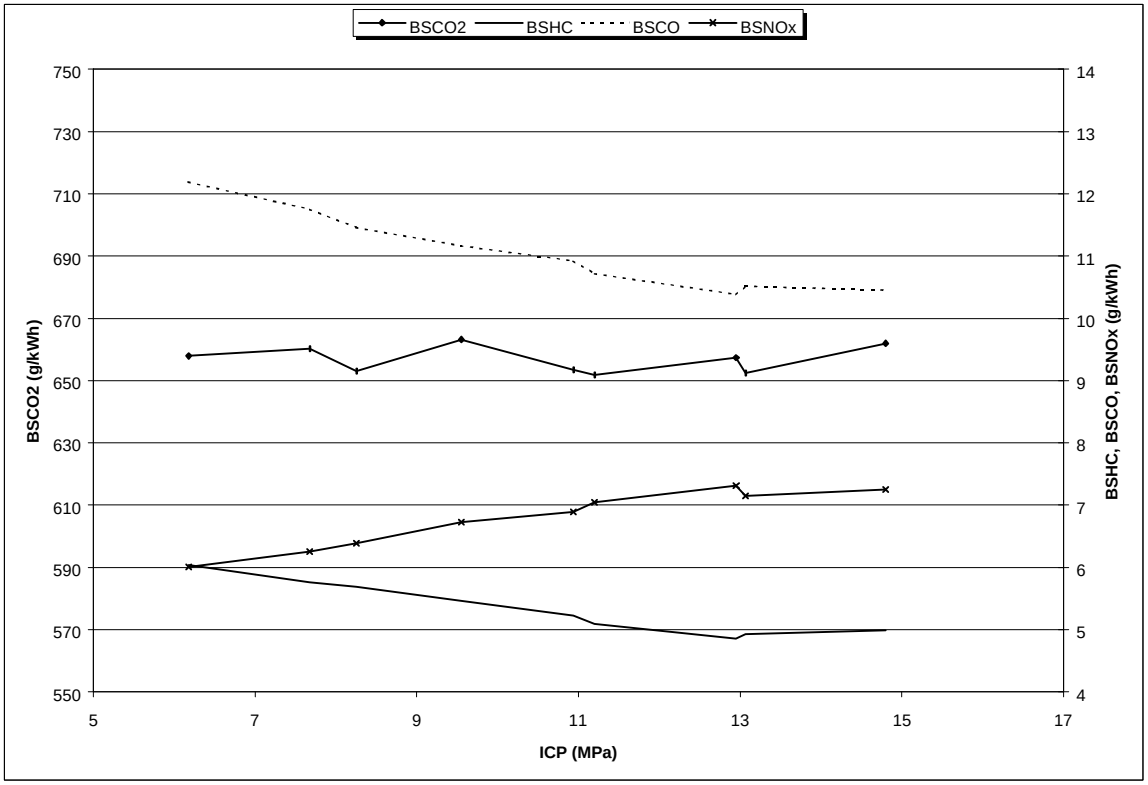

Figure 30: Dual fuel emissions vs. ICP (1500 rpm; 335 N-m; 4.75° BTDC)

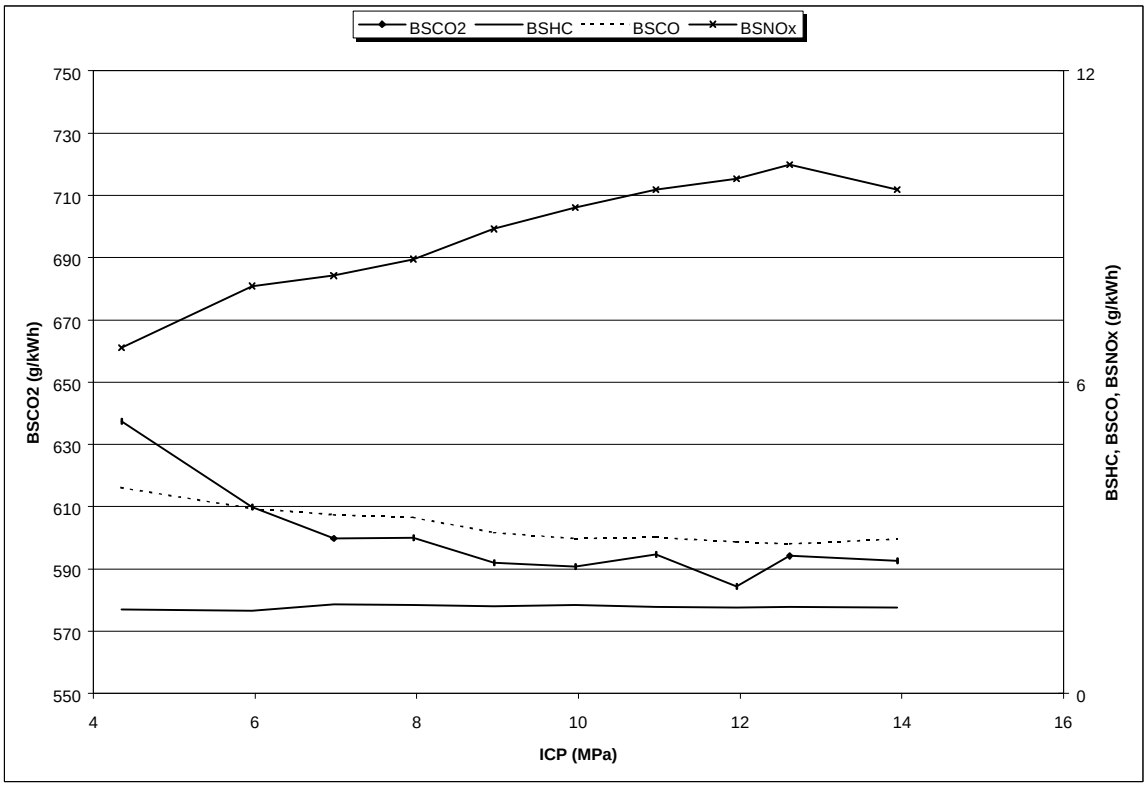

Figure 31: Dual fuel emissions vs. ICP (1500 rpm; 580 N-m; 2.5° BTDC)

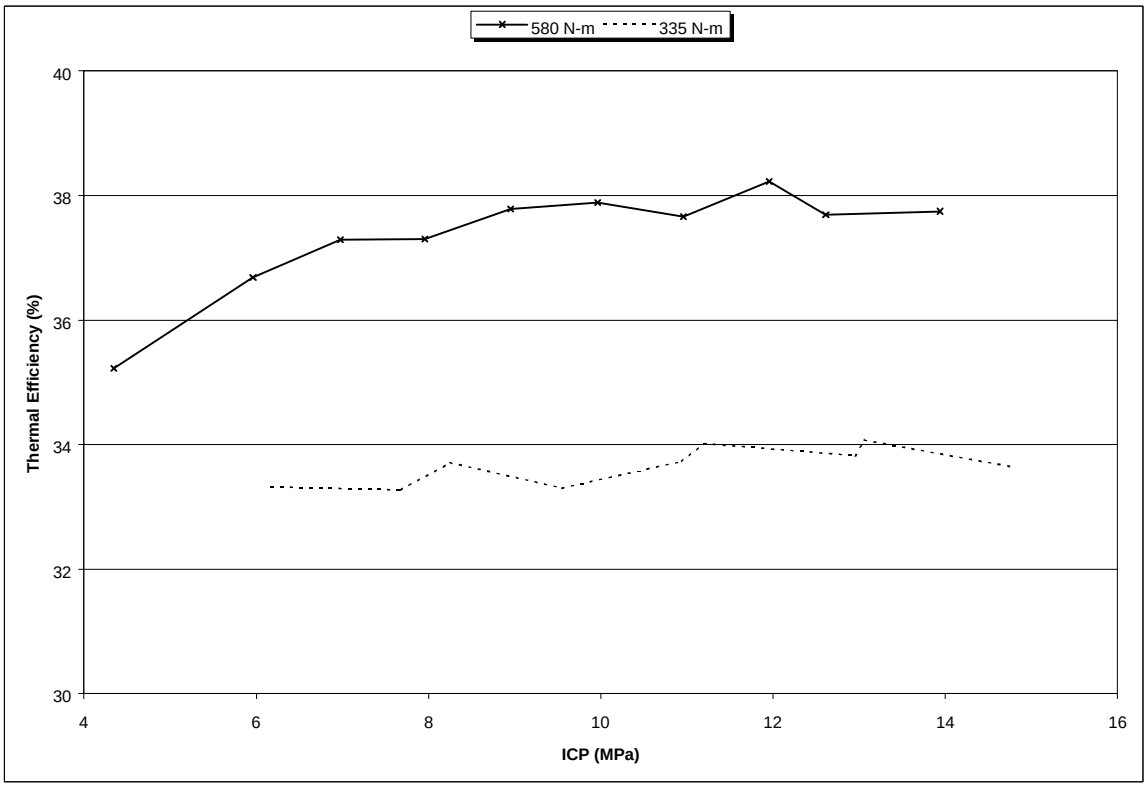

Figure 32: Dual fuel efficiency vs. ICP (1500 rpm; 335 N-m & 580 N-m)

	ICP (MPa)	Peak Pres. (kPa)
335 N-m	7	6562
	13	7770
580 N-m	7	8259
	13	9751

Table 8: Peak in-cylinder pressure for different ICP (335 N-m & 580 N-m)

From these data, the final optimum settings based on emissions and efficiency were determined to be:

	FIPW (μs)	ADV (° BTDC)	ICP (MPa)
335 N-m	1145	5.6	6
580 N-m	1398	2.4	5

Table 9: Dual fuel optimized FIPW, ADV, ICP (335 N-m & 580 N-m)

4.2.2 Dual Fuel Steady State Test Data Using WVU-ECU

With the optimum settings for FIPW, ADV, and ICP determined, the second set of comparative steady state tests was conducted with the engine running in dual fuel mode. The engine produced the following averaged emissions while running in the optimized dual fuel mode.

	PM (g/kWh)	THC (g/kWh)	NMHC (g/kWh)	CO (g/kWh)	CO_2 (g/kWh)	NO_x (g/kWh)
335 N-m	0.032	6.266	0.597	12.08	631.6	6.01
580 N-m	0.058	1.780	0.295	4.737	615.3	6.28

Table 10: Averaged DF emissions (335 N-m & 580 N-m)

As in the diesel tests, dilution bags were analyzed using a gas chromatograph. It can be seen that the primary hydrocarbon constituent is methane, which is not a regulated emission. The following methane percentages were adjusted for background methane levels and used to calculate the NMHC concentration before the emissions from each mode were averaged:

	Methane (ppm)	THC (ppm)	% Methane (less BG)
335 N-m 1	476.7	500.4	95.21
335 N-m 2	406.5	456.5	88.69
335 N-m 3	373.0	424.1	87.51
580 N-m 1	411.0	481.7	84.82
580 N-m 2	217.5	266.3	80.38
580 N-m 3	389.9	455.5	85.06

Table 11: Gas chromatograph data showing %MHC

In-cylinder pressure data were collected, and HRR, COV(IMEPg) and ignition delay were calculated. P-V diagrams were also generated. The COV(IMEPg) is below 10% (Table 12) which indicates stable combustion with minimal cycle-to-cycle

variations. This suggests that the engine would be driveable while operating under these conditions.

	COV(IMEPg) %	Ign. Delay °After SOI
335 N-m	7.85	15.80
580 N-m	6.20	17.74

Table 12: Dual fuel COV(IMEPg) & ignition delay (335 N-m & 580 N-m)

In Figures 33 & 34 it can be seen that there are two distinct pressure peaks. The first peak is due to compression of the gases in the cylinder with no heat addition from burning fuel - the motoring pressure trace. The second peak is due to late combustion of the diesel fuel and natural gas that takes place entirely after TDC. This reduces the peak pressure in the cylinder and therefore causes a reduction in NO_x.

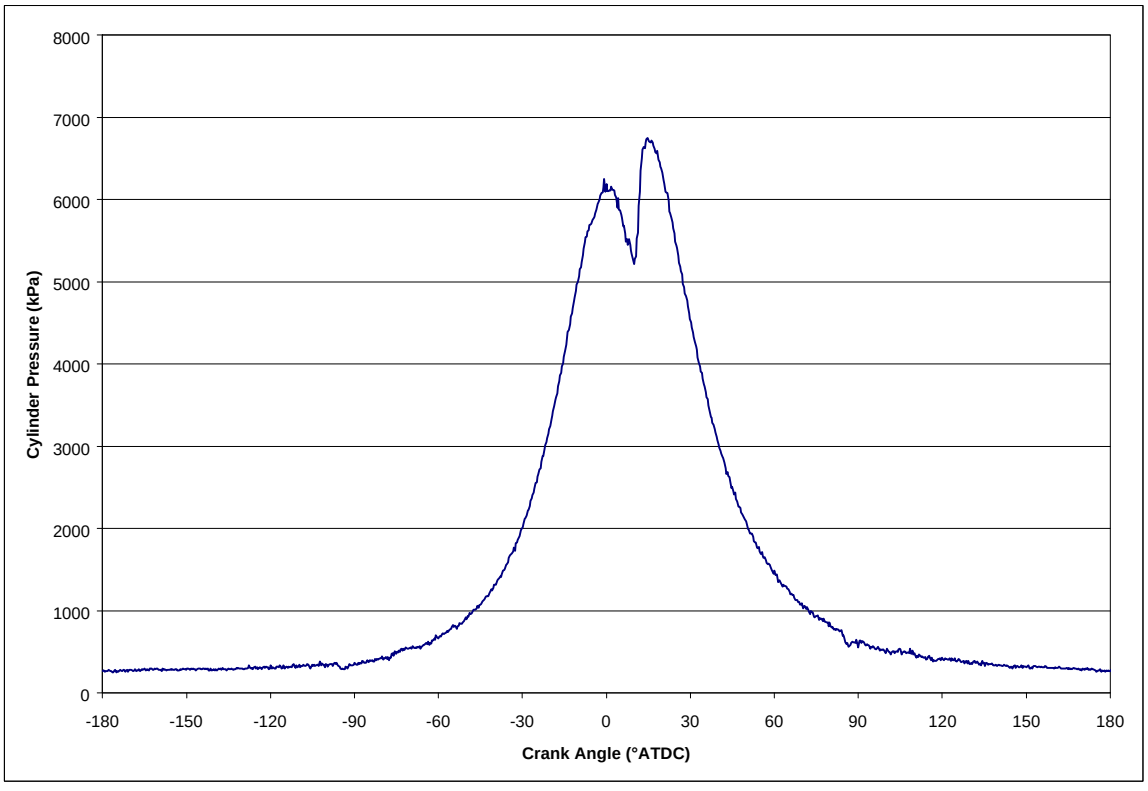

Figure 33: Dual fuel in-cylinder pressure vs. CA (1500 rpm; 335 N-m)

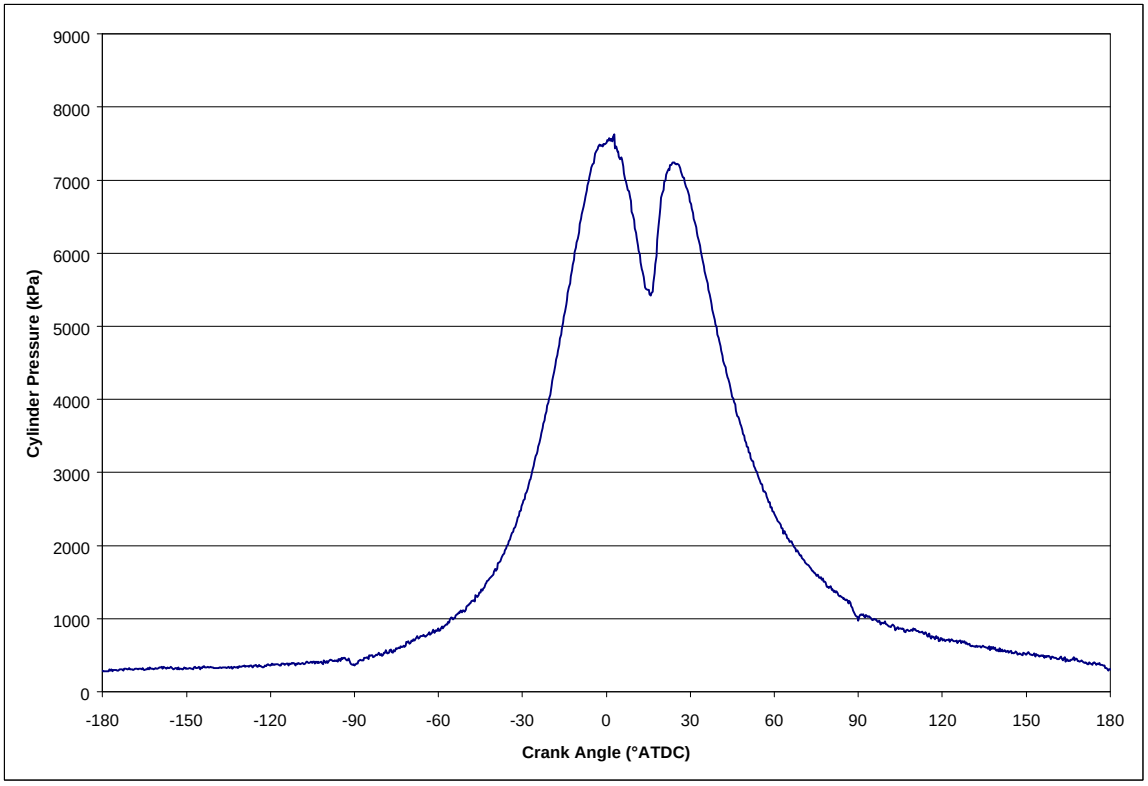

Figure 34: Dual fuel in-cylinder pressure vs. CA (1500 rpm; 580 N-m)

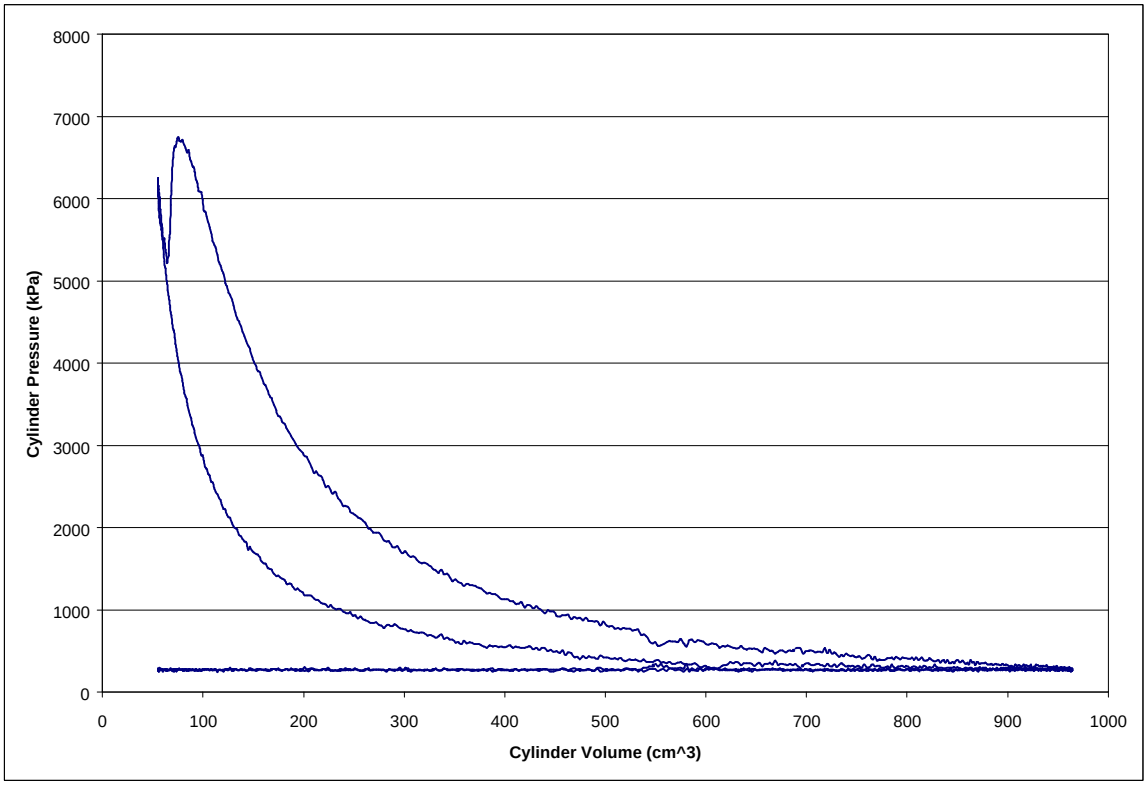

Figure 35: Dual fuel P-V diagram (1500 rpm; 335 N-m)

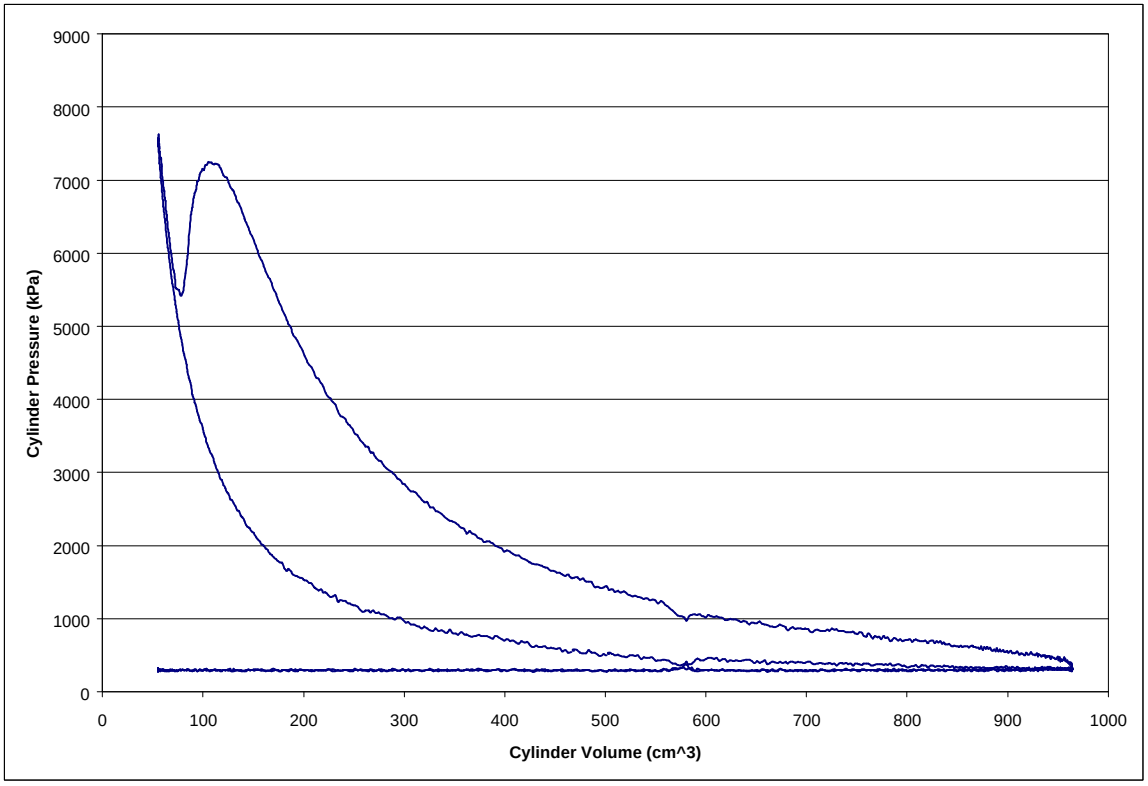

Figure 36: Dual fuel P-V diagram (1500 rpm; 580 N-m)

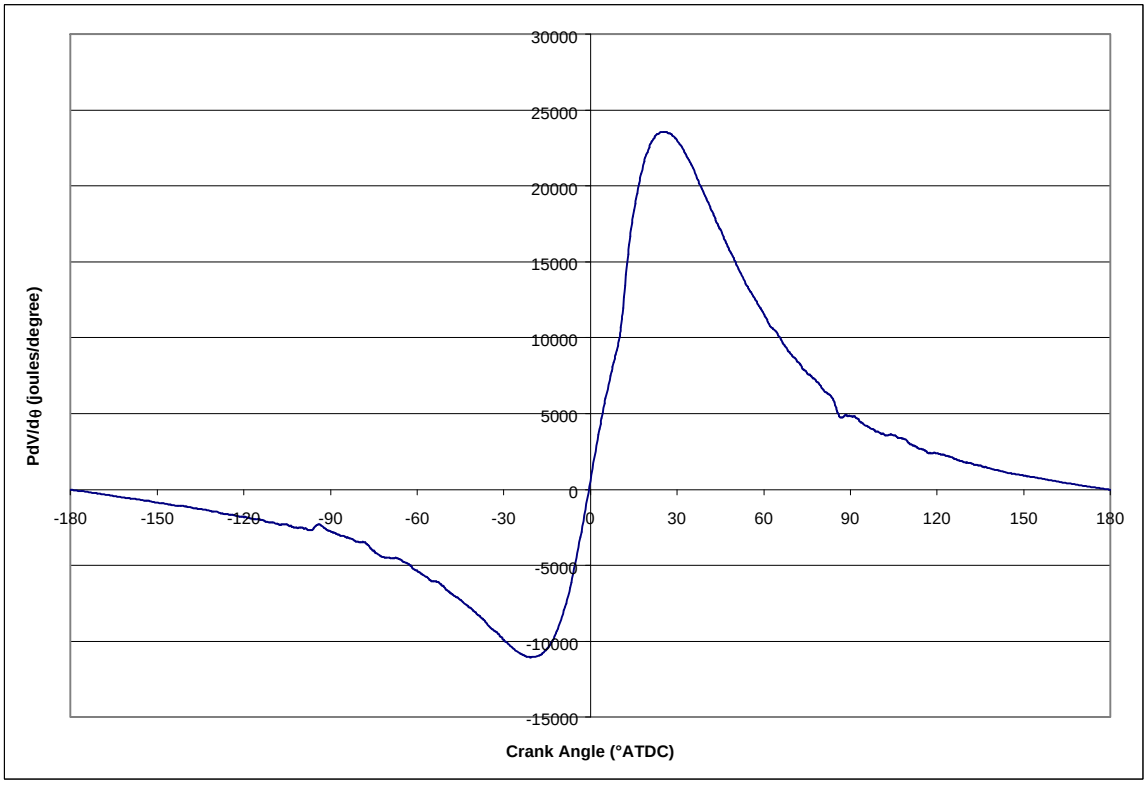

Figure 37: Dual fuel PdV/dθ vs. CA (1500 rpm; 335 N-m)

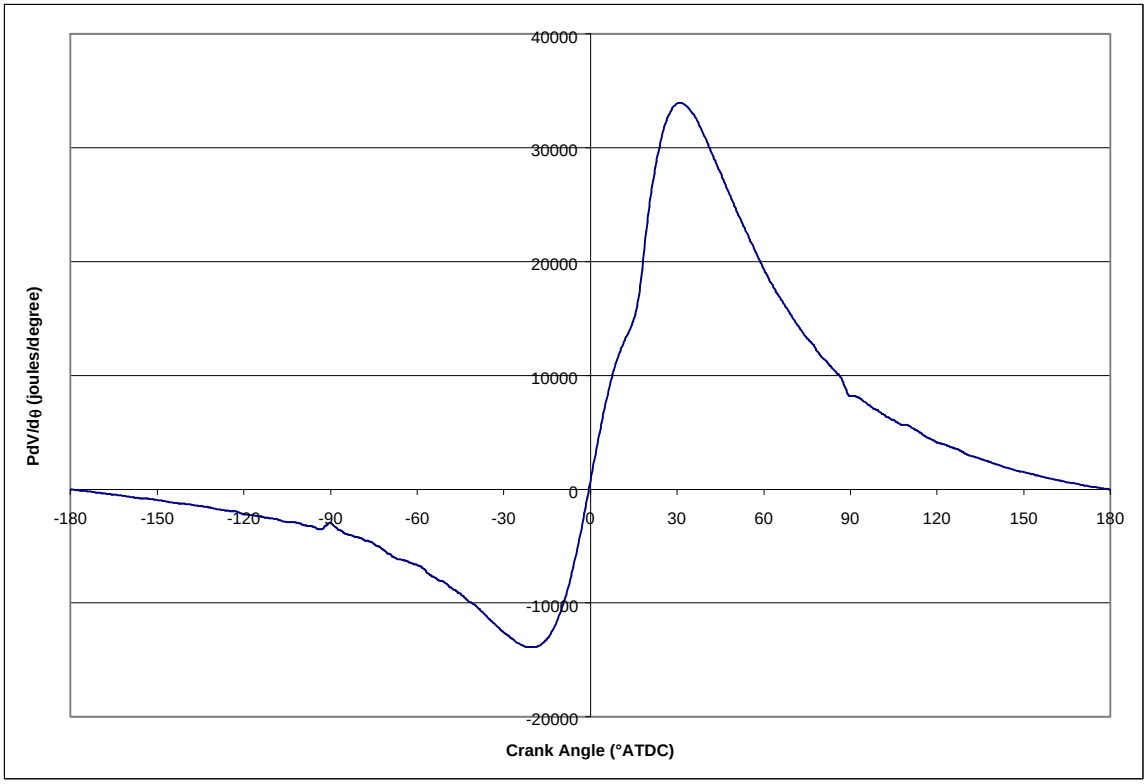

Figure 38: Dual fuel PdV/dθ vs. CA (1500 rpm; 580 N-m)

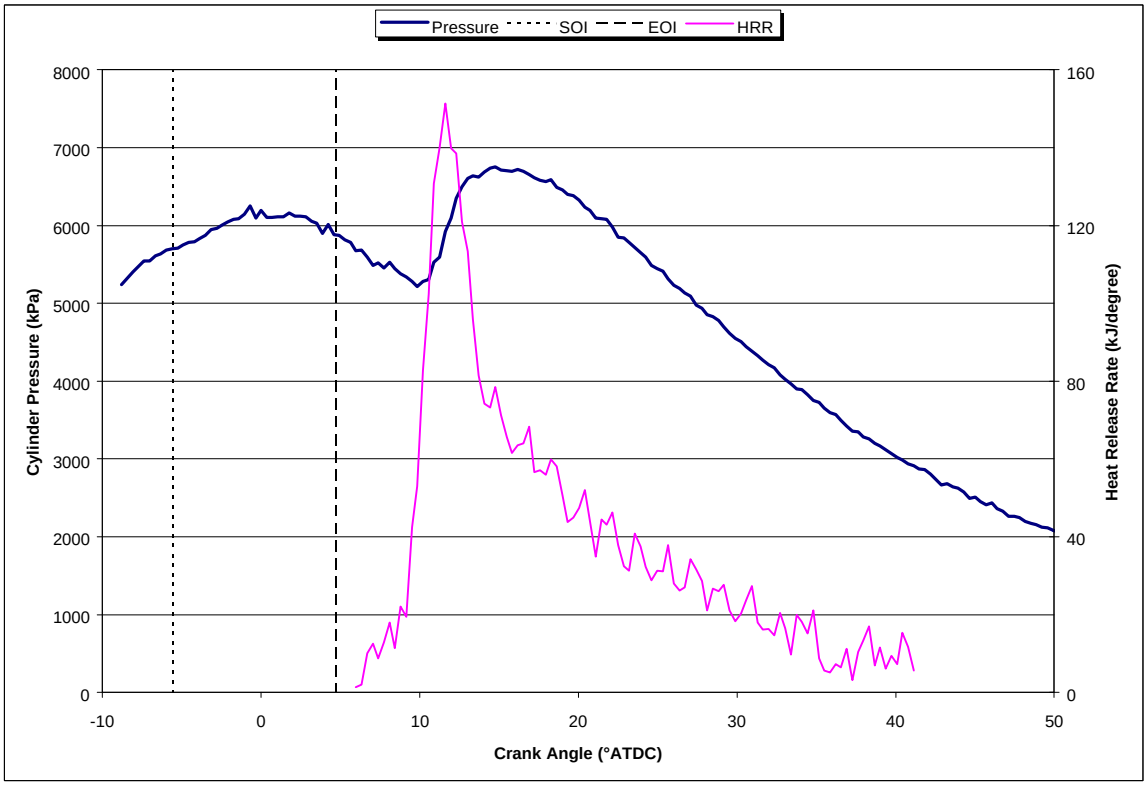

Figure 39: Dual fuel in-cylinder pressure & HRR vs. CA (1500 rpm; 335 N-m)

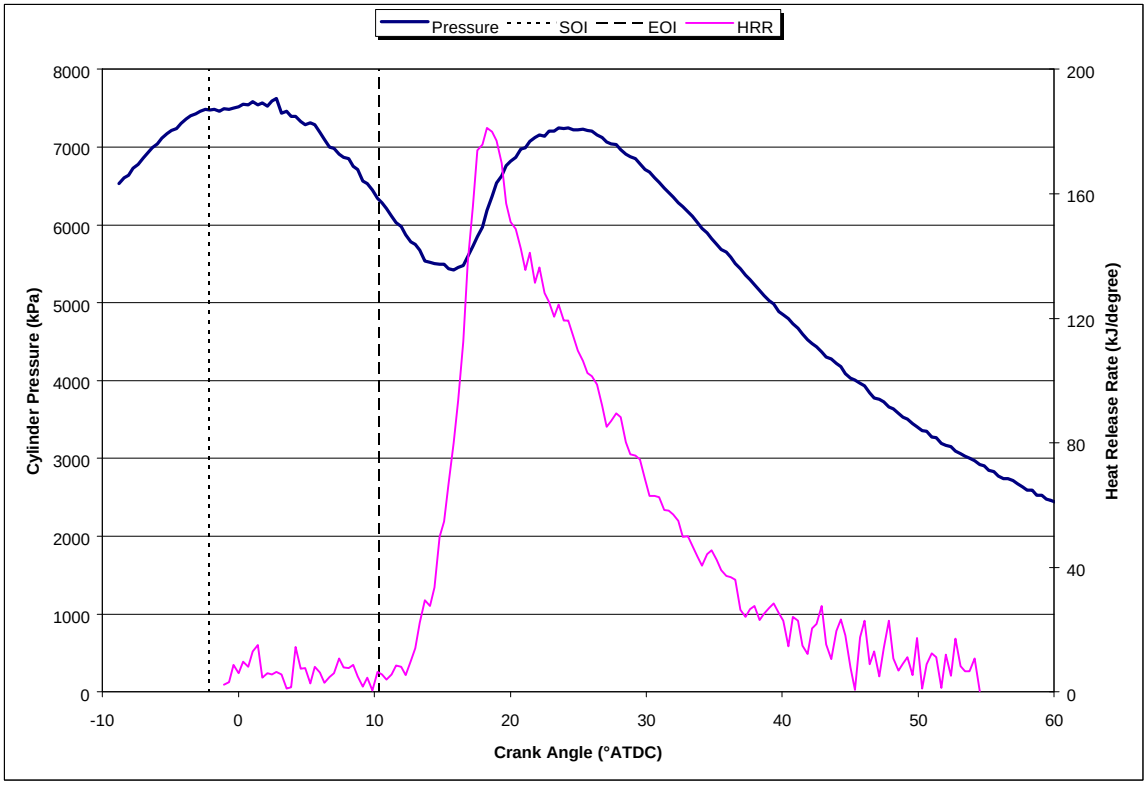

Figure 40: Dual fuel in-cylinder pressure & HRR vs. CA (1500 rpm; 580 N-m)

The amount of diesel replacement was also calculated for each mode, using the diesel fuel flow rate from the fuel counter and the carbon balance, to find the CNG flow rate.

	CNG (g/s)	D2 (g/s)	CNG/D2 (mass)	CNG/D2 (LHV)
335 N-m	3.016	1.229	2.454	2.840
580 N-m	5.620	1.388	4.049	4.686

Table 13: CNG/Diesel ratios (335 N-m & 580 N-m)

4.3 Comparison of Diesel and Dual Fuel Operation

The dual fuel and diesel steady state tests were compared to determine what, if any, emissions and efficiency benefits were produced. PM, CO_2, and NO_x emissions were significantly reduced compared to diesel operation, while there was a substantial increase

in NMHC for both modes and an increase in CO at 335 N-m. The dramatic increase in CO is probably due to very late combustion. CO formation is a necessary intermediate step in HC oxidation as shown in the following equation in which *R* represents the HC radical:

$$RH \Rightarrow R \Rightarrow RO_2 \Rightarrow RCHO \Rightarrow RCO \Rightarrow CO$$

The CO is then oxidized in the following reaction:

$$CO + OH \Leftrightarrow CO_2 + H$$

Since the combustion process is so late compared to diesel operation (see Figures 41 & 42), this reaction never takes place and therefore, high amounts of CO remain in the exhaust gas [23].

Emissions in g/kWh		1500 rpm, 335 N-m					
	PM	THC	NMHC	CO	CO_2	NO_x	NMHC + NO_x
Diesel (EEC-IV)	0.076	0.087	0.087	0.533	764.696	8.920	9.007
Dual Fuel	0.032	6.266	0.597	12.075	631.617	6.011	6.608
% difference	-57.9	7094	585	2165	-17.4	-32.6	-26.6
Emissions in g/kWh		1500 rpm, 580 N-m					
	PM	THC	NMHC	CO	CO_2	NO_x	NMHC + NO_x
Diesel (EEC-IV)	0.213	0.026	0.026	4.610	746.576	7.781	7.808
Dual Fuel	0.058	1.780	0.295	4.737	615.338	6.277	6.572
% difference	-73.0	6687	1025	2.8	-17.6	-19.3	-15.8

Table 14: Emissions comparison of DF & diesel (335 N-m & 580 N-m)

The engine obviously used less diesel fuel while operating in dual fuel mode. The exact quantity reduction was calculated and proved to be quite large.

	Diesel Operation (g/s)	Dual Fuel Operation (g/s)	Reduction %
335 N-m	3.5	1.3	64.6
580 N-m	6.0	1.4	76.7

Table 15: DF & diesel operation diesel fuel usage (335 N-m & 580 N-m)

Thermal efficiency for diesel and dual fuel operation was calculated and compared. As can be seen in Table 16, there is slight increase in thermal efficiency for dual fuel operation.

	Diesel Operation %	Dual Fuel Operation %	Difference %
335 N-m	34.71	34.85	0.14
580 N-m	35.26	36.67	1.41

Table 16: Comparison of diesel and dual fuel thermal efficiency

A comparison of the heat release rates for diesel and optimized dual fuel operation was conducted. Boost pressure was checked and was found to be nearly unchanged from diesel (335 N-m: 114 kPa, 580 N-m 134 kPa) to dual fuel operation (335 N-m: 115 kPa, 580 N-m 139 kPa). Figure 41 shows that at 335 N-m the diesel and dual fuel heat release rate curves are strikingly similar with slightly more heat released during the diffusion combustion phase for dual fuel operation than for diesel operation. However, in Figure 42, the diesel and dual fuel heat release rate profiles at 580 N-m are very different from the 335 N-m set point. There is no definitive premixed or diffusion combustion phase for diesel or dual fuel operation. This is probably due to the richer natural gas/air mixture which burns more rapidly than the leaner mixtures present in lighter load situations. In both the 335 N-m and the 580 N-m modes, the point of maximum heat release was later for dual fuel operation than for diesel.

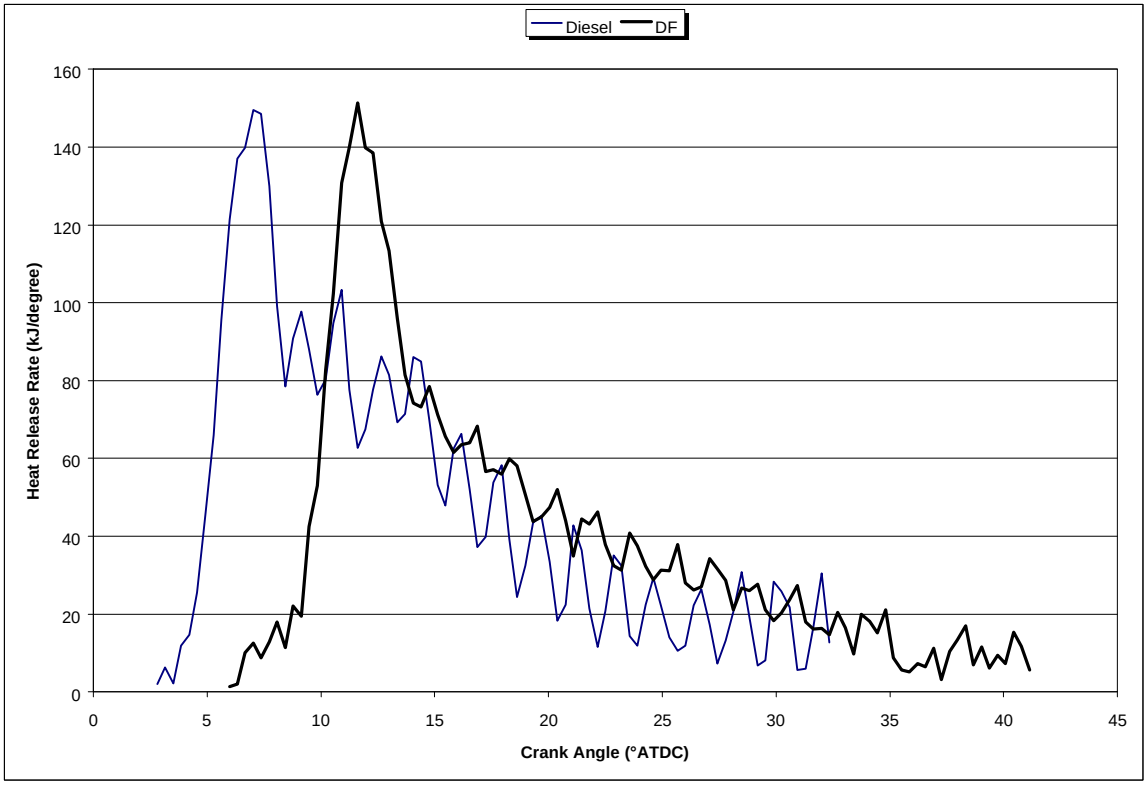

Figure 41: Dual fuel and diesel heat release rate comparison (1500 rpm; 335 N-m)

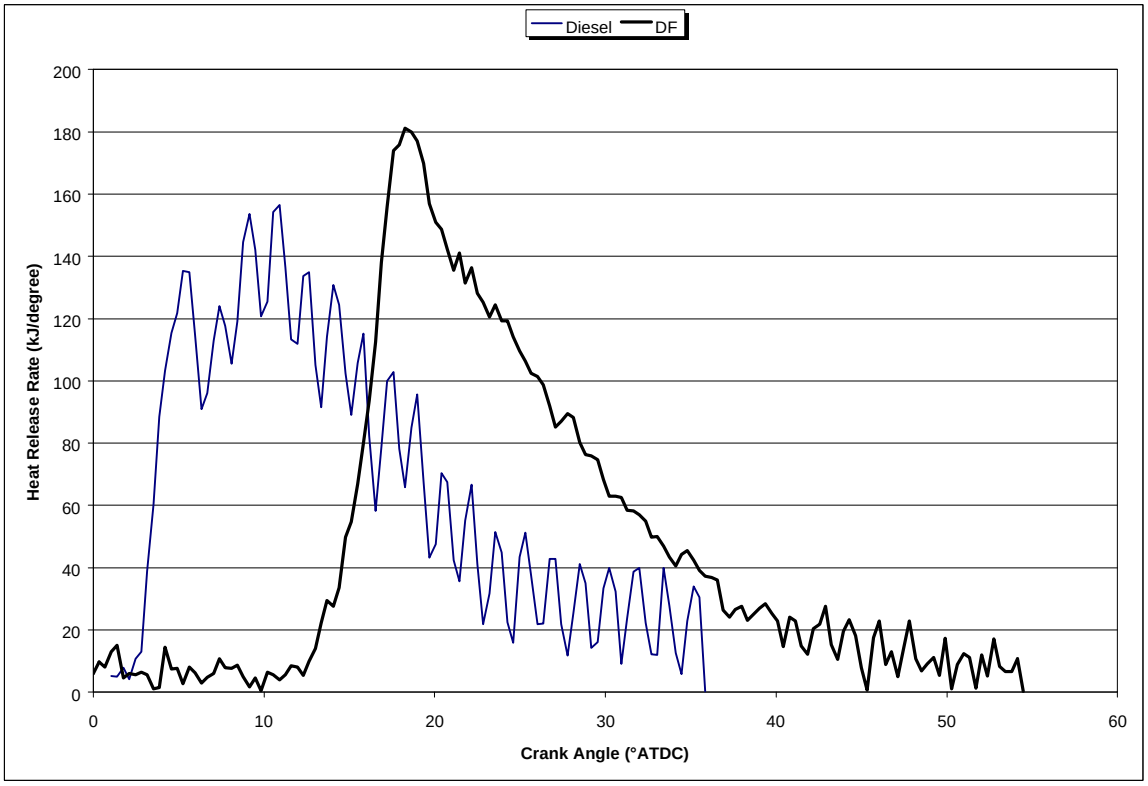

Figure 42: Dual fuel and diesel heat release rate comparison (1500 rpm; 580 N-m)

Figures 43 & 44 compare the in-cylinder pressures for the engine running in diesel-only and dual fuel mode. Figures 45 & 46 compare the PdV/dθ plots. It can be seen that the pressure traces, as well as the PdV/dθ plots are very different. This initially caused concern since the engine was producing the same power for the diesel-only and dual fuel modes. However, upon further investigation, it was found that the IMEPg for each operating condition was similar (6% difference for 335 N-m; 10% difference for 580 N-m). Ideally, the IMEPg would have been identical for each mode regardless of fuel type since the engine was producing the same power. The small differences in IMEPg can be explained by the cylinder-to-cylinder injector variations that cause some cylinders to produce less power than others. This behavior was observed while the engine was idling on diesel fuel only, when one of the instrumented cylinders was actually operating parasitically, rather than making a contribution to the overall output of the engine. Another explanation is that uneven mixing of the natural gas and air caused a lower fuel/air ratio in one or more of the cylinders which would account for the lowered IMEPg in those cylinders. Since only two cylinders out of eight were instrumented for pressure, it must be assumed that some of the other cylinders were making up the IMEPg difference. An entirely different explanation of this behavior is that since the ICP was lower for the dual fuel operation (6 MPa at 335 N-m and 5 MPa at 580 N-m compared to 11 MPa for diesel-only operation) the parasitic losses to the high pressure oil pump were lowered. This would make the required IMEPg lower to achieve the same net power output.

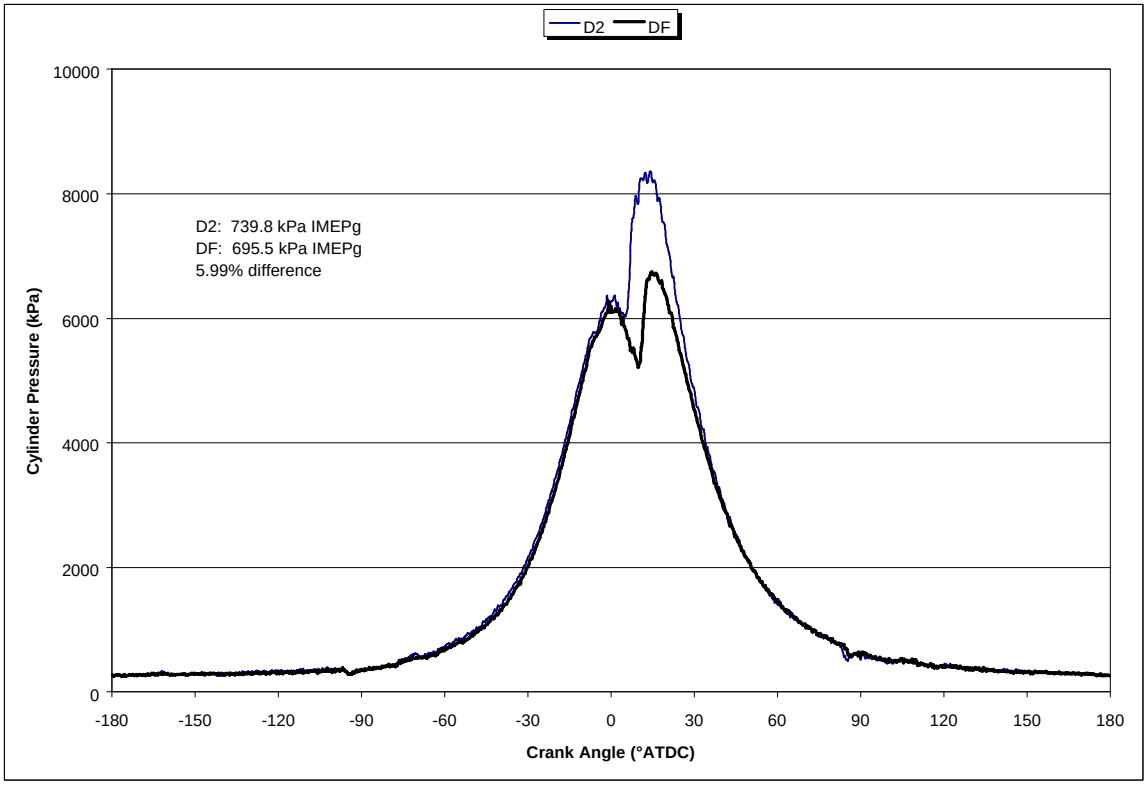

Figure 43: Dual fuel and diesel in-cylinder pressure and IMEPg comparison (1500 rpm; 335 N-m)

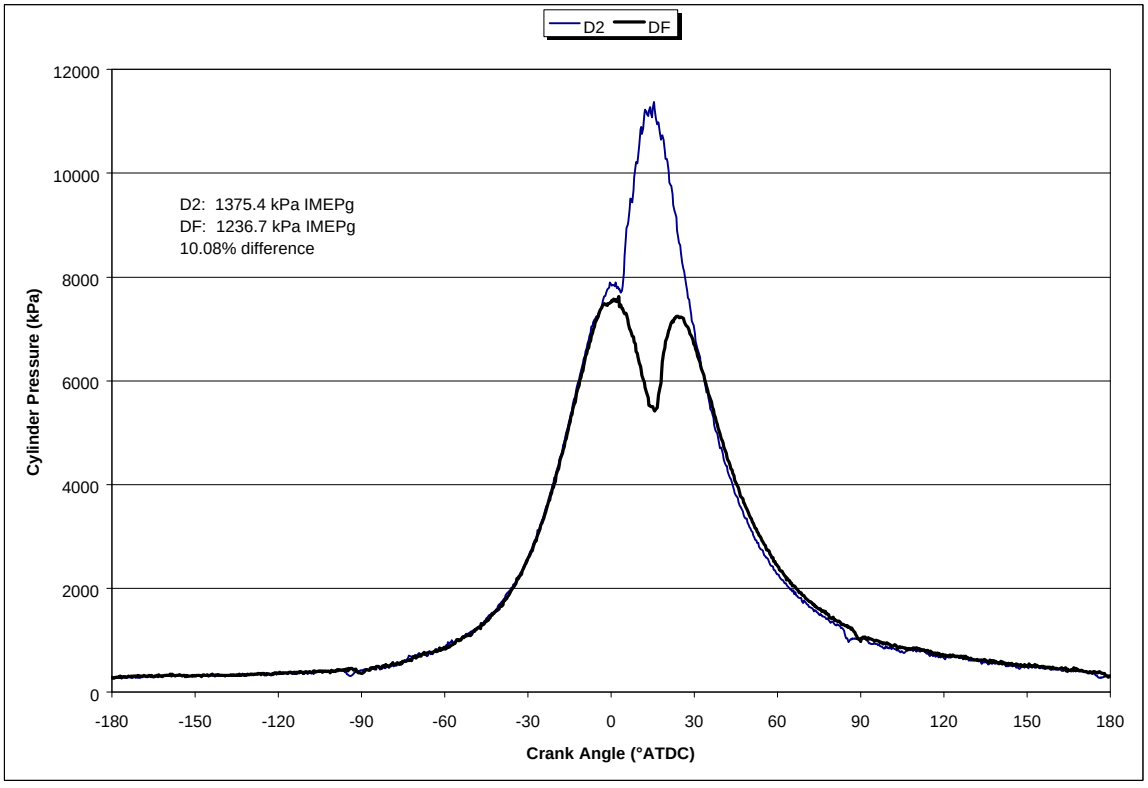

Figure 44: Dual fuel and diesel in-cylinder pressure and IMEPg comparison (1500 rpm; 580 N-m)

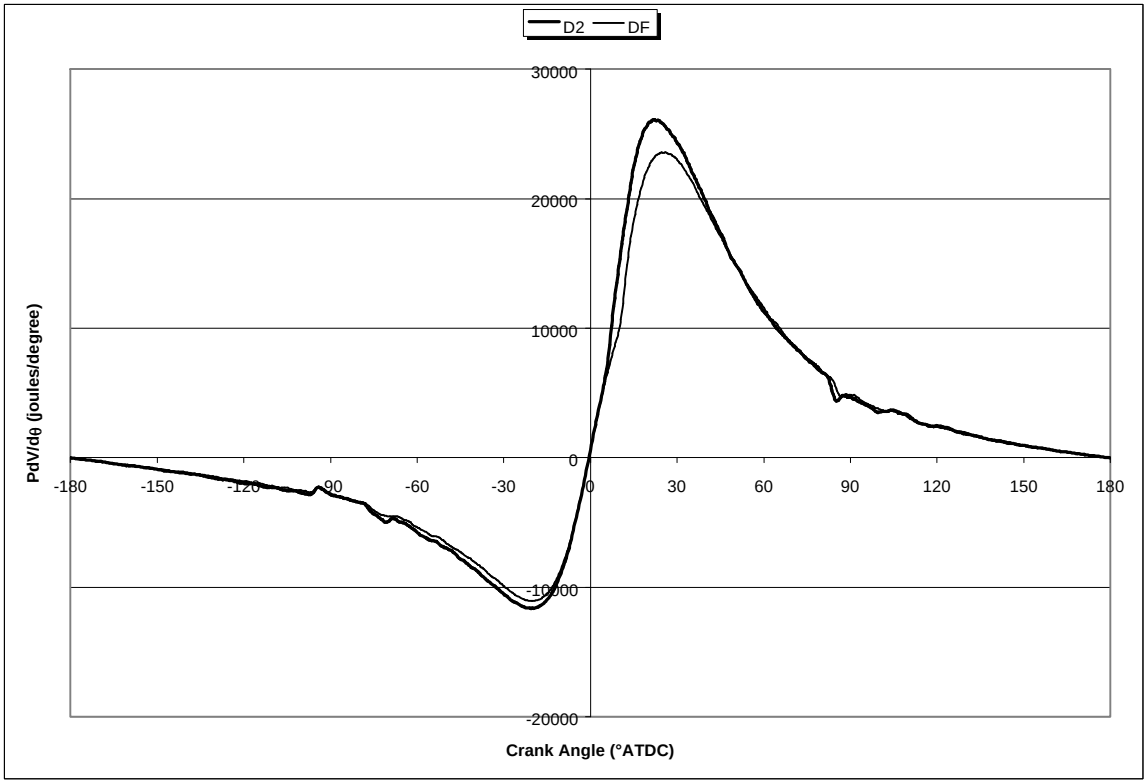

Figure 45: Dual fuel and diesel PdV/dθ comparison (1500 rpm; 335 N-m)

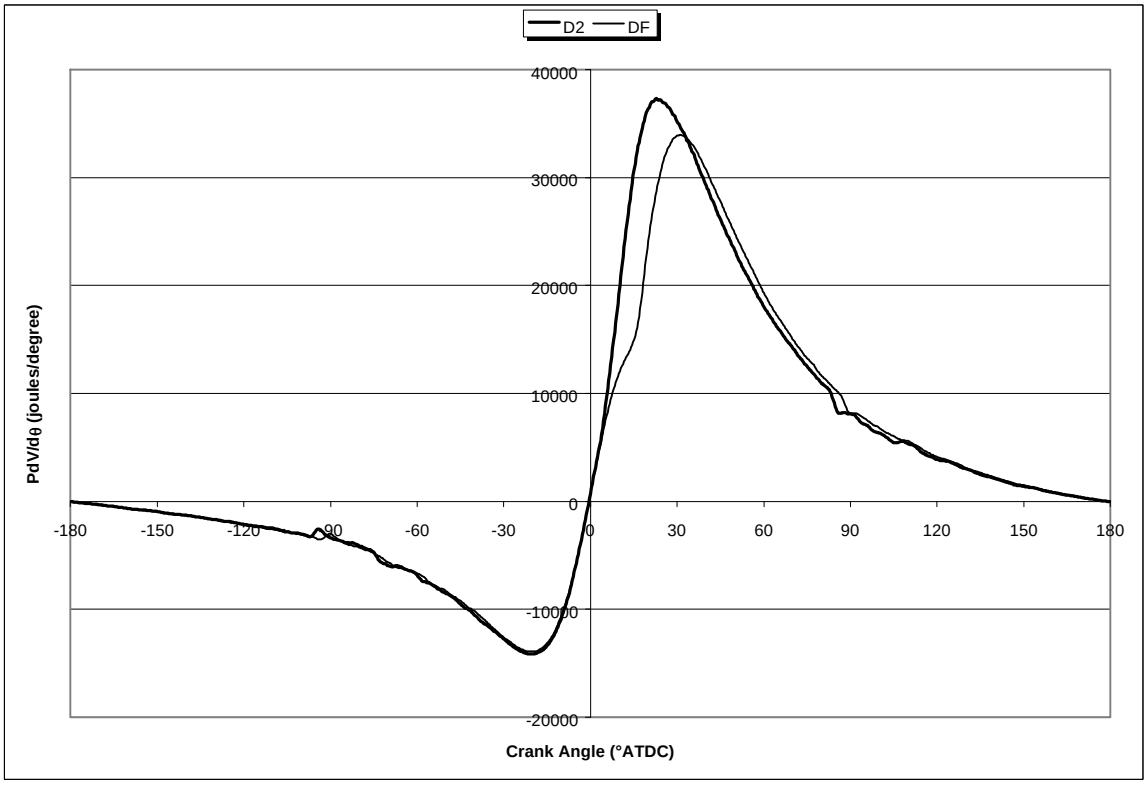

Figure 46: Dual fuel and diesel PdV/dθ comparison (1500 rpm; 580 N-m)

5 Conclusions & Recommendations

Over the course of this project, a direct injected diesel engine was converted to pilot-injected dual fuel operation with natural gas. However, many small intermediate steps were required to determine if any real emissions and efficiency benefits would be realized from this conversion. First, the engine had the be tested in its original configuration, and then a completely new engine control unit had to be designed, built, and fitted to perform extensive sweep testing of engine operation parameters including FIPW, ADV, ICP, and CNG flow, among others. Optimized dual fuel operation parameters were found using the information gathered from these sweeps. Finally, the engine was tested in optimized dual fuel mode to compare and confirm any emissions and efficiency improvements that resulted.

The comparative data presented in Chapter 4 shows that there were indeed significant improvements in emissions of NO_x and PM for dual fuel operation. Even more noteworthy is the fact that reduction in NO_x and PM come with a slight increase in thermal efficiency. These benefits appear with a dramatic decrease in diesel fuel usage compared to diesel-only operation. However, these benefits come with a price. Both THC and NMHC, as well as CO production, increased substantially over diesel-only levels. Although this is a concern, it should not cause alarm because CO and HC are easily reduced by exhaust after-treatment with an oxidation catalyst. This research also showed that the HEUI injection system is well suited for use in a dual fuel conversion since it allows for flexible fuel injection, critical for reducing the dual fuel emissions.

Admittedly, the scope of this research is limited as only two set points were investigated. However, it does prove that emissions and efficiency improvements over

diesel-only operation can be obtained with a dual fuel conversion and provides the groundwork for more extensive research. Future work should focus on optimizing the engine for more speeds and loads with the final goal being a complete dual fuel control scheme with special attention to further reduction of pilot quantities. Once the engine is fully optimized for steady state dual fuel operation, then transient tests may be attempted.

Other methods of emissions reduction should also be researched. Some methods include exhaust gas recirculation which was named earlier as a means to reduce HC emissions at light load, turbocharger air bypass, and possibly an investigation of different pilot fuels such as dimethyl ether and Fischer-Tropsch fuels.

An attempt to further minimize diesel usage should also be made. Modified HEUI injectors capable of injecting micro pilot quantities of diesel fuel could be used. The use of a well matched set of micro pilot injectors would also alleviate the cylinder-to-cylinder injection variations that caused the apparent IMEPg differences between dual fuel and diesel-only operation.

In general, it can be seen from this research that dual fuel engines are a viable way to use environmentally and economically appealing natural gas directly as a vehicular fuel. A dual fuel engine, when properly optimized, can produce lower emissions than a diesel engine with diesel-like thermal efficiency, while offering a significant reduction in diesel fuel usage and acceptable driveability.

References

1. Weaver, C. S. and Turner, S. H., "Dual Fuel Natural Gas/Diesel Engines: Technology, Performance, and Emissions," SAE Paper 940548.

2. Varde, K. S., "Propane Fumigation in a Direct Injection Type Diesel Engine," SAE Paper 831354.

3. Daisho, Y., Takahashi, Y. I., Nakayama, S., Kihara, R., Saito, T., "Controlling Combustion and Exhaust Emissions in a Direct-Injection Diesel Engine Dual-Fueled with Natural Gas," SAE Paper 952436.

4. Brogan, T. R., Graboski, M. S., Macomber, J. R., Helmich, M. J., Schaub, F. S., "Operation of a Large Bore Medium Speed Turbosupercharged Dual Fuel Engine on Low BTU Wood Gas," ASME 1993 ICE-Vol. 20 pp. 51-66.

5. Aly, H.and Siemer, G., "Experimental Investigation of Gaseous Hydrogen Utilization in a Dual-Fuel Engine for Stationary Power Plants," ASME 1993 ICE-Vol. 20 pp. 67-79.

6. Poonia, M. P., Ramesh, A., Gaur, R. R., "Effect of Intake Air Temperature and Pilot Fuel Quantity on the Combustion Characteristics of a LPG Dual Fuel Engine," SAE Paper 982455.

7. Dardalis, D., Matthews, R. D., Lewis, D., Davis, K., "The Texas Project, Part 5 - Economic Analysis: CNG and LPG Conversions of Light-Duty Vehicle Fleets," SAE Paper 982447.

8. Liss, W. E., Thrasher, W. H., "Natural Gas as a Stationary and Vehicular Fuel," SAE Paper 912364.

9. Hupperich, P., Dürnhoiz, M., "Time-Controller Pilot Injection for Stationary and Heavy-Duty Gas Engines," SAE Paper 971713.

10. Karim, G. A., Liu, Z., Jones, W., "Exhaust Emissions from Dual Fuel Engines at Light Load," SAE Paper 932822.

11. Gebert, K., Beck, N. J., Barkhimer, R. L., Wong, H., "Strategies to Improve Combustion and Emission Characteristics of Dual Fuel Pilot Ignited Natural Gas Engines," SAE Paper 971712.

12. Karim, G. A., "An Examination of Some Measures for Improving the Performance of Gas Fuelled Diesel Engines at Light Load," SAE Paper 912366.

13. Liu, Z., Karim, G. A., "The Ignition Delay Period in Dual Fuel Engines," SAE Paper 950466.

14. Li, X., Chippior, W. L., Gülder, O., L., "Effects of Cetane Enhancing Additives and Ignition Quality on Diesel Engine Emissions," SAE Paper 972968.

15. Gunea, C., Razavi M. R. M., Karim, G. A., "The Effects of Pilot Fuel Quality on Dual Fuel Engine Ignition Delay," SAE Paper 982453.

16. Gebert, K., Beck, N. J., Barkhimer, R. L., Wong, H., "Development of Pilot Fuel Injection System for CNG Engine," SAE Paper 961100.

17. Liu, Z., Karim, G. A., "A Predictive Model for the Combustion Process in Dual Fuel Engines," SAE Paper 952435.

18. Miyoshi, N., Matsumoto, S., Katoh, K., Tanaka, T., Harada, J., Takahashi, N., Yokota, K., Sugiura, M., Kasahara, K., “Development of a new Concept Three-Way Catalyst for Automotive Lean-Burn Engines,” SAE Paper 950809.

19. Penetrante, B. M., Bruasaco, R. M., Merritt, B. T., Pitz, W. J., Vogtlin, G. E., Kung, M. C., Kung, H. H., Wan, C. Z., Voss, K. E., "Plasma Assisted Catalytic Reduction of NO_x," SAE Paper 982508.

20. Lancaster, D. R., Krieger, R. B., Lienesch, J. H., "Measurement and Analysis of Engine Pressure Data," SAE Paper 750026.

21. Heywood, J. B., Internal Combustion Engine Fundamentals, McGraw-Hill, New York, NY, 1988.

22. Matekunas, F. A., "Modes and Measures of Cyclic Combustion Variability," SAE Paper 830337.

23. Degobert, P., Automobiles and Pollution, SAE Publications, Warrendale, PA, 1995.

Appendix A: Natural gas analysis

A sample of the natural gas used in testing was taken from the West Virginia University supply and sent to Gas Analytical Services, Inc., of Bridgeport, WV for analysis. The following analysis was used for all calculations involving natural gas.

Natural gas fractional analysis			
Component	MOL%	M	MOL% * M
methane	96.113	16.043	15.419409
ethane	2.571	30.07	0.7730997
propane	0.359	44.097	0.1583082
I-butane	0.05	58.124	0.029062
N-butane	0.09	58.124	0.0523116
I-pentane	0.01	72.151	0.0072151
N-pentane	0	72.151	0
nitrogen	0.598	28.016	0.1675357
CO2	0.149	44.011	0.0655764
oxygen	0	32	0
hexanes	0.06	86.178	0.0517068
Apparent Molecular Weight:			16.724224

Table 17: Natural gas analysis

Appendix B: Natural gas control valve calibration

The IMPCO natural gas control valve was supplied with the following calibration information. This information was used to generate a calibration equation which was used to convert the signal from the gas mass sensor to engineering units.

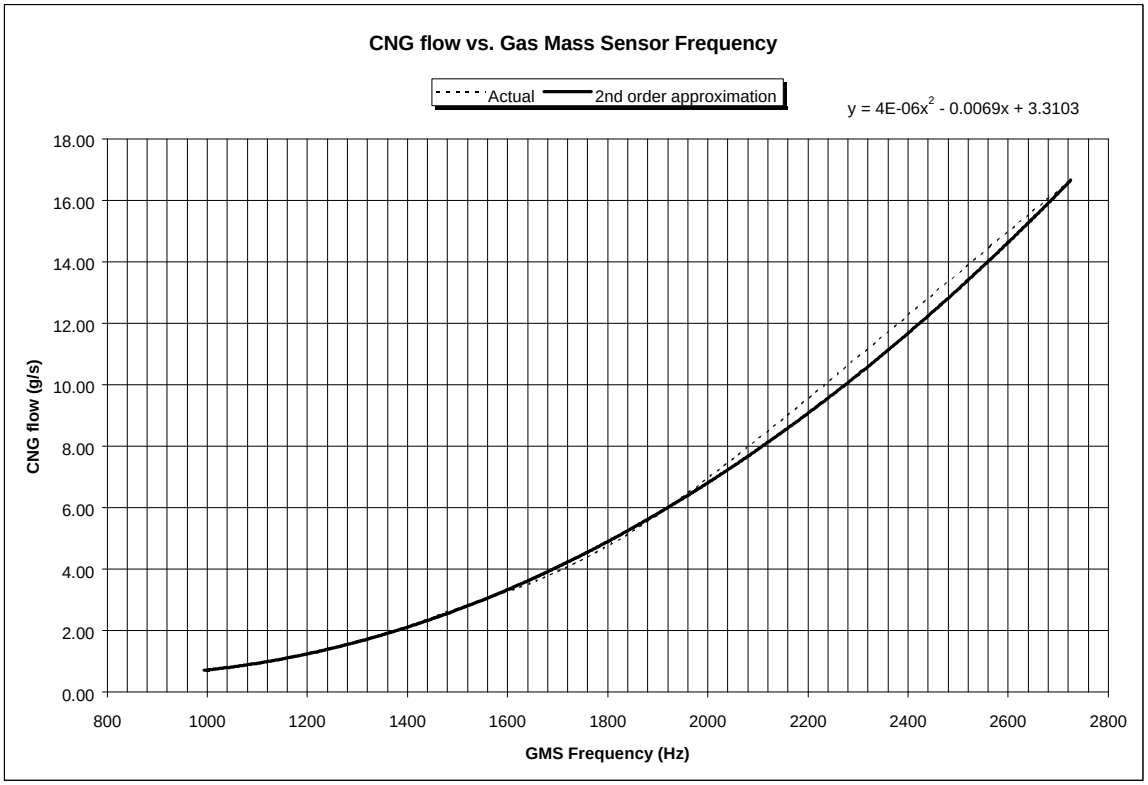

Figure 47: IMPCO gas mass sensor calibration

Appendix C: WVU-ECU Pinout diagram

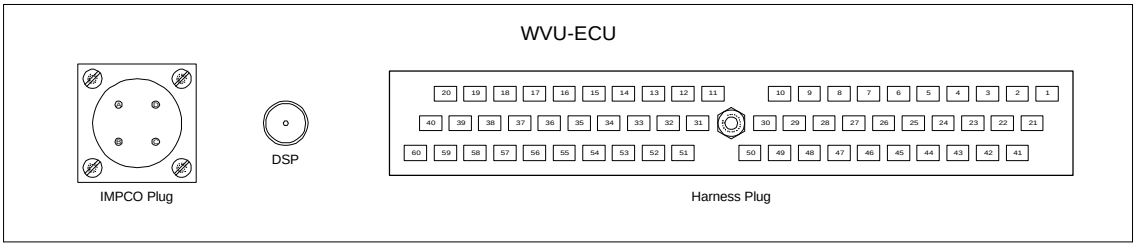

Figure 48: View of the interface end of the WVU-ECU

IMPCO Plug		Harness Plug	
A	+12V	7	ECT
B	GND	14	EOT
C	MCV(desired)	20	GND
D	GMS(measured)	21	ICPR
		22	FDCS
		24	IDM_F
		26	VREF(+5V)
		27	ICP
		31	CAMP GND
		33	IDM_EN
		34	FIS
		37	+12V
		40	GND
		45	MAP
		46	SIGGND
		47	APS
		50	CNG Flow (MCV)
		51	CNG Flow (GMS)
		56	CAMP
		57	+12V
		60	GND

Table 18: WVU-ECU Pinouts*

* The DSP (Digital Signal Processing) connection was an additional signal provided for another project and was not used in this research.

Appendix D: WVU-ECU Wiring diagrams

The following pages contain the circuit diagrams for the WVU-ECU.

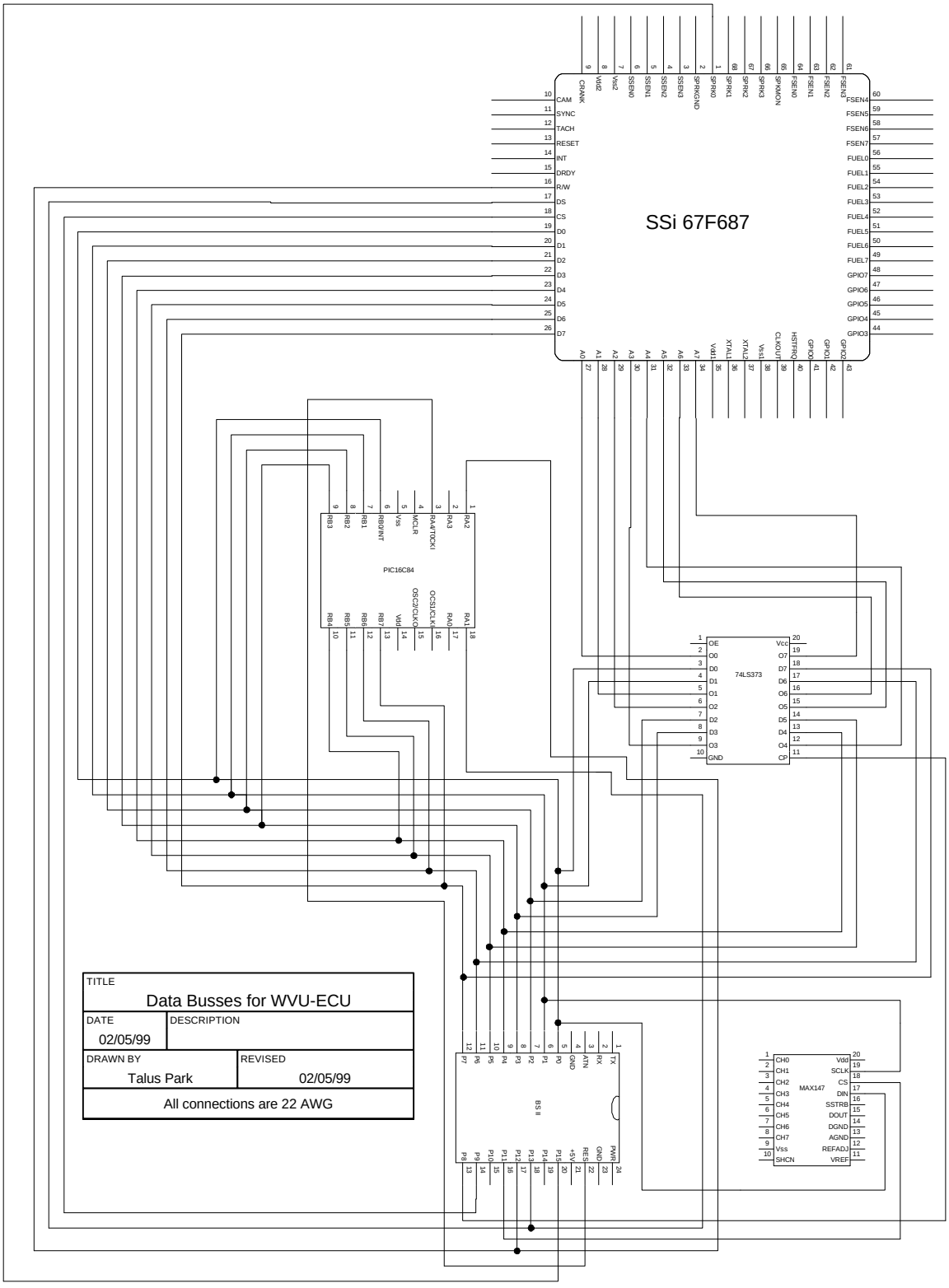
SSi 67F687
PIC16C84
74LS373
MAX147
BSII
TITLE
Data Busses for WVU-ECU
DATE
02/05/99
DESCRIPTION
DRAWN BY
Talus Park
REVISED
02/05/99
All connections are 22 AWG

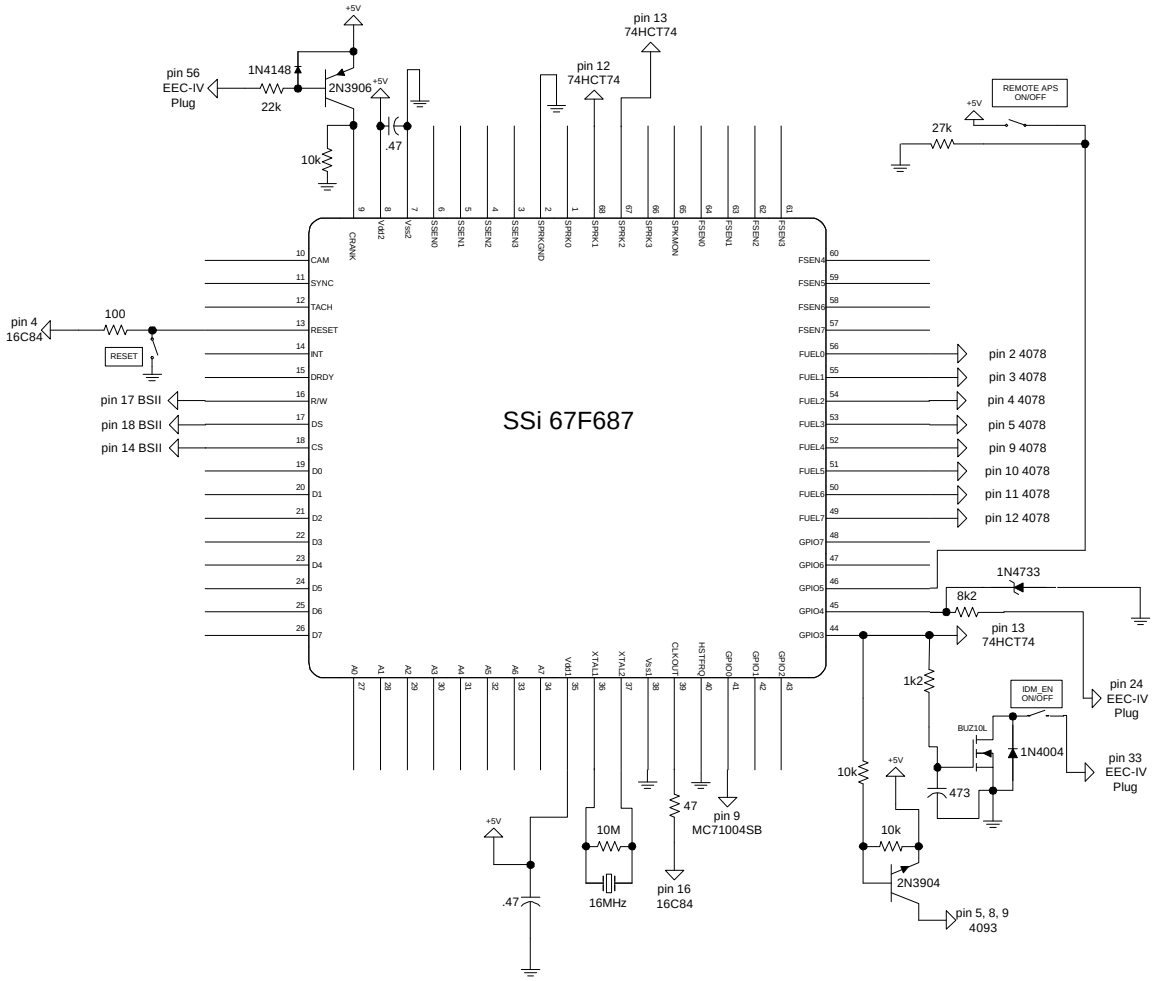

TITLE	Engine Interface Peripheral
DATE: 2/10/99	DESCRIPTION: All connections except data busses.
DRAWN BY: Talus Park	REVISED: 2/10/99
All connections are 22 AWG	

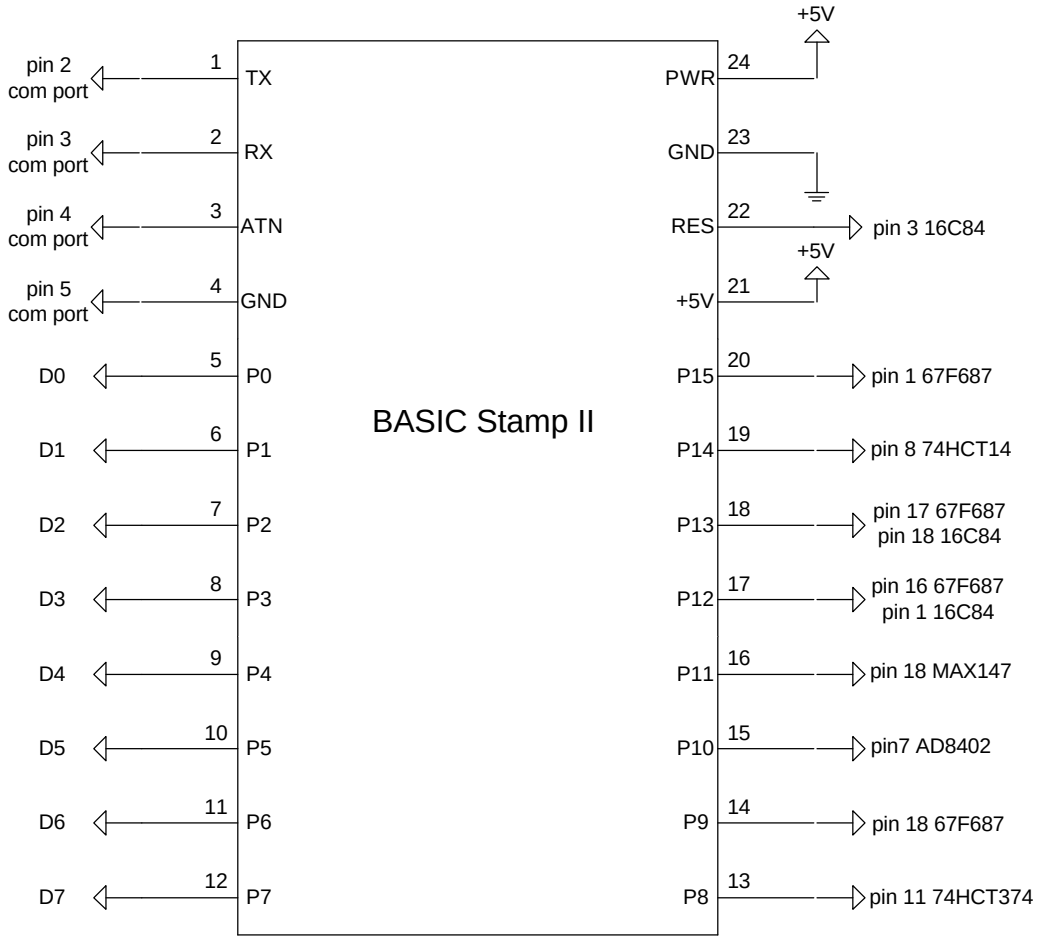

TITLE	
Run-Time Microcontroller	
DATE 2/9/99	DESCRIPTION All connections except data busses.
DRAWN BY Talus Park	REVISED 2/9/99
All connections are 22 AWG	

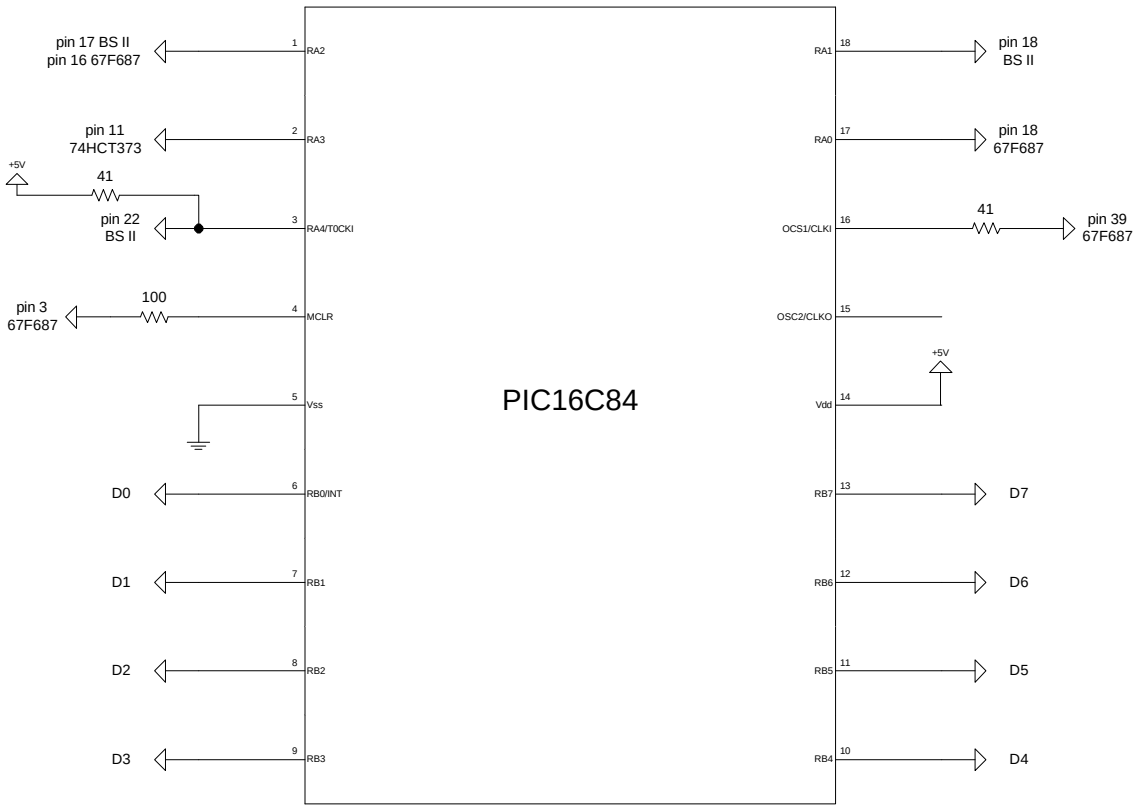

TITLE	
Initialization Microcontroller	
DATE	DESCRIPTION
2/10/99	All connections except data busses.
DRAWN BY	REVISED
Talus Park	2/10/99
All connections are 22 AWG	

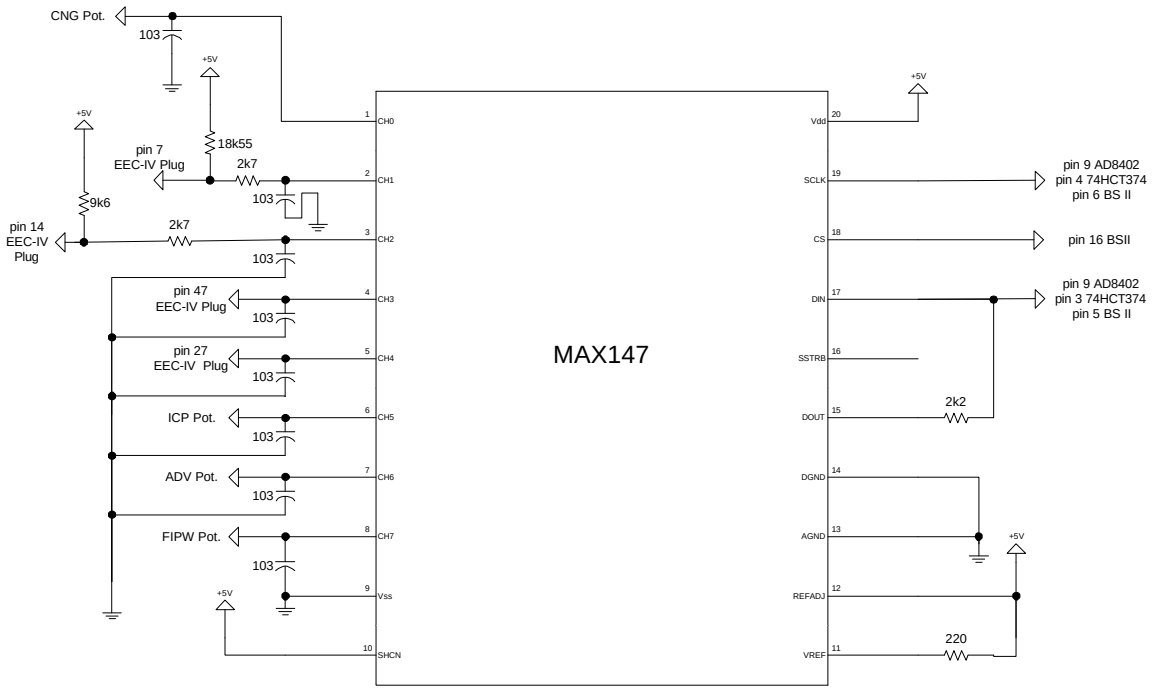

TITLE	12 bit Analog to Digital Converter
DATE: 2/7/99	DESCRIPTION: All connections except data busses.
DRAWN BY: Talus Park	REVISED: 2/7/99
All connections are 22 AWG	

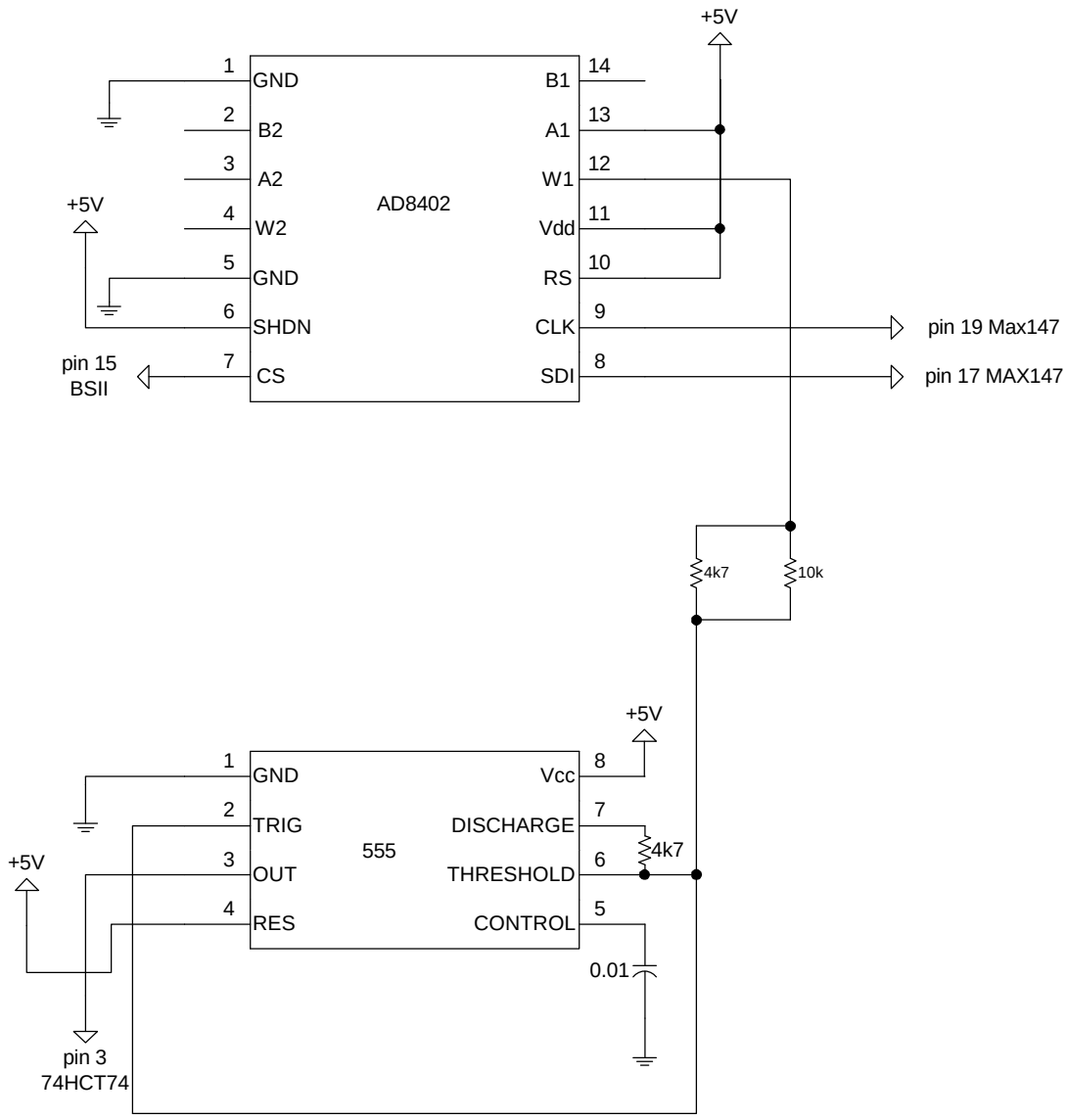

TITLE	
Variable PWM generator	
DATE: 2/10/99	DESCRIPTION: All connections except data busses.
DRAWN BY: Talus Park	REVISED: 2/10/99
All connections are 22 AWG	

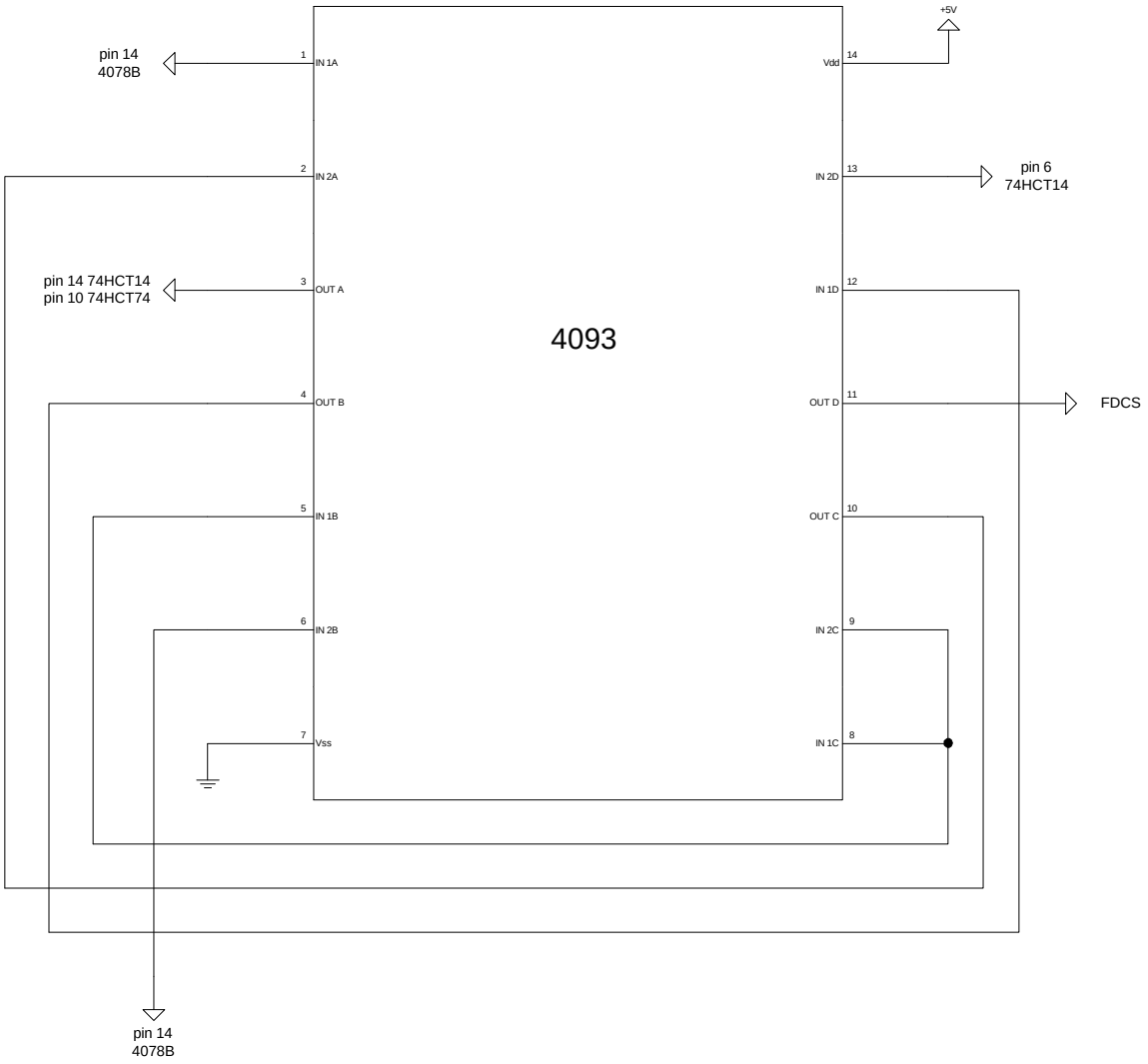

TITLE	EEC-IV / BASIC Stamp Switch
DATE: 2/10/99	DESCRIPTION: All connections except data busses.
DRAWN BY: Talus Park	REVISED: 2/10/99
All connections are 22 AWG	

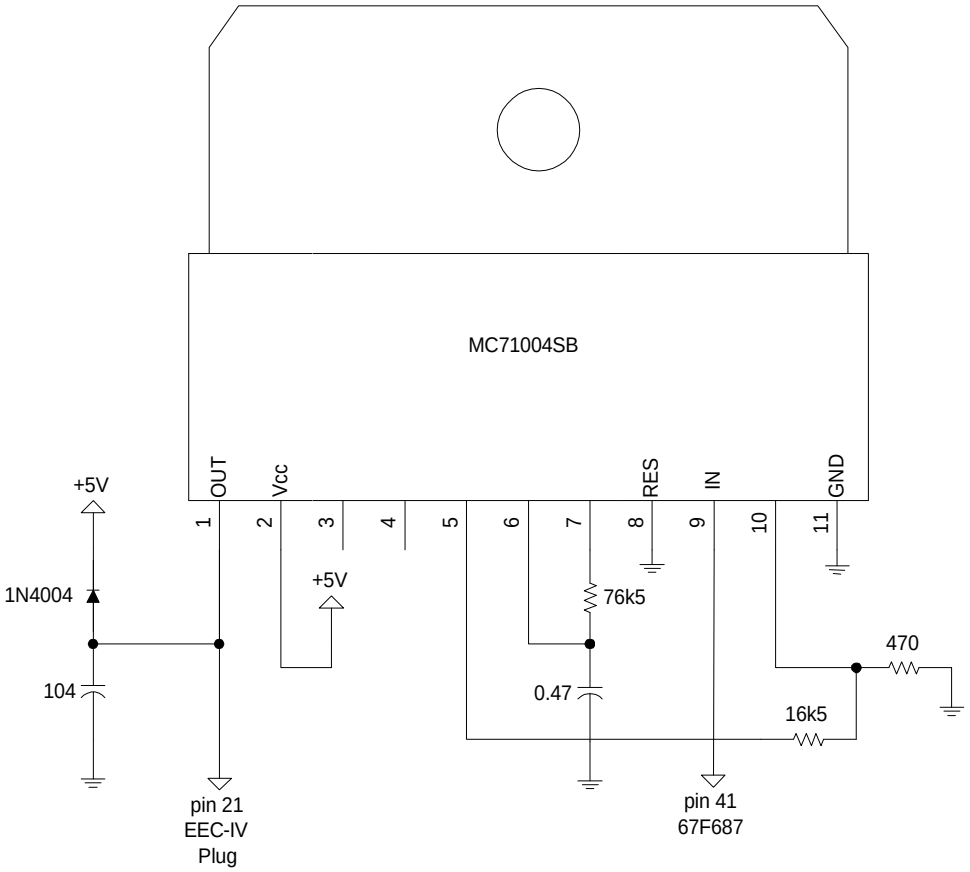

TITLE	
ICP Regulator Control	
DATE 2/9/99	DESCRIPTION All connections except data busses.
DRAWN BY Talus Park	REVISED 2/9/99
All connections are 22 AWG	

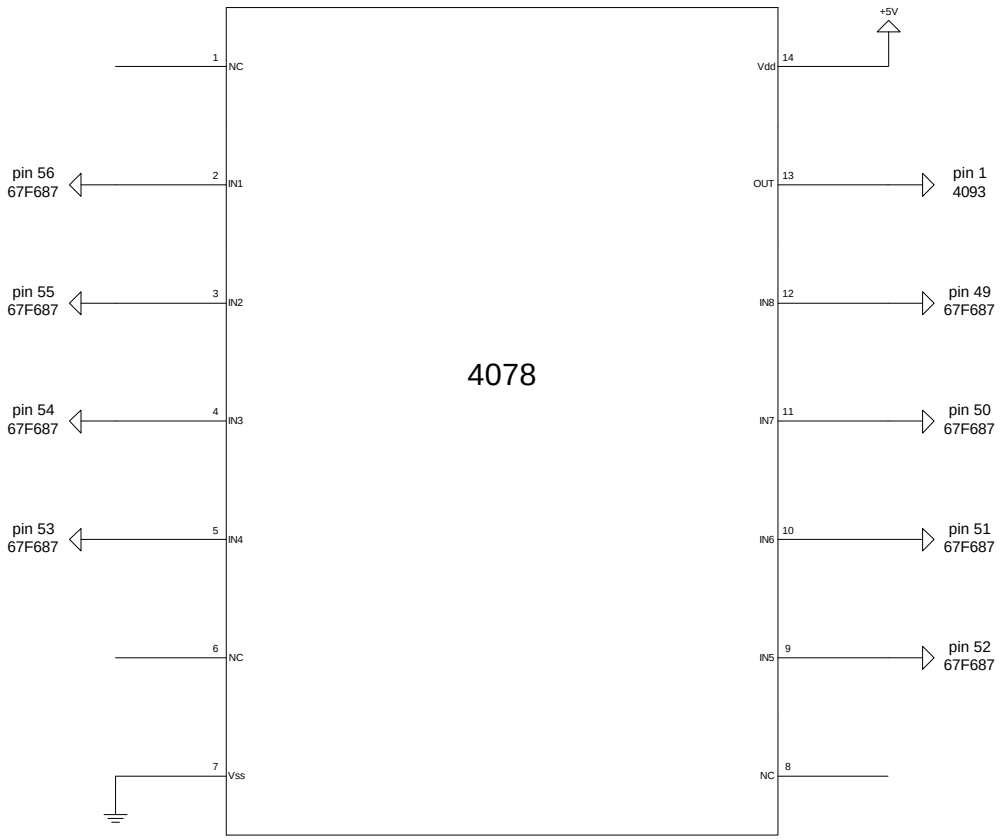

TITLE	
FIPW Combiner	
DATE 2/10/99	DESCRIPTION All connections except data busses.
DRAWN BY Talus Park	REVISED 2/10/99
All connections are 22 AWG	

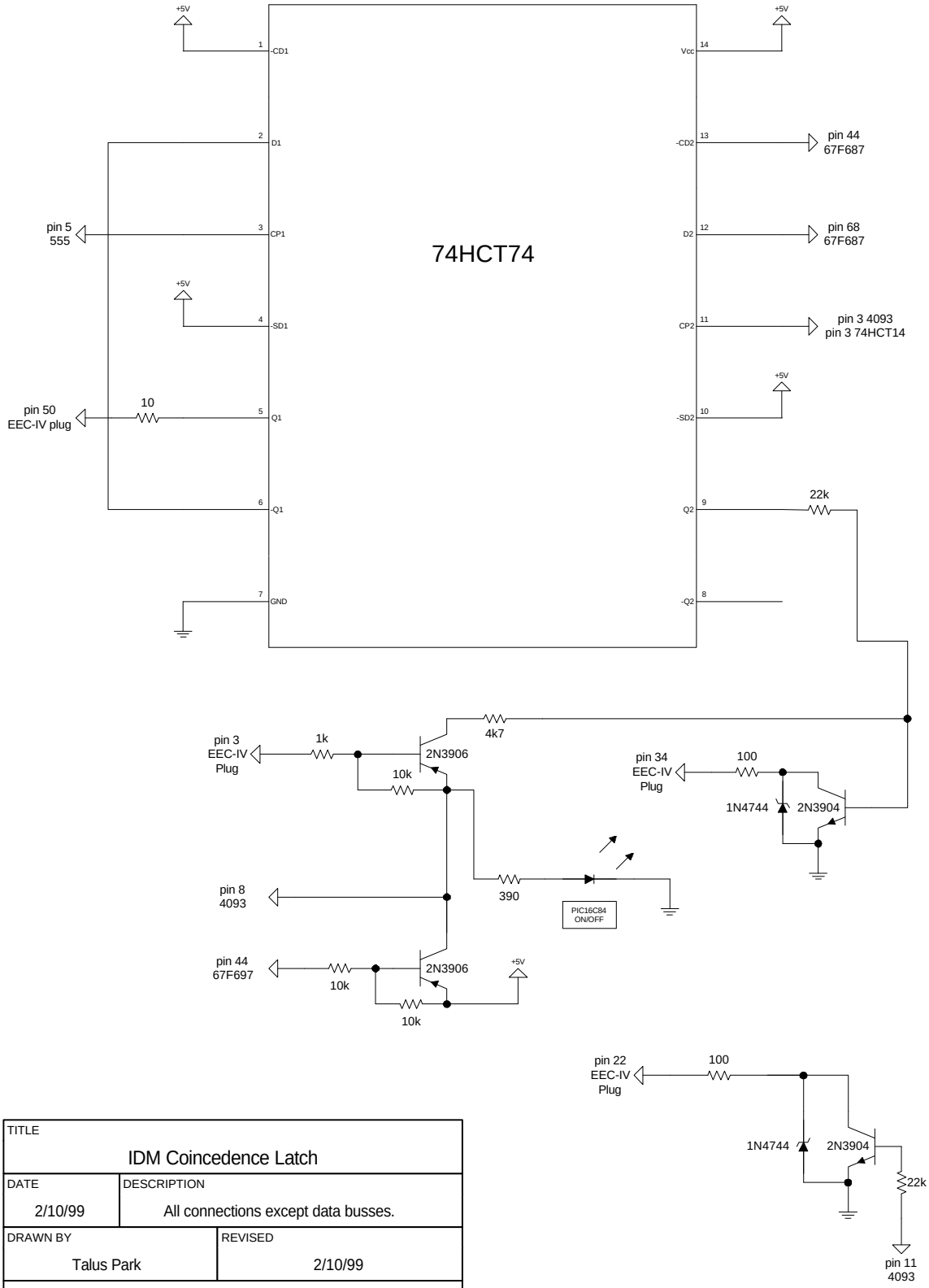

TITLE	IDM Coincedence Latch
DATE: 2/10/99	DESCRIPTION: All connections except data busses.
DRAWN BY: Talus Park	REVISED: 2/10/99
All connections are 22 AWG	

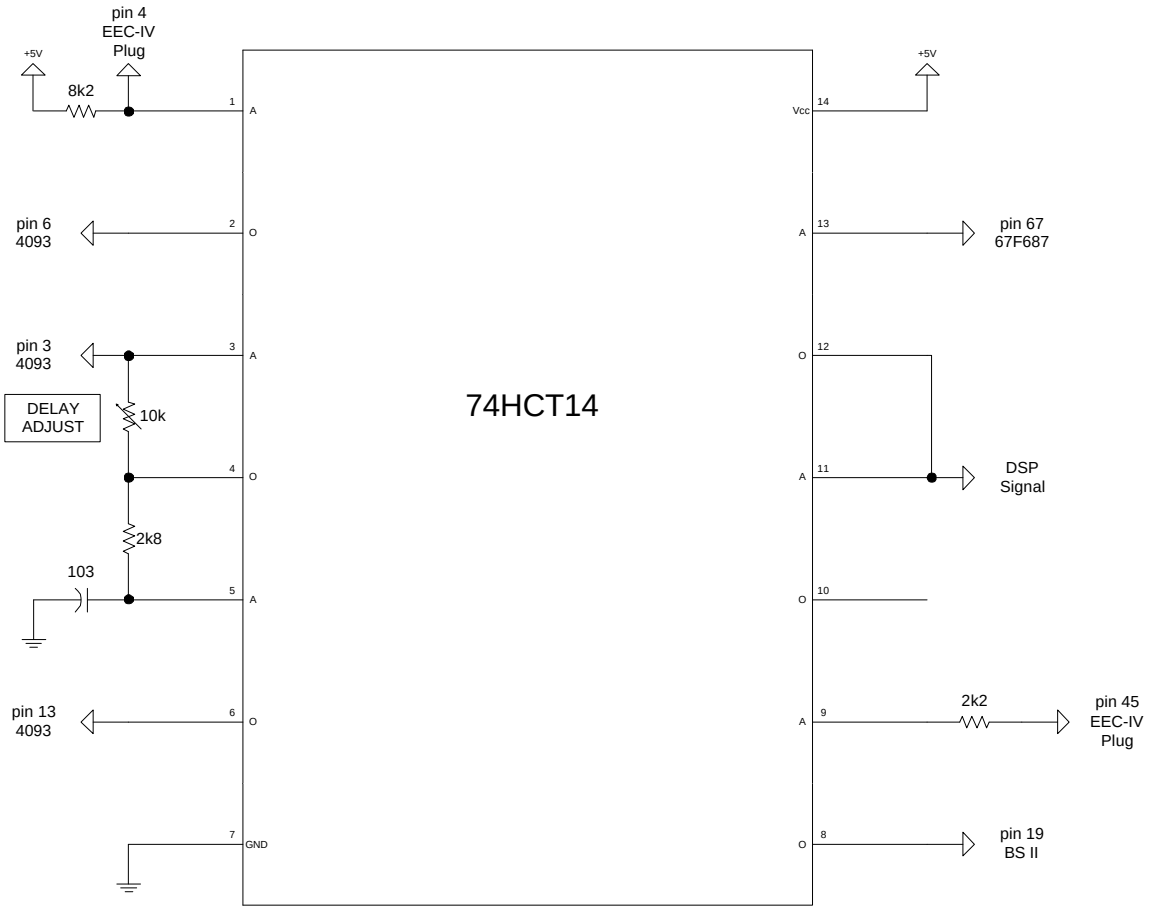

TITLE	
Schmitt Trigger	
DATE 2/10/99	DESCRIPTION All connections except data busses.
DRAWN BY Talus Park	REVISED 2/10/99
All connections are 22 AWG	

Appendix E: PIC16C84 Code

The Microchip PIC16C84 machine code listing for initializing the SSi67F687:

```
;Navistar Initialization Routines
;
; RJA, TP - 06/12/1998
;

        list p=16C84, r=hex
        include "p16cxx.inc"

;variables:

W_temp  equ 0Ch
S_temp  equ 0Dh

lataddr equ 0Eh

eipdata equ 0Fh
counter equ 10h

InjPress equ 11h

DelVal  equ  12h

;constants

MinInjPress     equ     .10
MinIdleFuel     equ     .109     (435/4 usec)

;definitions

#define cs687   PORTA,0
#define ds      PORTA,1
#define rw      PORTA,2
#define addlat  PORTA,3
#define BS2res  PORTA,4

#define CARRY   STATUS,C
#define ZERO    STATUS,Z
#define T0OV    INTCON, T0IF

;start here:

        org 0
        goto init

        org 4
        goto int_vec

        org 10

init:
        clrf INTCON             ;reset all interrupts and enables
```

```
        movlw B'00001101'
        movwf PORTA
        clrf PORTB

        bsf STATUS, RP0         ;set to page 1
        clrf TRISA              ;set port a to all outputs
        movlw 0FFh              ;set port b to all inputs
        movwf TRISB

        movlw B'10000111'       ;set up Timer0 to /256
        movwf TMR0              ;(option register)

        clrf STATUS             ;clear all status flags and pages

        clrf INTCON             ;clear all interrupts
        clrf PCLATH             ;clear program counter high part

;-----------------------------------------------------

;Initialize '687

; --- set up general purpose i/o ----

        movlw 0E7h      ;GOER
        movwf lataddr
        movlw 0Fh       ;set 7-4 as in, 3-0 as out
        movwf eipdata
        call eipwrite

        movlw 0E8h      ;GMSR
        movwf lataddr
        movlw 11h       ;set 0 to PWM, 1,2,3 as out, 4 as edge, 5,6,7
as in
        movwf eipdata
        call eipwrite

        movlw 0E9h      ;GESR
        movwf lataddr
        movlw 10h       ;ES4
        movwf eipdata
        call eipwrite

        movlw 0E6h      ;GOUT
        movwf lataddr
        movlw 0         ;clear all outputs
        movwf eipdata
        call eipwrite

        movlw 0E0h      ;PWMCTL
        movwf lataddr
        movlw 04h       ;set pwm0 & pwm1 to 411Hz
        movwf eipdata
        call eipwrite

;--- switch on IDM ----

        movlw 0F1h              ;SPRK
```

```
        movwf lataddr
        movlw 02h               ;drop cam phasing
        movwf eipdata
        call eipwrite

        movlw 0E6h              ;GOUT
        movwf lataddr
        movlw 08h               ;DO3
        movwf eipdata
        call eipwrite

;--- set injection control pressure ----

        movlw 0E1h              ;PWMDC0
        movwf lataddr
        movlw MinInjPress
        movwf eipdata
        call eipwrite

; --- set up ept ----

        movlw 0F6h              ;GCR
        movwf lataddr
        movlw 0B1h              ;reset to page 1 addressing, hard
                                ;shutdown
        movwf eipdata
        call eipwrite

; --- clear eip ram ----

        bsf STATUS, RP0         ;set to page 1
        clrf TRISB              ;set port b to outputs
        bcf STATUS, RP0         ;set back to page 0

        clrf counter            ;zero the '687 RAM

II1:
        movf counter, W
        movwf PORTB

        bcf addlat
        bsf addlat

        clrf PORTB

        bcf rw
        bcf cs687
        bsf ds
        bcf ds
        bsf cs687
        bsf rw

        incf counter
        movlw 078h
        subwf counter, W
        btfss CARRY
        goto II1
```

```
; --- load ept parameter table ----

        movlw 00h       ;CWSP00
        movwf lataddr
        movlw 03Ch
        movwf eipdata
        call eipwrite

        movlw 01h       ;CWTH00
        movwf lataddr
        movlw 01h
        movwf eipdata
        call eipwrite

        movlw 02h       ;CWSP01
        movwf lataddr
        movlw 51h       ;20.25 x 4 degrees
        movwf eipdata
        call eipwrite

        movlw 03h       ;CWTH01
        movwf lataddr
        movlw 17h
        movwf eipdata
        call eipwrite

        movlw 04h       ;CWSP02
        movwf lataddr
        movlw 27h       ;9.75 x 4 degrees
        movwf eipdata
        call eipwrite

        movlw 40h       ;PRACH1
        movwf lataddr
        movlw 05h       ;angle of tooth 22; section 3       345ø
        movwf eipdata
        call eipwrite

        movlw 41h       ;PRACL1
        movwf lataddr
        movlw 64h       ;angle of tooth 22; section 3        345ø
        movwf eipdata
        call eipwrite

        movlw 42h       ;PRTN01
        movwf lataddr
        movlw 16h       ;tooth 22; section 3
        movwf eipdata
        call eipwrite

        movlw 60h       ;PATRN1
        movwf lataddr
        movlw 01h
        movwf eipdata
        call eipwrite
```

```
movlw 61h       ;PATRN2
movwf lataddr
movlw 0F9h
movwf eipdata
call eipwrite

movlw 62h       ;PATRN3
movwf lataddr
movlw 0FAh
movwf eipdata
call eipwrite

movlw 63h       ;PATRN4
movwf lataddr
movlw 0FBh
movwf eipdata
call eipwrite

movlw 64h       ;PATRN5
movwf lataddr
movlw 0FCh
movwf eipdata
call eipwrite

movlw 65h       ;PATRN6
movwf lataddr
movlw 0FDh
movwf eipdata
call eipwrite

movlw 66h       ;PATRN7
movwf lataddr
movlw 0FEh
movwf eipdata
call eipwrite

movlw 67h       ;PATRN8
movwf lataddr
movlw 0FFh
movwf eipdata
call eipwrite

movlw 68h       ;PAREG1
movwf lataddr
movlw 21h
movwf eipdata
call eipwrite

movlw 69h       ;PAREG2
movwf lataddr
movlw 0C0h
movwf eipdata
call eipwrite

movlw 6Ah       ;PAREG3
movwf lataddr
movlw 42h
```

```
movwf eipdata
call eipwrite

movlw 6Bh       ;PAREG4
movwf lataddr
movlw 21h
movwf eipdata
call eipwrite

movlw 6Ch       ;CRKCFG
movwf lataddr
movlw 89h       ;digital input, no invert
movwf eipdata
call eipwrite

movlw 6Dh       ;CAMCFG
movwf lataddr
movlw 15h       ;digital input, no invert
movwf eipdata
call eipwrite

movlw 70h       ;PMREG1
movwf lataddr
movlw 02h
movwf eipdata
call eipwrite

movlw 71h       ;PMREG2
movwf lataddr
movlw 60h
movwf eipdata
call eipwrite

movlw 72h       ;PMREG3
movwf lataddr
movlw 17h
movwf eipdata
call eipwrite

movlw 74h       ;PMREG5
movwf lataddr
movlw 3Ch
movwf eipdata
call eipwrite

movlw 75h       ;PMREG5(dup)
movwf lataddr
movlw 3Ch
movwf eipdata
call eipwrite

movlw 0C3h      ;EPTRST
movwf lataddr
movlw 18h       ;15 cam degrees (30 crank degrees)
movwf eipdata
call eipwrite
```

```
; ---------   end of page 1 assignments ----

        movlw 0F6h      ;GCR
        movwf lataddr
        movlw 090h       ;reset to page 0, hold spark and fuel off
        movwf eipdata
        call eipwrite

;--- set spark 0 for engine speed sensor ---

; spark 0:

        movlw  00h      ;start: 0ø
        movwf lataddr
        movlw 00h
        movwf eipdata
        call eipwrite

        movlw 01h
        movwf lataddr
        movlw 00h
        movwf eipdata
        call eipwrite

        movlw 02h       ;stop: 7.5ø
        movwf lataddr
        movlw 00h
        movwf eipdata
        call eipwrite

        movlw 03h
        movwf lataddr
        movlw 1Eh
        movwf eipdata
        call eipwrite

;--- set spark 1 and 3 for cylinder identification CI ---

;spark 1:

        movlw 04h       ;start: 320ø
        movwf lataddr
        movlw 05h
        movwf eipdata
        call eipwrite

        movlw 05h
        movwf lataddr
        movlw 00h
        movwf eipdata
        call eipwrite

        movlw 06h       ;stop: 140ø
        movwf lataddr
        movlw 02h
        movwf eipdata
        call eipwrite
```

```
        movlw 07h
        movwf lataddr
        movlw 30h
        movwf eipdata
        call eipwrite

;--- set spark 2 for DSP triggering ---

;spark 2

        movlw 08h
        movwf lataddr
        movlw 03h       ;start: 225ø
        movwf eipdata
        call eipwrite

        movlw 09h
        movwf lataddr
        movlw 84h
        movwf eipdata
        call eipwrite

        movlw 0Ah
        movwf lataddr
        movlw 00h       ;stop: 45ø
        movwf eipdata
        call eipwrite

        movlw 0Bh
        movwf lataddr
        movlw 0B4h
        movwf eipdata
        call eipwrite

;--- set spark 1 and 3 for cylinder identification CI ---

;spark 3:

        movlw 0Ch       ;start: 320ø
        movwf lataddr
        movlw 05h
        movwf eipdata
        call eipwrite

        movlw 0Dh
        movwf lataddr
        movlw 00h
        movwf eipdata
        call eipwrite

        movlw 0Eh       ;stop: 140ø
        movwf lataddr
        movlw 02h
        movwf eipdata
        call eipwrite
```

```
        movlw 0Fh
        movwf lataddr
        movlw 30h
        movwf eipdata
        call eipwrite

;--- set up fuel ram ---

        movlw 20h       ;FSTRH0
        movwf lataddr
        movlw 0h
        movwf eipdata
        call eipwrite

        movlw 21h       ;FSTRL0
        movwf lataddr
        movlw 0h
        movwf eipdata
        call eipwrite

        movlw 22h       ;FPTH0
        movwf lataddr
        movlw 0h
        movwf eipdata
        call eipwrite

        movlw 23h       ;FPTL0
        movwf lataddr
        movlw MinIdleFuel
        movwf eipdata
        call eipwrite

;---- enable some outputs ---

        movlw 0F2h      ;FUEL
        movwf lataddr
        movlw 00h       ;turn all fuel outputs low
        movwf eipdata
        call eipwrite

        movlw 0F7h      ;SMAP
        movwf lataddr
        movlw 0Dh       ;enable spark 0, 2 and 3
        movwf eipdata
        call eipwrite

        movlw 0F6h      ;GCR
        movwf lataddr
        movlw 00h       ;allow all outputs
        movwf eipdata
        call eipwrite

        movlw 0F0h      ;MASK
        movwf lataddr
        movlw 00h       ;reset interrupt mask to allow outputs
        movwf eipdata
        call eipwrite
```

```
;--- hand control over to Basic Stamp...

        bsf STATUS, RP0         ;set to page 1
        movlw 0FFh              ;set port a and b to all inputs
        movwf TRISA
        movwf TRISB

        bcf STATUS, RP0         ;set to page 0

;*****************************************************************

main_loop:
        nop
        goto $-1                ;wait here forever

;*****************************************************************

;Subroutines:

ShortDelay:             ;128us increments
        movwf DelVal
        comf DelVal, W
        movwf TMR0
        bcf T0OV
        btfss T0OV
        goto $ - 1
        retlw 0

LongDelay:              ;in 32.7 ms increments

        movwf counter   ;counts in 128us increments
        clrf TMR0
        bcf T0OV
        btfss T0OV
        goto $ - 1
        decfsz counter
        goto $ - 4
        retlw 0

eipwrite:

        bsf STATUS, RP0         ;set to page 1
        clrf TRISB              ;set TRISB to outputs
        bcf STATUS, RP0         ;set back to page 0
        movf lataddr, W         ;write out lataddr
        movwf PORTB
        bcf addlat              ;set latch enable low
        bsf addlat              ;set latch enable high
        movf eipdata, W         ;outl = eipdata
        movwf PORTB
        bcf rw                  ;set to write
        bcf cs687               ;set 687 cs low
        bsf ds                  ;toggle ds high
        bcf ds                  ;ds low
        bsf cs687               ;set 687 cs high
        bsf rw                  ;high rw
```

```
        bsf STATUS, RP0         ;set to page 1
        movlw 0FFh
        movwf TRISB             ;set port b to inputs
        bcf STATUS, RP0         ;set back to page 0

        return

eipread:

        bsf rw
        bsf STATUS, RP0         ;set to page 1
        clrf TRISB              ;set TRISB to outputs
        bcf STATUS, RP0         ;set back to page 0
        movf lataddr, W
        bcf addlat
        bsf addlat
        bsf STATUS, RP0         ;set to page 1
        movlw 0FFh
        movwf TRISB             ;set port b to inputs
        bcf STATUS, RP0         ;set back to page 0
        bcf cs687
        bsf ds
        movf PORTB, W
        movwf eipdata
        bcf ds
        bsf cs687
      return

;-----------------------------------------------------------

int_vec:
push:
        movwf W_temp            ;copy W to temp
        swapf STATUS, W         ;swap status to be saved into W
        movwf S_temp            ;save status to STATUS temp

Which_Int:

        btfsc INTCON, RBIF      ;is it RB Port Change?
        goto RB_Change_Int

        btfsc INTCON, INTF      ;is it External Int?
        goto Ext_Int

        btfsc INTCON, T0IF      ;is it Timer0?
        goto T0_Int

        goto End_Int

RB_Change_Int:

        ;int handler goes here...

        bcf INTCON, RBIF        ;clear the rb int flag
        goto End_Int
```

```
Ext_Int:

        bcf INTCON, INTF        ;clear the ext int flag
        goto End_Int

T0_Int:
        bcf INTCON,T0IF         ;clear the timer0 interrupt flag bit

End_Int:

pop:
        swapf S_temp, W         ;swap nibbles in STATUS_temp and place
                                ;result in W
        movwf STATUS            ;move W into STATUS register
        swapf W_temp, 0         ;swap nibbles in W_temp
        swapf W_temp, W         ;swap nibbles in W_temp and place
                                ;result in W

        retfie

;---------------------------
        end
```

Appendix F: BASIC Stamp II code

The BASIC Stamp II PBASIC code used in the to execute the run-time operations:

```
'Navistar Engine Controller
'=========================
'
'   10/27/98
'
'    Local or remote CNG control: RJA/TP
'
'
'VARIABLE ASSIGNMENTS:

setadc var word
readadc var word
readsp var word
Temp var word
FIPW var word
FIStart var word
speed var word
APSVal var word

InjPress var byte

lataddr var byte
epromdata var byte
eipdata var byte
chann var byte
counter var byte
fcount var byte
flags var byte

'CONSTANT ASSIGNMENTS:

addlat      con 8       'address latch
cs687       con 9       'eip chip select
csvares con 10          'variable resistor chip select
csadc con 11            'adc chip select
rw    con 12            'eip read/write
ds    con 13            'eip data strobe

MinIdleFuel con   435 / 4     'microseconds
MaxInjTime  con  3050 / 4     'microseconds
MaxIdleFuel con  1200 / 4     'microseconds
MinInjPress con   10    'duty cycle units /256
MaxInjPress con   50    'duty cycle units

'FLAGS assignment:

RunFlag     var   flags.BIT0

'=============================================================================
=
```

```
Initialization:

      RunFlag = 0 'engine not running

      outc = $0F  'deselect all peripherals
      dirh = $3F  'set lower six bits of upper byte to out
      dirl = $FF  'set whole of lower byte to out

'-----------------

      counter = 20      'initialize counters

'set start-up fuel injection pulse width

      FIPW = MinIdleFuel
      gosub SetFIPW

' set fuel injection start angle

      FIStart = (358 * 4) - 1
      gosub SetInjStart

' set injection control pressure

      InjPress = MinInjPress
      gosub SetInjPress

' Engine starting

WaitForStart:

      pulsin 15,1,readadc     'Read 15ø pulse width
      debug dec5  readadc

      if readadc = 0 then WaitForStart

'else engine is running

'resume normal service

'turn off EEC interface

      lataddr = $0E6    'GOUT
      eipdata = $08
      gosub eipwrite

'allow cam phasing output

      lataddr = $F7     'SMAP
      eipdata = $0F     're-enable cam phasing
      gosub eipwrite

      lataddr = $F6     'GCR
      eipdata = $0      'programmed output control
      gosub eipwrite

      lataddr = $F0     'MASK
```

```
      eipdata =$0 'reset all interrupts
      gosub eipwrite

'==== START OF MAIN PROGRAM LOOP ===================================

main_loop:

      outc = $0F  'deselect all periphs

      lataddr = $C2           'check for SISR errors
      gosub eipread

'     if eipdata = 0 then end_o_error 'else reset interrupt mask

      debug "S"
      debug hex2 eipdata      'print error code
      debug ","

      lataddr = $F3           'check for sync errors
      gosub eipread
      debug "e"
      debug hex2 eipdata      'print error code
      debug ","

      lataddr = $F0           'MASK
      eipdata =$0
      gosub eipwrite

end_o_error:

      pulsin 15,1,readadc     'Read 15ø pulse width
      debug dec5  readadc

      speed = 62490 / readadc 'in 20 rpm increments

      debug "sp"
      debug dec4 speed
      debug ","

'read the setting potentiometers

      gosub ReadFIPpot
      if readadc > 435 then R1
      readadc = 435
R1:
      FIPW = readadc / 4
R2:
      gosub ReadAdvpot
      FIStart = 1440 - (readadc / 25)           '0ø to 40øBTDC

      gosub ReadICPpot

      lataddr = $E1     'PWMDC0 is used for ICP pwm
      eipdata = 10 + (readadc / 50) '10/256 to 50/256 duty cycle
      gosub eipwrite

'read the physical inputs
```

```
      gosub ReadATS           '
      debug dec4 readadc
      debug ","
      gosub ReadECT           '
      debug dec4 readadc
      debug ","
      gosub ReadEOT
      debug dec4 readadc
      debug ","
      gosub ReadAPS           '
      APSVal = readadc  'store APS adc value
      debug dec4 readadc
      debug ","
      gosub ReadICP
      debug dec4 readadc
'     debug ","
'     gosub ReadMAP           '
'     debug ","
'     debug dec4 readadc

'Check for local/remote analog input switch (via APS)

      lataddr = $E5           'GINP
      gosub eipread
      Temp = eipdata & $20    'check bit 5
      if Temp = 0 then R3     'local

'Use APS to set CNG

      Temp = APSVal / 16            'copy aps/16 into temp
      goto R4

R3:
      gosub ReadCNGPot
      Temp = readadc / 16           'convert to 8 bits

R4:
      Temp = Temp & $FF       'clear high bits
      low csvares             'clear variable resistor cs
      shiftout 0,1,1,[Temp\16]      'to resistor1 at address0
      high csvares                  'set variable resistor cs

'-----
      goto fuel_okay

'for idle mode:   750 rpm

      if speed < 37 then fuel_up

fuel_down:

      FIPW = FIPW - 4         'decrease fuelling
        if FIPW > MinIdleFuel then fuel_okay
      FIPW = MinIdleFuel
      goto fuel_okay
```

```
fuel_up:
      FIPW = FIPW + 2         'increase fuelling
        if FIPW < MaxIdleFuel then fuel_okay
      FIPW = MaxIdleFuel

fuel_okay:

rev_limiter:
      if speed < 120 then set_fuel  '1200 RPM

        FIPW = MinIdleFuel

set_fuel:
      gosub SetInjStart
      gosub SetFIPW

'-----
'
finish_up:
      debug 13

end_off:
      goto main_loop      'and return to beginning of main loop
end

'====== END OF MAIN LOOP  ======================================

'Subroutines:

eipwrite:

      dirl = $FF  'set data port to all out
      outl = lataddr
      low addlat  'set latch enable low
      high addlat 'set latch enable high
      outl = eipdata
      low rw            'set to write
      low cs687   'set 687 cs low
      high ds           'toggle ds
      low ds
      high cs687  'set 687 cs high
      high rw
      return

eipread:
      high rw
      dirl = $FF  'set to write out
      outl = lataddr
      low addlat
      high addlat
      dirl = 0    'set the direction to  read in
      low cs687
      high ds
      eipdata = inl
      low ds
      high cs687
      return
```

```
getadc:
      setadc = %10001110 | (chann << 4)   'unipolar, SE, int clk
      low csadc
      shiftout 0,1,1,[setadc]
      shiftin 0,1,2,[readadc\12]
      high csadc
      return

ReadMAP:

      pulsin 14,1,readadc     'Read MAP sensor frequency
      return

ReadATS:
      chann = 0
      gosub getadc

      return

ReadECT:
      chann= 4
      gosub getadc

      return

ReadEOT:
      chann = 1
      gosub getadc

      return

ReadAPS:
      chann = 5
      gosub getadc

      return

ReadICP:
      chann = 2
      gosub getadc

      return

ReadICPpot:
      chann = 6
      gosub getadc

      return

ReadAdvpot:
      chann = 3
      gosub getadc

      return

ReadFIPpot:
```

```
      chann = 7
      gosub getadc

      return

ReadCNGPot:
      chann = 0
      gosub getadc

      return

SetInjStart:

      Temp = FIStart    'in .25 cam degrees resolution

      for fcount = 0 to 7

      if Temp < $5A0 then SI1
      Temp = Temp - $5A0
SI1:
      lataddr = $20 + (fcount << 2)
      eipdata = Temp.HIGHBYTE
      gosub eipwrite

      lataddr = $21 + (fcount << 2)
      eipdata = Temp.LOWBYTE
      gosub eipwrite

      Temp = Temp + 180 'increment by 45øx 4 for each injector

      next

      return

SetFIPW:
      'FIPW in 4 microsecond resolution

   for fcount = 0 to 7

      lataddr = $22 + (fcount << 2)
      eipdata = FIPW.HIGHBYTE
      gosub eipwrite

      lataddr = $23 + (fcount << 2)
      eipdata = FIPW.LOWBYTE
      gosub eipwrite

   next

      return

SetInjPress:
      lataddr = $E1
      eipdata = InjPress
      gosub eipwrite

      return
```